**ISTANBUL TECHNICAL UNIVERSITY ★ EURASIA INSTITUTE OF EARTH SCIENCES**

**INVESTIGATION OF IMPACTS OF AEROSOLS ON EASTERN MEDITERRANEAN REGION CLIMATE**

**Ph.D. THESIS**

**Tuğba AĞAÇAYAK**

**Department of Climate and Marine Sciences**

**Earth System Science Programme**

**Anabilim Dalı :**   **Herhangi Mühendislik, Bilim**
**Programı :**   **Herhangi Program**

**FEBRUARY 2014**

**ISTANBUL TECHNICAL UNIVERSITY ★ EURASIA INSTITUTE OF EARTH SCIENCES**

**INVESTIGATION OF IMPACTS OF AEROSOLS ON EASTERN
MEDITERRANEAN REGION CLIMATE**

**Ph.D. THESIS**

**Tuğba AĞAÇAYAK**
**(601072004)**

**Department of Climate and Marine Sciences**

**Earth System Science Programme**

**Thesis Advisor: Assoc. Prof. Dr. Tayfun KINDAP**
Anabilim Dalı : Herhangi Mühendislik, Bilim
**Assoc. Prof. Dr. Alper ÜNAL**
Programı :   Herhangi Program

**FEBRUARY 2014**

**İSTANBUL TEKNİK ÜNİVERSİTESİ ★ AVRASYA YER BİLİMLERİ ENSTİTÜSÜ**

**AEROSOLLERİN DOĞU AKDENİZ BÖLGESİ İKLİMİ ÜZERİNE ETKİSİNİN ARAŞTIRILMASI**

**DOKTORA TEZİ**

**Tuğba AĞAÇAYAK**
**(601072004)**

**İklim ve Deniz Bilimleri Anabilim Dalı**

**Yer Sistem Bilimi Programı**

**Tez Danışmanı: Doç. Dr. Tayfun KINDAP**
**Anabilim Dalı : Herhangi Mühendislik, Bilim**
**Doç. Dr. Alper ÜNAL**
**Programı :  Herhangi Program**

**ŞUBAT 2014**

**Tuğba Ağaçayak**, **a Ph.D.** student of **ITU Eurasia Institute of  Earth Sciences** student ID 601072004 successfully defended the **dissertation** entitled "**INVESTIGATION OF IMPACTS OF SAHARAN DUST ON EASTERN MEDITERRANEAN REGION CLIMATE**", which she prepared after fulfilling the requirements specified in the associated legislations, before the jury whose signatures are below.

**Thesis Advisor :**     **Assoc. Prof. Dr. Tayfun KINDAP**     ...............................
İstanbul Technical University

**Co-advisor :**     **Assoc. Prof.Dr. Alper ÜNAL**     ...............................
İstanbul Technical University

**Jury Members :**     **Prof. Dr. Selahattin İNCECİK**     ...............................
İstanbul Technical University

**Prof. Dr. Cemal SAYDAM**     ...............................
Hacettepe University

**Prof. Dr. Mete TAYANÇ**     ...............................
Marmara University

**Prof. Dr. Orhan YENİGÜN**     ...............................
Boğaziçi University

**Assoc. Prof. Dr. Ali DENİZ**     ...............................
Istanbul Technical University

**Date of Submission : 3 February 2014**
**Date of Defense      : 24 February 2014**

*I dedicate this dissertation to the memory of*

*my beloved friend Zeynep Gülcan ÇOLAK*

**FOREWORD**

This thesis is based on the work carried out at Istanbul Technical University, Eurasia Institute of Earth Sciences, where I studied as a PhD student and worked as a research assistant. I have done a six months research with Dr. Marc Mallet for my thesis study at CNRS, University Paul Sabatier, Toulouse-France with support of TUBITAK. I am grateful to many people who have supported me until the end.

First of all, I would like to express my appreciation to my supervisors Assoc. Prof. Dr. Tayfun KINDAP and Assoc. Prof. Dr. Alper ÜNAL for their guidance in every step of my PhD. I would like to thank Prof. Dr. Mehmet KARACA and Prof. Dr. Nüzhet DALFES for their academic support throughout the whole study. I would like to thank all the committee members for their recommendations, especially to our precious professor Prof. Dr. Ferruh ERTÜRK who has passed away in August 2011. I also would like to thank to all my professors that I have attended their lectures during my bachelor, masters and PhD studies at ITU.

I appreciate Dr. François DULAC from LSCE for his recommendations and Dr. Marc MALLET from CNRS for his collaboration, hospitality and guidance. I am grateful to him for being such a good advisor and being so caring to his students. He helped me not to feel like a "foreigner" during my stay in the Laboratoire D'Aerologie. I am also grateful to all the members of LA for their friendship.

I would like to thank all my colleagues at EIES, Dr. Luca POZZOLI for his support, guidance, patience and motivation; Dr. Ozan Mert GÖKTÜRK and Dr. Deniz BOZKURT for their friendship and help during my PhD, Dr. Yasemin EZBER, for her precious friendship, contribution to my studies and moral support whenever I need, Assist. Prof. Ayşe Gül GÜNGÖR for her kind help and friendship.

I wish to express a very special thank you to my dear friends Zeynep ATALAY, Özge ÇETİNKAYA, Diren DEMİR, Pınar ÖZBAY for their valuable friendship; my late friends Onan GÜREN, Nagehan İLHAN, Berfin KALAY, Gönül ULUDAĞ for being with me during the last year of my PhD. I would like to thank to my dear friend Sumita KEDIA, for making me not to feel lonely in Toulouse and for the lovely memories we had together.

Finally, I am grateful to my family, especially to my parents Asuman and İsmail AĞAÇAYAK for their everlasting support and understanding, and my sister and my brother for their support and joy.

Hopefully this thesis will have useful implications for future studies.


February 2014                                                              Tuğba AĞAÇAYAK

x

# TABLE OF CONTENTS

## ABBREVIATIONS

| | |
|---|---|
| **AERONET** | : Aerosol Robotic Network |
| **AOD** | : Aerosol Optical Depth |
| **App** | : Appendix |
| **BC** | : Black Carbon |
| **DMS** | : Dimethly Sulfide |
| **DREAM** | : Dust REgional Atmospheric Model |
| **ECHAM5** | : ECMWF Hamburg |
| **ICTP** | : International Center for Theoretical Physics |
| **IPCC** | : Intergovernmental Panel on Climate Change |
| **LW** | : Long-wave |
| **GLCC** | : Global Land Cover Characterization |
| **GHG** | : Greenhouse Gas |
| **MODIS** | : Moderate Resolution Imaging Spectroradiometer |
| **MISR** | : Multi-angle Imaging SpectroRadiometer |
| **NCAR** | : The National Center for Atmospheric Research |
| **NH** | : Northern Hemisphere |
| **NO$_X$** | : Nitrogen oxides |
| **NOAA** | : National Oceanic and Atmospheric Administration |
| **OC** | : Organic Carbon |
| **OMI** | : Ozone Monitoring Instrument |
| **PM** | : Particulate Matter |
| **RegCM** | : Regional Climate Model |
| **SLP** | : Sea level pressure |
| **SO$_2$** | : Sulfur dioxide |
| **SSA** | : Single Scattering Albedo |
| **SW** | : Short-wave |
| **TOA** | : Top of Atmosphere |
| **VOC** | : Volatile Organic Compound |

## LIST OF TABLES

# LIST OF FIGURES

# INVESTIGATION OF IMPACTS OF AEROSOLS ON EASTERN MEDITERRANEAN REGION CLIMATE

## SUMMARY

Eastern Mediterranean is a region which has increasing population growth with low Environmental Performance Indicator. Air pollution is one of the problems, which decreases the environmental quality. It is known that long-range transport of Saharan dust is one of the main contributors to the air pollution problem. The purpose of the first section of this study is to investigate the relationship between high particulate matter concentrations and mineral dust transport using regional climate modelling, satellite data as well as in-situ observations and to determine the aerosol optical properties and radiative effects of aerosols for a dust transport episode.

PM$_{10}$ values for the selected regions for the episode in Turkey and at 10 different stations in Istanbul for the period 2004-2010 were provided by the Turkish Ministry of Environment. Daily mean PM$_{10}$ concentrations exceeding the European standard of 50 μg/m$^3$ were found to be on average, 49 days for the Spring period, 45 days for the Winter period, and 41 days for the Fall period for Istanbul. DREAM model output suggests that high PM$_{10}$ concentrations correlate highly with mineral dust transport episodes from Saharan desert (i.e., 23% for winter and 58% for spring). During the period between March 21st and 24th, 2008, observed daily mean of PM$_{10}$ concentrations reach up to 180 μg/m$^3$ in Marmara Region.

Model results highly correlated with PM$_{10}$ concentrations and satellite image. It is found that RegCM4.1 is able to model March 2008 episode and it can capture the dust pattern correctly in comparison with the satellite image. On March 23th 2008, when the dust episode affecting Aegean and Marmara Regions intensively, daily mean PM$_{10}$ was 102.6 μg/m$^3$ in Aegean Region and 117.3 μg/m$^3$ in Marmara Region according to the data provided by Turkish Ministry of Environment and Urbanization.

Model performance was checked through the AOD model outputs and AERONET observations. Three stations were selected which are affected stations such as Erdemli and Sevastopol and control station Eilat. Correlation coefficient was calculated around 0.6. On March 23th, AOD is 1.11 in Aegean Region and 0.87 in Marmara Region according to the RegCM4.1 model results. Mean dry deposition was 201.13 mg/m$^2$ and 96.67 mg/m$^2$ and column burden was 1009.9 mg/m$^2$ and 745.37 mg/m$^2$ respectively.

Dust transport causes changes in radiative forcing because of the highly scattering feature of mineral dust. Short wave radiation at surface and at ToA decreased around 71.4 W/m$^2$ and 33 W/m$^2$ in Aegean Region and 61.9 W/m$^2$ and 28.8 W/m$^2$ in Marmara Region respectively. Long wave radiation at surface and ToA increased around 10.7 W/m$^2$ and 4.4 W/m$^2$ in Aegean Region and 6.9 W/m$^2$ and 4 W/m$^2$ in Marmara Region respectively. The first part of this study shows the atmospheric

properties and radiative forcing during an important dust episode affecting west of Turkey.

As a second aim of this study, climatic effect of mineral dust was evaluated. Dust from Saharan Desert is an important component of the climate of the Mediterranean basin. The emissions and transport of dust from Sahara to Europe depends on meteorological conditions, therefore climate change can affect the sources of mineral dust and its transport pathways. On the other hand dust has also an effect on climate by modifying the radiative budget in the atmosphere. The objective of this study is to identify the effect of mineral dust on the climate of Mediterranean. In order to quantify this effect, we simulated with the regional climate model RegCM-4.1 for three 10-years time periods (1991-2000, 2041-2050, and 2091-2100). The model domain covers the entire Mediterranean Sea, including the Saharan Desert between 25°N and Northern Europe at 50°N. The horizontal resolution is 27 km x 27 km with 18 vertical layers from surface to 50 hPa. The ECHAM5 simulations of scenario A1B were used to provide boundary and initial conditions to RegCM simulations. To show the effect of dust on climate, we performed 2 simulations, for each 10-year period with dust and without dust.

A comprehensive analysis of the dust budget, including surface emissions, burden, deposition for present and future climate are presented in this study. Compared to present climate, a shift of mineral dust emissions towards southern latitudes of Saharan Desert was observed for the future. In the southern part of the domain dust emissions increased by 15% and 20% in 2040s and 2090s, respectively. This is due to a change in the general pattern of surface winds, which are strengthening at lower latitudes, probably due to a strengthening and relocation of the Azores anticyclone towards north in future climate conditions. This generates a change in dust burden over the Mediterranean and decreases particularly in the Eastern Mediterranean (10%) and increases in the West Mediterranean (8%). The changes in burden of dust determine also a change in the distribution of the aerosol optical depth (AOD) and the dust radiative forcing. In the 2040s AOD increased by 15% in the Western Mediterranean and decreased by 10% in the Eastern Mediterranean. Similar changes were also simulated for the end of the 21st century.

The impact of dust on the net radiative budget was quantified for the single 10-years periods by comparing the simulations with dust and without dust. Shortwave net radiation at surface was decreasing up to 20 $W/m^2$ over the source regions and 8 $W/m^2$ over Mediterranean Sea and South Europe. Shortwave net radiation at the top of atmosphere was decreasing 3 $W/m^2$ over the source region. Similarly we present also the changes on surface temperature and precipitation for the single 10-years periods. Dust caused an average temperature decrease of 0.2 C° over Europe and 0.5 C° over the African continent for the period 1991-2000. A similar impact was found for the 2041-2050 period. Smaller temperature changes simulated for the end of the 21st century. No significant changes were observed in precipitation for the 3 periods.

# AEROSOLLERİN DOĞU AKDENİZ İKLİMİNE ETKİLERİNİN DEĞERLENDİRİLMESİ

## ÖZET

Doğu Akdeniz Bölgesi artan nüfusu ve düşük çevresel performans göstergeleriyle çevre ve atmosfer bilimlerinde gün geçtikçe önem kazanmaktadır. Hava kirliliği, bölgedeki çevre kalitesini azaltan problemlerden biridir. Sahra tozunun uzun mesafeli taşınımı hava kirliliğine etki eden en önemli etkenlerden biridir. Bu tezin ilk bölümünde amaç, öncelikle mineral tozun partikül madde konsantrasyonları üzerindeki etkisini araştırmak, toz taşınımını modelleyerek, sonuçları uydu görüntüleri ve yer gözlemleri ile karşılaştırmak, aerosol optik değerleri belirlemek, tozun radyatif etkisini bir toz episoduyla karşılaştırmaktır.

Çevre ve Şehircilik Bakanlığı'ndan İstanbul'daki 10 farklı istasyon için, 2004-2010 yılları aralığı partikül madde verisi temin edilmiştir. Saatlik olarak alınan veri, günlük ortalamaya ve sonra da aylık ortalamaya çevrilmiştir. Günlük verilerin öncelikle Avrupa Komisyonu Standardı olan 50 $\mu g/m^3$'yi aşıp aşmadığı kontrol edilmiştir. İstanbul'da bahar ayında ortalama 49 gün, kış döneminde ortalama 45 gün, sonbaharda 41 gün sınırı aşmıştır. DREAM Model çıktılarına göre (Nickovic et al. 2001; Perez et al. 2006) yüksek $PM_{10}$ konsantrasyonları mineral toz taşınımıyla önemli şekilde koraledir (23% kış ve 58% ilkbahar).

Çalışmanın ilk kısmında RegCM4.1 modeli Sahra tozunun etkilerini ayrıntılı şekilde incelemek amacıyla kullanılmıştır. 21-24 Mart 2008 tarihleri arasındaki periyotta, günlük ortalama partikül madde konsantrasyonları Marmara Bölgesi'nde 180 $\mu g/m^3$'ye ulaşmaktadır.

Model sonuçları, $PM_{10}$ konsantrasyonları ve uydu görüntüleriyle iyi şekilde korale çıkmıştır. RegCM4.1 Mart 2008 episodunu iyi şekilde modellemiştir ve toz taşınımını uydu görüntülerine benzer şekilde gerçekleştirdiği gözlenmiştir. Ege ve Marmara Bölgeleri'ni yoğun şekilde etkileyen 23 Mart 2008 gününde, Ege'de günlük ortalama 102 $\mu g/m^3$ ve Marmara'da 117.3 $\mu g/m^3$ $PM_{10}$ konsantrasyonu ölçülmüştür. Ölçüm değerleri Çevre ve Şehircilik Bakanlığı'ndan elde edilmiştir.

Model performansı AOD model çıktılarına ve AERONET gözlemlerine göre değerlendirilmiştir. Kontrol için Erdemli, Sivastopol ve Eilat istasyonları seçilmiştir. Gözlem ve model sonuçları korelasyon katsayısı 0.6'dır. Aynı gün model çıktılarına göre Ege Bölgesi'nde 1.11 olarak hesaplanan AOD, Marmara Bölgesi için 0.87 olarak hesaplanmıştır. Ortalama kuru çökelme sırasıyla 201.13 $mg/m^2$ ve 96.67 $mg/m^2$ olarak hesaplanırken, kolon derinliği 1009.9 $mg/m^2$ ve 745.37 $mg/m^2$ olarak hesaplanmıştır.

Mineral toz taşınımı, tozun saçıcı özelliği nedeniyle ayrıca radyatif güdümlemeyi de etkilemektedir. Kısa dalga boylu radyasyon yüzeyde ve atmosferin tepesinde, Ege Bölgesi'nde 71.4 $W/m^2$ ve 33 $W/m^2$ azalırken, Marmara Bölgesi'nde 61.9 $W/m^2$ ve

28.8 W/m$^2$ azalmaktadır. Uzun dalga boylu radyasyon yüzeyde ve atmosfer tepesinde Ege Bölgesi'nde 10.7 W/m$^2$ ve 4.4 W/m$^2$ artarken, Marmara Bölgesi'nde and 6.9 W/m$^2$ ve 4 W/m$^2$ artmaktadır.

Bu çalışmada Türkiye'nin batısında etkili olmuş bir episot için atmosferik özellikler ve radyatif güdümleme incelenmiştir. Bu çalışmanın ikinci aşaması, mineral tozların iklim üzerine etkisinin değerlendirilmesidir. Sahra'dan gelen mineral tozların iklim üzerine önemli etkisi bulunmaktadır. Mineral tozlar özellikle saçıcı özelliğe sahip oldukları için gelen radyasyonun bir kısmının geri yansıtılmasına ve dolayısıyla sıcaklıkların azalmasına sebep olmaktadır. Öte yandan Sahra'dan tozun taşınması meteorolojik koşullara bağlıdır. Dolayısıyla iklim değişikliği de mineral toz kaynaklarını ve taşınım yollarını etkileyebilmektedir. Bu nedenle geri besleme mekanizması çift yönlü değerlendirilmelidir.

Çalışmanın ikinci aşamasının amacı, mineral tozların Akdeniz iklimi üzerine etkisinin değerlendirilmesidir. Bu etkiyi değerlendirmek için, bölgesel iklim modeli RegCM4.1 ile 10 senelik 3 ayrı dönemin (1991-2000, 2041-2050, ve 2091-2100) simülasyonu yapılmıştır. Her bir dönem ayrı ayrı toz içeren ve içermeyen durumlar için çalıştırılmıştır.

Model domaini bütün Akdeniz Bölgesi'ni içermektedir. Model sınırları Sahra Çölü 25° kuzey enleminden, Kuzey Avrupa'da 50° kuzey enlemine kadar, batıda 15°, doğuda 45° boylamına kadardır. Yatayda çözünürlük 27 km x 27 km, dikeyde 18 sigma seviyesidir. Atmosfer tepesi 50 hPa'dır. Model başlangıç ve sınır koşulları ECHAM5 simülasyonları A1B senaryosu simülasyonlarından alınmıştır. A1B senaryosu bütün enerji kaynaklarının dengeli kullanıldığı bir senaryodur.

Toz bütçesinin genişlemesine bir analizi için, yüzey emisyonları, kolon yükü, çökelme, aerosol optik derinlik üzerine her dönem için detaylı bir araştırma yapılmıştır. Gelecekteki iklim için ortaya konulan sonuçları referans periyotla kıyaslayınca, gelecekteki dönemde toz emisyonlarının daha güneye doğru kaydığı gözlenmiştir. Domainin güney bölümünde emisyonların 2041-2050 döneminde %15, 2091-2100 döneminde %20 arttığı görülmektedir. Bu durum yüzey rüzgarlarının genel paterninin değişmesinden kaynaklanmaktadır. Rüzgarlar aşağı enlemlerde güçlenir. Bu da özellikle Azor antisiklonlarının kuzeye doğru kayarak güçlenmesinden kaynaklanır. Bu durum toz yükünün domainin batısında %8 artmasına, Doğu Akdeniz'de %10 azalmasına sebep olmaktadır. Kolon yükü ayrıca aerosol optik derinliği ve toz radyatif güdümlemeyi de etkilemektedir. 2041-2050 döneminde Batı Akdeniz'de aerosol optik derinlik % 15 artarken, Doğu Akdeniz'de %10 azalmaktadır. 2091-2100 döneminde de benzer değişiklik görülmektedir.

Tozun net radyasyon bütçesi üzerinde etkisi her 10 yıllık periyotta tozun dahil olduğu ve olmadığı durumlar için değerlendirilmiştir. Yüzeyde kısa dalga boylu net radyasyon, tozun kaynağı olan Sahra bölgesinde 20 W/m$^2$ kadar azalırken, Güney Avrupa ve Akdeniz Bölgesi'nde 8 W/m$^2$ kadar artmıştır. Kısa dalga boylu net radyasyon atmosferin tepesinde 3 W/m$^2$ kadar azalmıştır. Benzer şekilde 10 yıllık dönemler için sıcaklık ve yağış değişiklikleri de incelenmiştir. Tozun her dönemde Avrupa üzerinde 0.2 C° sıcaklık azalmasına, Afrika üzerinde 0.5 C° sıcaklık azalmasına sebep olacağı görülmüştür. Yağışta 3 dönem için de anlamlı bir değişiklik olmamıştır.

# 1. INTRODUCTION

Aerosols are liquid or solid particles emitted to the atmosphere by natural and anthropogenic sources (IPCC, 2007). They affect the earth's radiative balance directly (through scattering and absorption of solar and infrared radiation) or indirectly (through interactions with clouds).

Natural aerosol species include mineral dust, sea salt, volcanic ash, and biogenic emissions from land and ocean, while anthropogenic aerosols are mainly emitted by fossil fuel combustion and biomass burning. Among these sources, mineral dust is the most important component as globally, approximately 3000 Tg dust is emitted every year in the form of mineral dust (% 12 of total aerosols) (Zender et al., 2003).

Aerosols are classified according to their formation mechanism. These classifications include primary aerosols particulates that are emitted to the atmosphere directly; and secondary aerosols, particulates that are formed in the atmosphere through chemical reactions (Sportisse, 2008). Table 1.1 presents source of aerosols and their estimated fluxes. Primary natural aerosols make 97% of total aerosols, and it includes mineral dust (12%), sea salt (84%), volcanic dust, and biological debris. Primary anthropogenic aerosols make 2% of total aerosols. These aerosols are industrial dust, black carbon, and organic aerosols. Secondary anthropogenic aerosols are sulfates from $SO_2$ and nitrates from NOx, which make about 1% of total aerosols. Secondary natural aerosols are sulfate from dimethyl sulfide, sulfate from volcanic $SO_2$, and organic aerosols from biogenic VOC.

Aerosol diameters are in the range between a few nanometers to 100 μm. Particles from combustion can be from few nanometers to 1 μm whereas natural aerosols are generally bigger than 1 μm. Aerosol size distribution is defined accordingly to the size of the particles. It is hard to define all the particle's diameters, as their diameter is changing temporally and spatially. Therefore "size bin" term, which is the range to classify the aerosols according to their diameters, is used (Seinfeld, 2006). Size bin range can be chosen differently in models according to the specific needs. In order to show the

difference in aerosol size, $PM_x$ term is used. Particulate matter with diameter smaller than x micrometer is shown as $PM_x$. For example particulates less than 2.5 μm is referred to $PM_{2.5}$. Total suspended particulate matter (TSP) is the mass concentration smaller than 40-50 μm.

**Table 1.1 :** Source and estimated flux of aerosols (Seinfeld, 2006).

| Source | Estimated Flux (Tg/yr) | Reference |
|---|---|---|
| **NATURAL - Primary** | (97%) | |
| Mineral Dust | 2980  (12%) | Zender et al. 2003 |
| Seasalt | 10100 (84%) | Gong et al. 2002 |
| Volcanic Dust | 30 | Kiehl and Rodhe 1995 |
| Biological Debris | 50 | Kiehl and Rodhe 1995 |
| **NATURAL - Secondary** | | |
| Sulfate from DMS | 12.4 | Liao et al. 2003 |
| Sulfate from Volcanic $SO_2$ | 20 | Kiehl and Rodhe 1995 |
| Organic Aerosol from biogenic VOC | 11.2 | Chung and Seinfeld 2002 |
| **ANTROPOGENIC - Primary** | (2%) | |
| Industrial Dust | 100 | Kiehl and Rodhe 1995 |
| Black Carbon | 12 Tg C | Liousse et al. 1996 |
| Organic Aerosol | 81 Tg C | Liousse et al. 1996 |
| **ANTROPOGENIC -Secondary** | (1%) | |
| Sulfates from $SO_2$ | 48.6 Tg S | Liao et al. 2003 |
| Nitrates from NOx | 21.3 Tg $NO_3^-$ | Liao et al. 2003 |

Aerosol's can be examined by electron microscopy and defined by different modes according to their number or volume. Figure 1.1 shows their distribution. Volume modes are accumulation and coarse mode. Primary emissions, secondary sulfates, nitrates and coagulation of small particles are in accumulation mode. The accumulation mode can be formed by two modes, which are condensation and droplet submode in some cases. Primary particles and growth of smaller particles by coagulation can be in

the condensation mode where droplet mode is created during the cloud processing. Aerosols in coarse mode are caused by the mechanical processes such as wind and erosion. Sources of coarse mode aerosols are mainly natural, some secondary sulfates and also nitrates (Seinfeld, 2006). When aerosols are classified according to their number, they can be grouped as Nucleation mode (smaller than 10 nm) and Aitken mode (10-100 nm). Nucleation mode is found less in the atmosphere and depends on the atmospheric conditions. Aitken nuclei can be primary particles and also secondary material condensed on the primary particles.
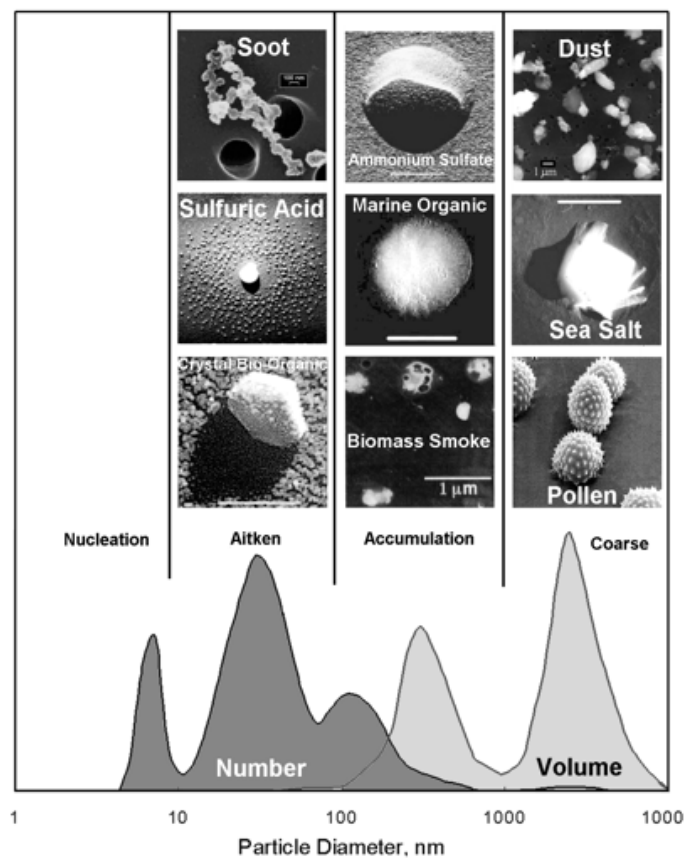


**Figure 1.1 :** Examples of different aerosol types from electron microscope images as a function of the aerosol mode together with typical number and volume distributions (Brasseur et al., 2003).

Aerosols can also be classified according to their sources such as urban aerosols (Figure 1.2, top left), marine aerosols, rural continental aerosols, remote continental aerosol, free tropospheric aerosols, polar aerosols, and desert aerosols (Figure 1.2, bottom left). Sources of urban aerosols are industries, transportation, power plants, natural sources and secondary particles. Mass distribution is accumulation mode and coarse mode in urban (Figure 1.2, top right), however number distribution is mostly smaller than 0.1 μm. Coarse particles in urban area are mainly natural aerosol or industrial residuals.

Primary particles from industry and secondary aerosols are in aitken or accumulation mode. Marine aerosols are in three modes, which are the aitken mode (D < 0.1 μm), accumulation mode (0.1 < D < 0.6 μm) and the coarse mode (D > 0.6 μm) with a concentration in the range of 100-300 cm$^3$. In the rural areas, source of aerosol is mainly natural and less anthropogenic. Diameters are in two modes around 0.02 and 0.08 μm. Mass distribution is around 7 μm. Remote continental aerosols are primary particles and secondary oxidation particles. Modes are 0.02, 0.1, and 2 μm (Jaenicke, 1993).
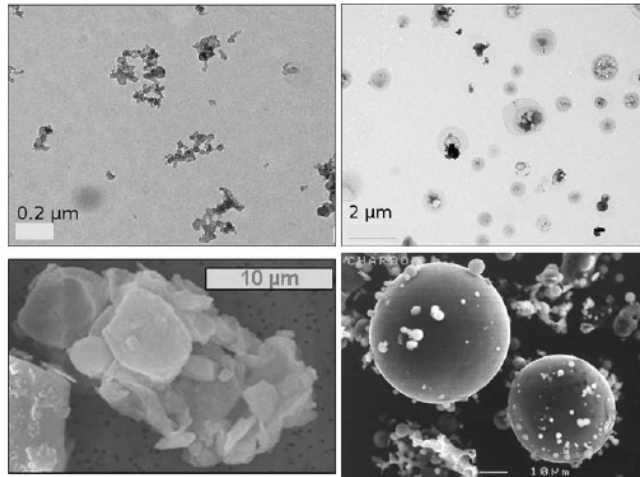


**Figure 1.2 :** Image of aerosols by an electron microscope (Sportisse, 2008).

Free tropospheric aerosol can be found in the mid and upper level of troposphere. Modes are 0.01 and 0.25 μm. They can be formed at the upper troposphere because of the low temperature and low aerosol surface area. Polar aerosols have very low concentration and found near Arctic and Antartica. Mean diameter is around 0.15 μm and modes are 0.75 and 8 μm. Desert aerosol can be transported by the wind velocity and modes are 0.01 μm, 0.05 μm and 10 μm (Jaenicka, 1993). Major elements in soil are Si, Al, Fe, Ca (Warneck, 1988). Particles can be transported across Atlantic to USA and across Mediterranean to Europe. Particles around 100 μm can be found near the source region and smaller than 10 μm can be transported to far points even more than 5000 km (Seinfeld, 2006). Figure 1.1 shows the typical number and volume distribution of aerosols. Soot, sulfuric acid and organics can be given as examples for aitken mode aerosols. Ammonium sulfate, marine organics, biomass smoke can be given as examples for accumulation mode. Dust, sea salt, and pollen are in coarse mode.

IPCC (2000) had a classification of aerosols according to their size and hemispheric distribution. This is given in Table 1.2. As stated earlier, mineral dust is the second highest annual emissions (2150 Tg/yr). It should be noted that 84% of mineral dust is in

the Northern Hemisphere. Approximately 81% (1750 Tg/yr) is emitted in the range of 2-20 μm, 13% in the range of 1-16 μm, and the rest 5% in the range <1 μm.

**Table 1.2 :** Estimation of aerosol emissions (IPCC, 2000).

| Type | Total (Tg/yr) | Range | North | South |
|---|---|---|---|---|
| Sea Salt | 3344 | 1000-6000 | 43% | 57% |
| Diameter < 1 μm | 54 | 18-100 | | |
| Diameter in [1, 16] μm | 3290 | 1000-6000 | | |
| Mineral aerosol (dust) | 2150 | 1000-3000 | 84% | 16% |
| Diameter < 1μm | 110 | | | |
| Diameter in [1, 16] μm | 290 | | | |
| Diameter in [2, 20] μm | 1750 | | | |
| Organic Aerosol | | | | |
| Biomass burning | 54 | 45-80 | 50% | 50% |
| Fossil Fuel Combustion | 28 | 10-30 | 98% | 2% |
| Biogenic | 56 | 0-90 | 98% | 2% |
| Elemental Carbon | 12.3 | | | |
| Biomass Burning | 5.7 | 5-9 | 50% | 50% |
| Fossil Fuel Combustion | 6.6 | 6-8 | 98% | 2% |
| Industrial Emissions | 100 | 40-130 | | |

Mixing state is important in aerosol distribution. There are three different mixing states of aerosols. These are; single internal mixing, multiple internal mixing, and external mixing. In single internal mixing, chemical components are mixed completely. In multiple internal mixing, there are some species, which are well mixed. External mixing is the state, in which the species are not mixed (Sportisse, 2008). Multiple external mixing is the state that is most realistic because of the coagulation and ageing processes.

Aerosols can be classified according to their components as well: carbon containing aerosols and non-carbon aerosols. Aerosols, which are containing carbon are called organic aerosols. Actually most aerosols are a mixture of organic and inorganic species (Sportisse, 2008). Aerosols can include ammonium, nitrates, sulfates, organics, crustal species, sea salt, metal oxides, hydrogen ions, and water. Fine particles generally include sulfate, ammonium, organic and elemental carbon. Coarse particles on the other hand are mainly natural aerosols, and they are comprised of silicon, calcium,

magnesium, aluminium, iron and biogenic organic particles. Nitrate can be found in both fine and coarse mode.

Mineral dust can come out from soil or road. Soil dust particles contain minerals and organic matter such as quartz, feldspar, hematite, calcite, dolomite, epsomite, gypsum, clay and also organic matter such as plant and animal residuals (Jacobson, 2005). Because of the climatic and biogeochemical effect of mineral dust; transport, emission and features of dust became a significant subject for studies (Escudero et al., 2011).

## 1.1 Aerosols Dynamics

There are many processes, which play important role on size distribution and chemical composition. These processes are nucleation, coagulation, condensation and evaporation, mass transfer to cloud drops, heterogeneous reactions and loss processes (Sportisse, 2008).

Nucleation is the process which is the formation of new particles by conversion of gaseous molecules. These clusters have a size between 0.1-1 nm. Coagulation is the process which aerosols come together because of their Brownian motion. Condensation occurs when gaseous molecule condense on the aerosol or evaporates from the aerosol which is caused by the concentration difference. Condensation is fast for fine particles and slow for the coarse particles.

Some aerosols may lead cloud condensation nuclei formation as playing the condensation surface role which is the most important process for cloud drops formation. Size, chemical composition, and super-saturation of a particle is important for being nucleus for water droplet formation.

Loss processes are dry deposition which transfer the particle to the surface by gravitational settling and wet deposition which transfers the particle by rain, snow or fog. Figure 1.3 summarizes the dynamic processes of aerosols.
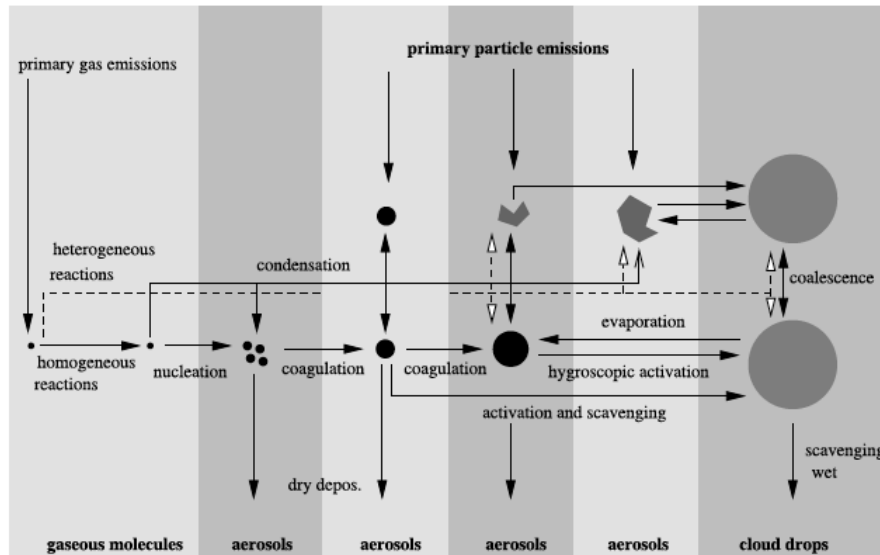
**Figure 1.3 :** Image of aerosol dynamics (Raes et al., 2000).

## 1.2 Effects of Aerosols and Climate Interactions

Aerosol studies are important because of their effect on health, air quality, cloud formation and climate impact (Jacobson, 2005). Aerosols have direct effect on global energy balance by absorption and scattering of radiation and have indirect effect by reflectance of clouds and precipitation (Hansen et al., 1997; Lohmann and Feichter, 2001; Ramanathan et al., 2001). As seen in Figure 1.4, direct effect of aerosols is scattering and absorption. This term was changed to "REari" which means aerosol-radiation interactions, and explains the combined scattering and absorption of radiation in the fifth report of IPCC (AR5).

Mainly, aerosols absorb or scatter radiation according to their physical properties. Most of the aerosols scatter the radiation. Color of the aerosol is also important. If the compound has high absorption feature like black carbon, incoming radiation will be absorbed. If the compound has high scattering feature like mineral dust incoming radiation will be reflected. This process is also depending on if the mineral dust has a contamination with other compounds. Aerosols also can change the albedo by covering the surface. For example, black carbon can transport to Arctic and causes melting of ice.

Behavior of pollutant according to their warming or cooling potential can be seen in Table 1.3. Greenhouse gases, which prevents the outgoing infrared radiation, stays globally, operates day and night. Their residence time is from decades to centuries, which has a total warming effect. Particles smaller than 1 μm, scatters the incoming

solar radiation. They vary in space and time, they operate the daytime and stay around 2 weeks, they cause a total cooling effect. Sulfate particles which cause the scattering of incoming solar radiation, are common in industrialized areas of northern hemisphere, they operate in daytime, stay around 2 weeks, and causes a total cooling effect. Mineral dust, which causes scattering in the visible part of the spectrum, transports to downwind of large arid regions, operates in daytime and causes a total cooling effect. Another kind of mineral dust, which causes absorbing in the infrared region, transports to downwind of large arid regions, operates at daytime and causes warming. Black carbon also absorbs in the visible part of the solar radiation in industrialized areas of northern hemisphere, operates at daytime, stays around 1 week and causes warming.
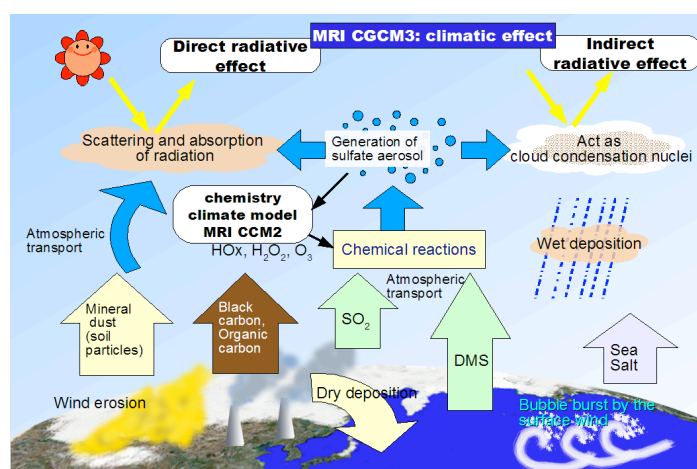


**Figure 1.4 :** Schematic evaluation of aerosols in atmosphere.

Climate change is the change in the mean state of the climate, for decades or longer time period. Natural processes and anthropogenic emissions may change the atmospheric composition and cause climate change. Figure 1.5 shows the important activities, which may affect the radiative forcing. Greenhouse gases increase the radiative forcing where anthropogenic aerosols have negative effect on radiative forcing (IPCC, 2007). As seen in Figure 1.5 uncertainty levels for aerosol radiative impact is rather high. Therefore, from global and regional climate change perspective radiative forcing of aerosols is critical. For example, long-lived greenhouse gases such as $CO_2$, $CH_4$, tropospheric ozone, stratospheric water vapour, black carbon on snow cause increase about 1.5 $W/m^2$ in radiative forcing while total aerosol decreases radiative forcing by 1 $W/m^2$. It is important to know that; climate change projections in the fourth assessment report of IPCC have not included the radiative effect of desert dust (Zhang et al., 2009). This was one of the biggest shortcomings of the study and was highlighted by IPCC. Since the fourth assessment report of IPCC, it recognizes the importance of

radiative forcing of aerosols and anthropogenic aerosols were taken into the consideration in the emission scenarios. Fifth assessment report of IPCC has included the cloud and aerosols but there are still uncertainties. Aerosol processes and properties which are important on climate are more defined than the previous assessment report. Most of the global circulation models have sulphur cycle and the direct and indirect effect of sulphate aerosol. Also they include the mass, size distribution, mixing state of multi component aerosol particles (IPCC, 2013).

**Table 1.3 :** Behaviour of pollutans.

| Type of pollutant | Act | Where? | When? | Residence Time | Effect |
|---|---|---|---|---|---|
| Greenhouse Gas | Preventing outgoing, infrared radiation | Uniform globally | Operates day and night | Decades to centuries | **Warming** |
| Particle < 1 µm | Scattering incoming solar radiation | Variable in space and time | Day time | 2 weeks | **Cooling** |
| Sulfate particles | Scattering incoming solar radiation | In industrialized areas of NH | Day time | 2 weeks | **Cooling** |
| Mineral Dust | Scattering in the visible part of the spectrum | Downwind of large arid regions | Day time | 2 weeks | **Cooling** |
| Mineral Dust | Absorbing in the infrared region | Downwind of large arid regions | Day time | 2 weeks | **Warming** |
| Black Carbon | Absorbing in the visible part of the solar radiation | In industrialized areas of NH | Day time | 1 week | **Warming** |
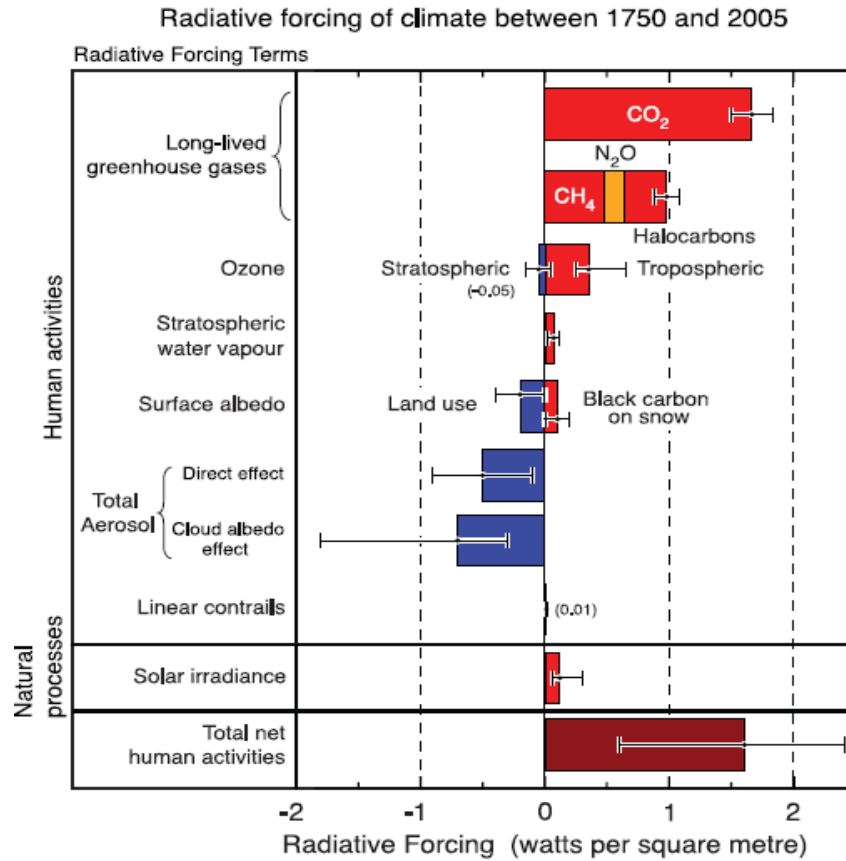
**Figure 1.5 :** Radiative Forcing of Climate Between 1750 and 2005 (IPCC, 2007).

## 1.3 Study Basin

Saharan Desert is the biggest hot desert in the world, located in the North of Africa. It has a 9.4 million $km^2$ area in total. It is the biggest mineral dust source in the world. It is a very important source which affects the air quality and climate of Mediterranean Region. Figure 1.6 shows a satellite image for Saharan Desert.
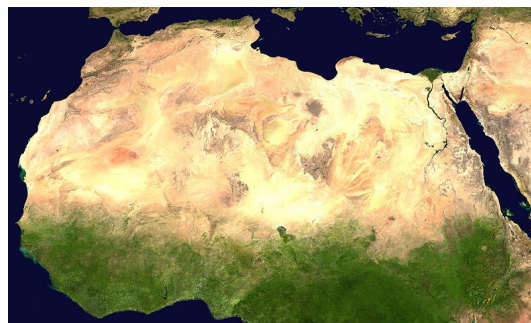


**Figure 1.6 :** Saharan Desert.

Figure 1.7 shows the nine regions causing desert dust. These regions are in North Africa (Sahara), South Africa, the Arabian Peninsula, Central Asia, Western China, Eastern China, North America, South America and Australia (Prospero et al., 2002; Tanaka and Chiba, 2006). It is calculated by Tanaka and Chiba (2006) that Sahara contributes 58% of the total global dust emission. In the figure, estimated emissions can be shown by the rounds.
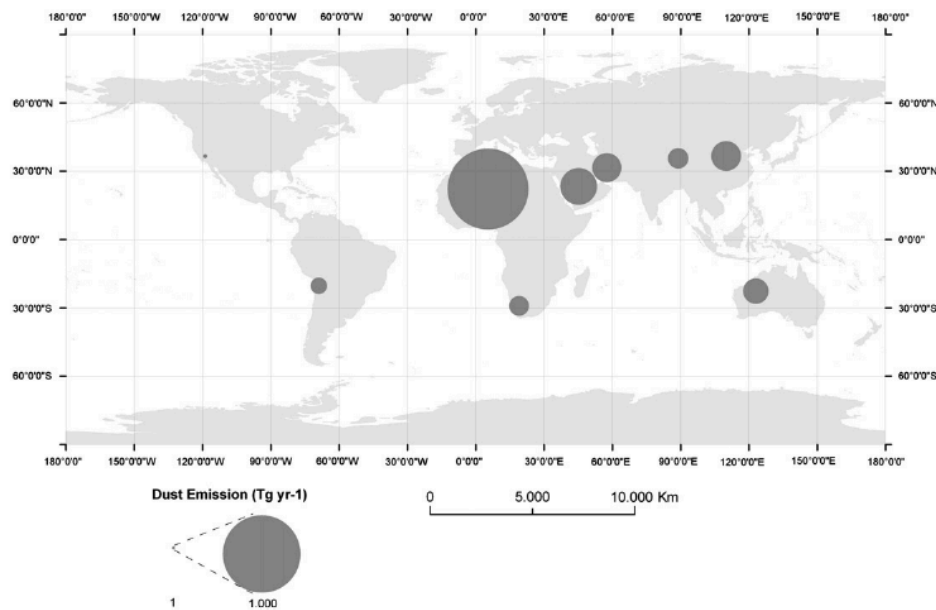


**Figure 1.7 :** Location of the source areas and scale of the dust emissions.
Adapted from Tanaka and Chiba, 2006.

## 1.4 Impact of Saharan Dust on Mediterranean

Anthropogenic or natural materials can be carried to the sea and land by atmospheric transport (Kubilay, 1997). Figure 1.8 shows the transport ways of Saharan dust. Dust can be transported to America, Caribbean's, and South America over Atlantic Ocean by path I around 3-5 days in summer and 1 week in winter, to Europe and Mediterranean Region over Mediterranean Sea by path II in 7-8 days, to Anatolia and Middle East by path III around 1 week (Engelstaedter et al., 2008).
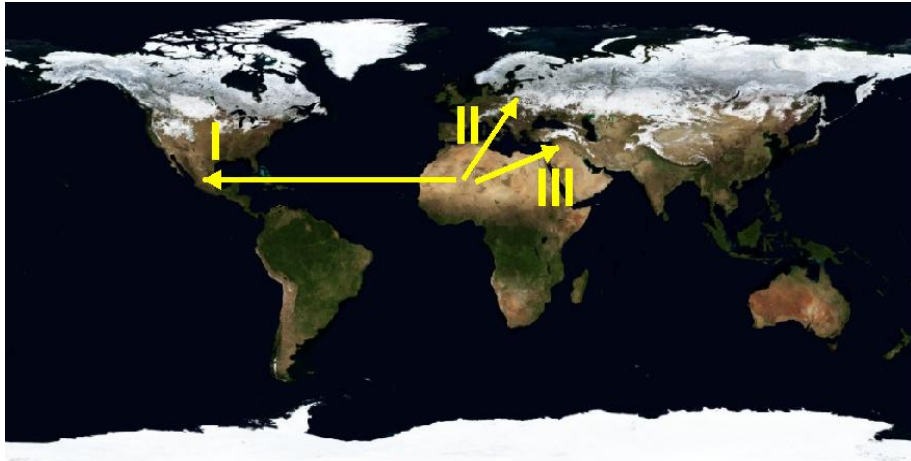
**Figure 1.8 :** Saharan Dust Transport.

Mediterranean Basin covers part of three continents, Europe, Asia and Africa. Land near the Mediterranean Sea has Mediterranean Climate with mild, rainy winter and dry, hot summers. Since it is formed by three different continents, there are many factors affecting the region. Mediterranean Region is used to be subject area to aerosol-climate studies. Both sea salt aerosols, North and Central African mineral dust, biomass burning, and North and Eastern Mediterranean source long range urban/industrial and biomass burning aerosols affect Mediterranean. Mineral dust is the most important aerosol type in Mediterranean Region, however radiative effects are not well defined (Santese et al., 2010). Besides investigation of effects of anthropogenic aerosols on climate is important because of the direct and indirect effects (Sathees et al., 2004). Figure 1.9 shows the countries that have coast to the Mediterranean Sea.



**Figure 1.9 :** Study Area

Mineral dust transported from Saharan desert is often a problem for the countries located on the coasts of the Mediterranean Sea. It has effect on air quality and visibility (increase in PM levels, decrease in visibility), radiative properties (decrease in SW, increase in LW, CCN), human health (asthma, allergy, migraine), and they also add minerals and nutrients to the ocean (Fe).

Saharan dust is an important natural source affecting the $PM_{10}$ level in the atmosphere (Jimenez et al, 2010) and Saharan dust episodes cause peaks in $PM_{10}$ concentration (Longueville et al., 2010). It leads increase in particulate matter concentration at the monitoring sites as a result of dust transport (Salvador et al., 2013). Sunnu et al (2008) also found that Saharan dust is more contributed to $PM_{10}$ in comparisons with particles with a size 5 and 2 μm in Ghana. Dust particles in the air can be transported long distances from the source regions and cause high levels of daily $PM_{10}$ concentrations, adding to the local pollution of anthropogenic origin and affect air quality whether they are natural or anthropogenic. In populated cities, this can be an important issue while trying to have conformity with the air quality standards imposed by legislation at country or regional level such as European Union.

According to the studies done on the effect of mineral dust on oceans, Kocak et al. (2004) found that trace elements (Al, Fe, and Mn) increases around 1.5 and 4 times during the transition season related to the dust transport. Saydam (2001) found that dust from specific deserts has the potential to produce bioavailable iron within cloud droplets and daytime wet dust deposition over the ocean surface results in the enhancement of coccolithophores. Also mineral dust has effect on health. Inhaled mineral dust with an diameter bigger than 10μm, stops in the upper respiratory tract where the particles get trapped in the mucous lining of the nasopharyngeal tract. They are normally of an only small health concern, unless the particles are of toxic mineralogy. If the dust particles have an aerodynamic diameter smaller than 10μm ($PM_{10}$ standard), they can penetrate more deeply into the lung passages to the tracheobronchial regions, where they also get trapped in a layer of mucus (Derbyshire, 2007; Plumlee and Ziegler, 2006).

Mediterranean Region is subject to aerosol-climate studies, since it is affected by air pollution and natural sources caused by the surrounding regions. From the air quality perspective, mineral dust can contribute significantly to $PM_{10}$ concentrations, potentially leading to violate the air quality standards. In Europe the Council Directive 1999/30/EC fix the limit values for particulate matter concentrations and sets the daily

limit $PM_{10}$ concentration to 50 μg/m$^3$, which may be exceeded for a maximum of 35 days per year. Mineral dust is particularly important for the countries in the Mediterranean region due to the large emissions from North Africa, which can be transported to Europe. Mineral dust is also important from the climate perspective. However aerosol radiative effects are not well defined (Santese et al., 2010).

Mediterranean Basin used to be the subject of many researchers due to its climate variability and climate change (e.g., Bolle 2003; Giorgi and Lionello 2008; Onol and Semazzi 2009; Evans 2009). Mediterranean is frequently exposed to African dust transport episodes throughout the year. Furthermore, the countries in the Eastern Mediterranean Region are generally characterized by lower environmental quality (e.g. Yale EPI, 2001) and high percentages of urban/rural population, with large cities such as Istanbul, Athens, and Cairo, where population is more exposed to high levels of pollutant concentrations. For this reason it is particularly important to develop air quality and climate models which are able to quantify the contribution of natural aerosols, like mineral dust, to particulate matter levels. There are many studies which analyzed the African dust impact on the Mediterranean (Tsidulko et al., 2002; Mace et al, 2003; Papayannis et al, 2005; Koçak et al., 2007; Mitsakou et al., 2008; Querol et al., 2009; Ganor et al., 2010). According to Astitha et al. (2008) 50% of the $PM_{10}$ exceedance days in Athens are caused by the Saharan dust contribution. It is shown that the most important season for Saharan dust episodes is spring in Alexandria and the Greater Nile Delta region (El-Askary et al., 2009).

At regional scale several climate modeling studies were performed with the Regional Climate Model (RegCM4) (Giorgi, 2012), focusing on dust transport episodes from the Saharan desert and the Mediterranean Sea. Konare et al. (2008) and Solmon et al. (2008) investigated the effect of desert dust on the West African monsoon with RegCM3 (Pal et al., 2000). They found that dust effect on shortwave (SW) radiative forcing causes a decrease in average precipitation over the Sahel Region comparable to those found during dry years (up to -2 mm day$^{-1}$), and quantified in 8% when including the effect of dust on longwave (LW) radiation (Solmon et al., 2008). Santese et al. (2010) used RegCM3 to investigate the direct and semi-direct aerosol radiative effects over Sahara and Europe during two dust outbreak episodes. They found that RegCM3 is able to model the evolution of observed AOD with time for the simulated dust episodes. RegCM3 slightly underestimates (~20%) observed AOD at stations closer to the dust

source region, but this underestimates increases with the distance from dust sources suggesting a somewhat weak long range transport by the model. A study conducted by Malavelle et al. (2011) used RegCM3 to simulate the optical properties and direct radiative forcing of mineral dust over West Africa, and total radiative forcing at ToA averaged for winter was calculated between $-5.25$ and $-4.0$ W/m$^2$ over dark surfaces, and around $-0.15$ W/m$^2$ over bright surfaces. Nabat et al. (2012) tested different parameterizations of dust emission size distribution within RegCM4 (Giorgi, et al., 2012). They showed that, both at episodic and seasonal scale, a new dust distribution (based on an analogy with the fragmentation of brittle materials) improve the AOD and geographic gradients of RegCM4 compared to ground based and satellite observations. They also estimated a 10-years average (2000-2009) SW direct radiative forcing of $-13.6$ W/m$^2$ at surface and $-5.5$ W/m$^2$ at top of atmosphere (TOA) over the Mediterranean Sea.

On the other hand it is hard to simulate atmospheric aerosol concentrations, chemical composition, and optical properties in global and regional climate models (IPCC, 2007). The simulation of atmospheric aerosol concentrations, chemical composition, and optical properties is one of the major uncertainties in global and regional climate models (IPCC, 2007). Both anthropogenic and natural aerosols affect the climate, but it is important to determine the anthropogenic aerosols to understand the effect of human activities on air quality and climate (Solmon et al., 2006). Since the effects of aerosols in regional scale is important, there are tools to evaluate anthropogenic aerosol in high-resolution regional climate models. Regional climate models, which provide better resolution than the global climate models can define the aerosol complexity (Solmon et al., 2006). RegCM3 was tested by Santese et al. for two episodes of mineral dust from Sahara onto the Central Mediterranean, during July 2003, including all aerosols (2010). Another study is done by Zhang et al. (2009) to test the dust aerosol over East Asia. In this study RegCM4.1 is tested only for dust aerosol which has importance to increase PM$_{10}$ concentrations during the spring months over Eastern Mediterranean. It is very significant to show the effect of dust episodes during spring months. Besides, dust episodes are frequent during every season where spring is mostly affected.

Eastern Mediterranean is affected by both anthropogenic and natural air pollution Lelieveld et al. (2002) suggested that, as indicated by several studies (Haywood, and Boucher, 2000 ; Formenti et al., 2001; Andreae et al., 2002). Mediterranean region's

troposphere shows among the highest aerosol radiative forcing over the entire world, especially during summer months. During the MINOS measuring campaign (August 2010, Finokalia, Crete, Greece) they measured at a station located in the center of East Mediterranean a mean contribution of 42% of dust to the total mass of coarse aerosol particles (diameter > 2 μm) and 4% of fine aerosols. From these measurements they estimated a mean radiative forcing from all aerosols of -18 W m$^{-2}$ at surface and -6.6 W m$^{-2}$ at TOA. Several studies, using in-situ observation, showed that high particulate matter concentration is related to increase in Saharan influence in the Eastern Mediterranean Region (Kubilay et al. 2000, 2005; Kocak et al. 2004; Kocak et al. 2007a, b; Kocak et al. 2009). In these studies it is shown that, although Saharan dust transport can occur in every season, dust impact is highest during March, April, May and October. It is also suggested that 70% of these events occur in the transition season and mineral dust episodes tend to last up to 10 days. Chemical composition analysis study in the Eastern Mediterranean conducted by Kocak et al., 2004 show that a) mineral dust burden increases from north to south according to the distance and b) trace elemens (Al, Fe, and Mn) increases around 1.5 and 4 times during the transition season related to the dust transport.

Since dust transport is very important in Mediterranean Region and it is affecting the air quality, aerosol optical properties and radiative forcing, this paper focuses on the effects of dust episodes on PM$_{10}$, aerosol optical properties and radiative forcing over Eastern Mediterranean using the new version 4.1 of RegCM model (Giorgi, 2012). In RegCM4, different soil and soil texture distribution from sub-grid emissions used according to Laurent et al. (2008). Dust emission size distributions are calculated according to Kok (2011), which has 12 more prognostic equations. Model outputs were analyzed for aerosol optical properties and radiative forcing (SW, LW). Results of this simulation are compared with AERONET sun/sky radiometer measurements and satellite data for evaluating the simulated aerosol optical properties.

## 1.5 Purpose and Thesis Plan

Climate modelling studies for Turkey were done at Eurasia Institute of Earth Sciences using RegCM3. In this study, three global climate model's (ECHAM5, CCSM3 and HadCM3) output used to run RegCM3 for the eastern Mediterranean–Black Sea region. Also NCEP/NCAR data were used for the validation of the model. This study showed

that, precipitation was overestimated by the model over the mountains. Winter precipitation and temperature modelled well by three GCM models. Summer precipitation and temperature are also modelled fine with ECHAM5 and HadCM3 (Bozkurt, 2012). It should be noted that these simulations did not include Saharan dust.

In this thesis study the aim is to reduce uncertainty in radiative estimates of climate modelling in inclusion of Saharan dust. For this purpose, RegCM4.1 is used both for short-term and long-term. This is the first modelling study done for Turkey accounting the dust impact on the climate system which has also high resolution. Objective of this study is to identify the effect of mineral dust on air quality and climate of Eastern Mediterranean.
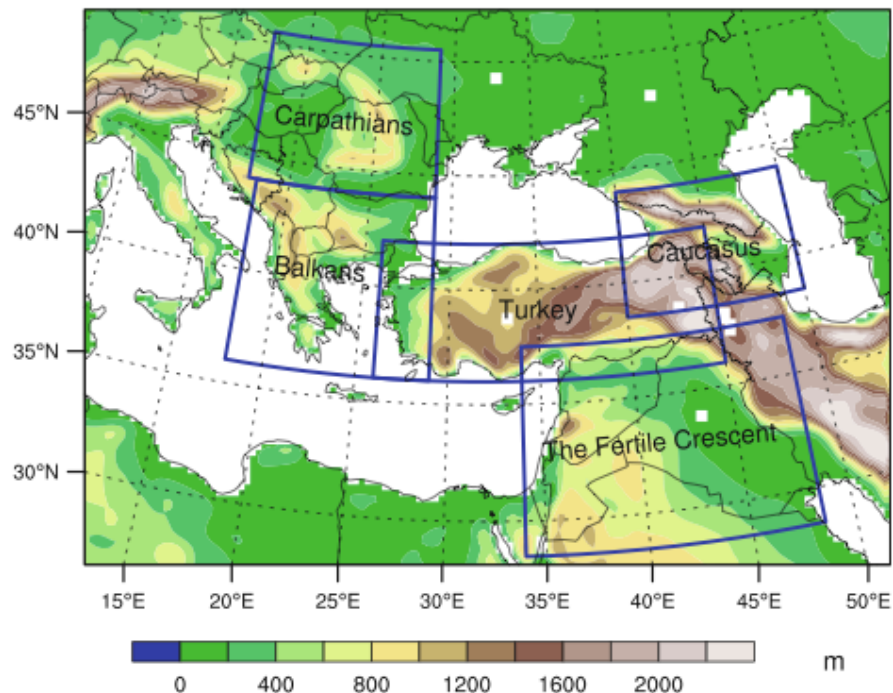


**Figure 1.10 :** Model domain of the study (Bozkurt, 2012).

In the short term study, an episodic study has been done to validate the model and to investigate the effect of dust on air quality. This study is done for March 2008 to show the effect of dust on radiative budget. Results are compared with satellite and Aeronet observations. Aerosol optical properties and radiative forcing (SW, LW) over the region are analyzed. In the long term study, three time periods are selected to be modeled, which are 1991-2000, 2041-2050 and 2091-2100. Then long term simulations are done to analyze the effect of dust on climate. First the past simulations for 1991-2000 then

future simulations 2041-2050 and 2091-2100 are completed. The reference period is taken for 1991-2000. This period is selected to make a selection for ten years periods with a same interval which is not including heat wave effect. The first future simulation is done for 2041-2050 which is the breaking point according to the studies of Gao (2006), Giorgi (2006). The second simulation period shows the end of century which used to be taken as the end period of climate simulations since the ECHAM5 data is available until 2100. Ten years periods are selected which are representing each term, because of the simulations with dust module has high computational cost and also take long time to model. All simulations were done for dust module activated and not activated since it is necessary to show the effect of dust in future.

First of all, the model setup was defined according to the experimental simulations. After defining the model setup, an episodic study was done. This episodic study is an evaluation and validation of the model. Following the episodic study, there is an experiment for the past period as a reference period and two experiments to show the effects of dust on precipitation and temperature, when the region was modelled with and without dust. First experiment is set without dust, which is the reference study for the comparison of mineral dust effect. The second experiment is accounting dust aerosol that shows the effects of mineral dust. RegCM-4.1 was used to simulate the effects of dust over Eastern Mediterranean. There are four different simulation terms, which are an episodic study, and three long term study as shown in the Table 1.4.

**Table 1.4 :** Simulation terms.

| Period | With dust simulation | Without dust simulation |
|---|---|---|
| 21-24 March 2008 | Epidu | Epino |
| 1991-2000 | PRDU | PRnoDU |
| 2041-2050 | NFDU | NfnoDU |
| 2091-2100 | 21DU | 21noDU |

In the second section of the thesis methodology is given. The third section gives the results and discussion, and the last section gives the conclusion and future works.

## 2.  METHODOLOGY

This section provides information on the methodology used in this study. First, RegCM (Regional Climate Model) and its modules are defined. Then the simulation set-up and datasets used for the short term and long term simulations are explained.

RegCM solves the primitive equation in the three-dimensional, sigma-coordinate system. It has been developed at the National Center for Atmospheric Research (NCAR) and improved at the Abdus Salam International Centre for Theoretical Physics (ICTP) (Zakey et al., 2006). The model is generally used for long term regional climate simulations. The first version of RegCM was produced by Dickinson et al. (1989) and Giorgi (1990) then later versions improved, RegCM2 by Giorgi et al (1993a), Giorgi et al. (1993b), RegCM2.5 by Giorgi and Mearns (1999) and RegCM3 by Pal et al. (2007). RegCM4.0 was released in June 2010 and RegCM4.1 was released in May 2011. RegCM4.2 was released in December 2011. In this study RegCM4.1 version is utilized.

RegCM4 has various packages that corporates the physics into the model (Pal et al., 2007). These are the solar and atmospheric radiation schemes described by Kiehl et al. (1996), the land surface processes represented via BATS by Dickinson et al. (1993), the boundary layer processes which uses the non-local parameterization described by Holtslag et al. (1990), the mass flux scheme of Grell (1993), and the sub-grid explicit moisture scheme of Pal et al. (2000). Furthermore, the RegCM4.1 has a new land surface, the planetary boundary layer and air-sea flux schemes, a mixed convection and tropical band configuration. Moreover, it has modifications to the pre-existing radiative transfer and boundary layer schemes and a full upgrade of the model code towards improved flexibility, portability and user friendliness. It is coupled to a 1D lake model, a simplified aerosol scheme (including OC, BC, $SO_4$, dust and sea spray) and a gas phase chemistry module (CBM-Z).

The aerosol model of RegCM4.1 includes sulphur dioxide, sulphate, hydrophobic and hydrophilic carbonaceous particles such as Black Carbon and Organic Carbon and dust particles. The dust emission module is improved by Zakey et al. (2006) following Marticorena et al. (1995) and Alfaro et al. (2001). The dust module of the model

includes the calculation of the emission and the optical properties, wet and dry removal of dust, and the transport of gravitational settling. This process is contingent on the wind conditions, soil characteristics and the particle size. The dust emission calculation is based on the soil aggregate saltation and sandblasting processes. The calculation has four steps, which are the specification of soil aggregate size distribution, the calculation of threshold friction velocity, the horizontal saltation of soil aggregate mass flux, and the vertical transportable dust particle mass flux (Zakey et al., 2006). It is important to define the dust process properly, in order to add dust module to the regional climate model (Elguindi et al., 2010).

There are important modules that include the dust effect in the RegCM model (Zakey et al., 2006). These modules can be activated with the BATS interface, according to the desert and semi desert land cover (Elguindi et al., 2010). As sketched in Figure 2.1, the BATS interface uses the vegetation and interactive soil moisture to modify the exchange of momentum, energy, and water vapour from surface to atmosphere. Then the BATS calculation is performed separately for the subgrid cells and surface fluxes are adapted to the coarse cell for an input to the atmospheric model.
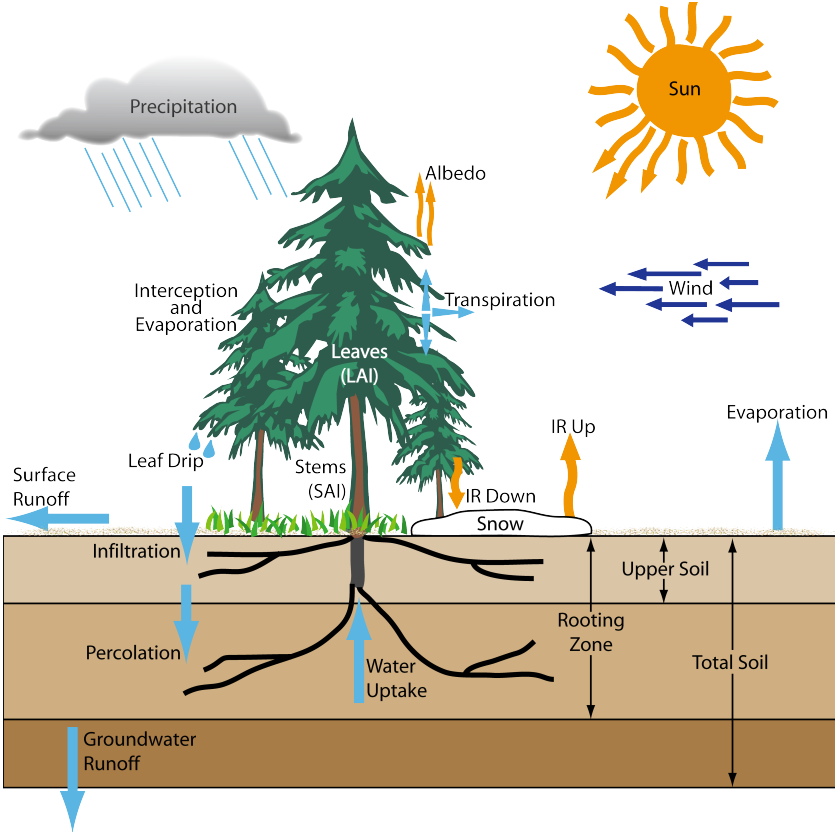


**Figure 2.1 :** Representation of BATS (Url-1).

RegCM4 has two new land use categories for urban and sub-urban environments. It is important to use the urban category to modify the surface albedo and alter the surface energy balance. This also creates impervious surfaces with effect on runoff and evapotranspiration. The vegetation cover, the roughness length, and the soil characteristics can be modified to describe these effects (Elguindi, 2011).

It is essential to include the mineral dust simulation in the climate model since it largely affects the radiative budget of Earth through direct and indirect effects (Sokolik et al., 2001; Tegen, 2003; Balkanski et al., 2007; Nabat, 2012). On the other hand, large uncertainties are associated to the simulation of atmospheric aerosol concentrations, the chemical composition and the optical properties in global and regional climate models (IPCC, 2007). Dust emissions, transport and deposition are simulated in various models in coherent manner (e.g. Guelle et al., 2000; Reddy et al., 2005b; Ginoux et al., 2001; Woodage et al., 2010), while dust burden and dust optical properties showed larger diversity. Huneeus et al. (2011) conducted a model inter comparison study comparing the results of 15 global aerosol model. This comparison showed large differences for simulated aerosol optical depth, within a factor of two, deposition on surface concentrations, within a factor 10. Based on comparison with observations they also suggest that a range of possible emissions for North Africa is 400 to 2200 Tg yr$^{-1}$ and for Middle East is 26 to 526 Tg yr$^{-1}$.

The mineral dust simulation of RegCM4.1 was described in detail by Elguindi et al., 2010, Zakey et al., 2006, Marticorena et al. (1995), and Alfaro et al. (2001). The dust emission process depends on the wind speed, the soil characteristics, and the particle size. The dust is emitted at size bins of 0.01, 1.00, 2.50, and 5.00 micrometers. The dust emission calculations include the soil aggregate saltation, and sand blasting processes. This calculation has several steps, including the specification of the soil aggregate for each model grid cell, the calculation of a threshold friction velocity leading erosion and saltation processes, horizontal saltating soil aggregate mass flux, and vertical transportable dust particle mass flux generated by the saltating aggregates (Elguindi, 2011). These parameterizations can be activated with the BATS interface. The RegCM4.1 mineral dust module has transport, gravitational settling, wet and dry deposition and calculations of optical properties (Zakey, 2006).

There are several developments on the dust module in RegCM. One of these developments is made on the aerosol radiative transfer calculations. RegCM4 has the

infrared spectrum, which has a role on large dust, and sea salt particles while RegCM3 has only the scattering and absorption of shortwave spectrum. Another one is the coupling of aerosols and atmospheric chemistry. There is a continuous development of the aerosol scheme of RegCM so that it can eventually be used for the long term simulations. Solmon et al. (2006) introduce the first aerosol scheme that includes the anthropogenic aerosols. Later, Zakey et al. (2006) developed a 4-bin desert dust module and a 2-bin sea salt scheme. In latest version, the dust emission scheme has a new emission calculation related to the different types of soil and soil texture of Laurent et al (2008) (Giorgi et al, 2012).

The aerosol scheme has different modes that can be selected as neither aerosol, nor dust used; biomass, $SO_2$+BC+OC, no dust; anthropogenic, $SO_2$+BC+OC, no dust; anthropogenic+biomass, $SO_2$+BC+OC, no dust; no aerosol, with dust; biomass, $SO_2$+BC+OC, with dust; anthropogenic, $SO_2$+BC+OC, with dust; anthropogenic+biomass, $SO_2$+BC+OC, with dust. In this study no aerosol with dust choice is activated in order to determine the effect of mineral dust aerosol on air quality and climate.

The RegCM has the preprocessing, the simulation and the post processing steps. The preprocessing step has also several steps that include Terrain, SST, ICBC and Aerosol, respectively. For example, there is a regcm.in file in the binary that is corrected accordingly to the needs of the study. This file will be used to launch all the post-processing steps as well. The first preprocessing step, Terrain, creates the simulation domain accordingly to the setup in the regcm.in file. After terrain is launched a DOMAIN.NC file is created. This file contains the topography and land use databases, projections and land sea mask. After this step, SST is run. SST launches the same regcm.in file and generates the SST.NC file. This step creates the necessary sea surface temperatures for the initial and boundary conditions for selected period set in the regcm.in file. Then ICBC is executed using the same file to generate the initial and boundary conditions for the model. ICBC.date.NC file contains surface pressure, surface temperature, horizontal 3D wind component, 3D temperature and mixing ratio for the selected period and time step in the namelist regcm.in file. After that, AEROSOL component is run with the same namelist file. It produces an AEROSOL.NC file. This file includes the emission dataset. After having all the preprocessing files ready, model can be run. It is necessary to define how many processors are used then the simulation can be started. In this study 16 processors are

used. After the simulation finishes, ATM, RAD, SRF and SAV files are created. Post processing is applied to these files to select necessary parameters and convert the sigma levels to pressure levels. These steps are summarized in the Figure 2.2.
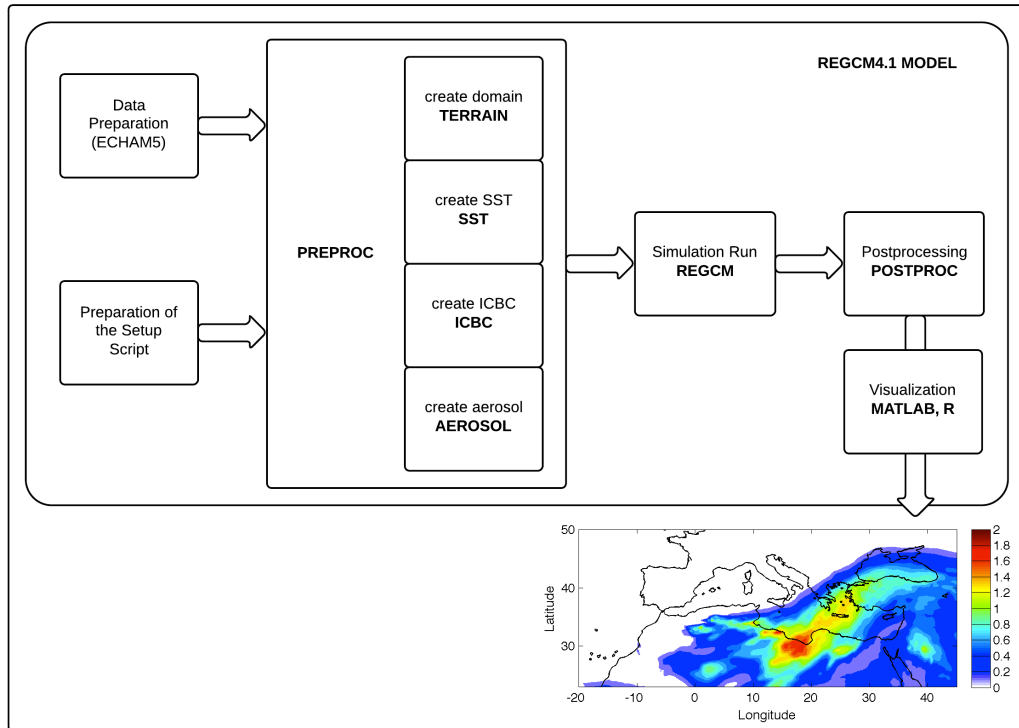


**Figure 2.2 :** Steps of RegCM-4.1 model run.

## 2.1  Simulation Set-up

The model domain includes Northern Africa, the Mediterranean Sea and a part of Europe, extending from about 20°N-50°N and 15°W-45°E, for a total of 128 x 256 grid cells at 27 km spatial resolution using Lambert Conformal projection (central latitude 40 N° and central longitude 20 E°).
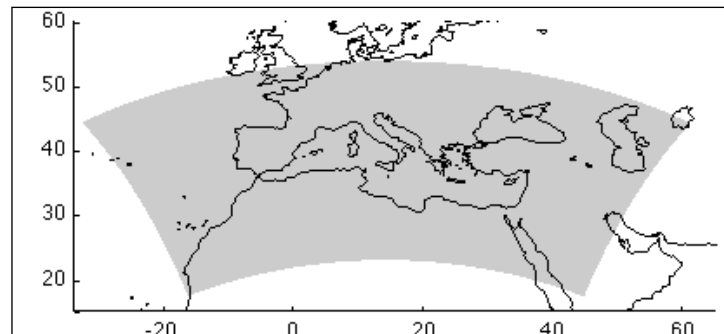


**Figure 2.3 :** Model Domain.

The domain shown in Figure 2.3 is selected according to many different tests of the model for an episodic event. First the episodic event is selected, then dust transport is checked by the satellite image. Many test cases are run in order to do the best model domain set-up. Model domain set-up is selected as reference to the short-term and long-term study, when the simulation outputs give similar pattern with the satellite image.

The domain is discretized using 128 x 256 grid cells at 27 km spatial resolution using Lambert Conformal projection (central latitude 40 N° and central longitude 20 E°). The vertical resolution is 18 vertical layers from surface to 50 hPa. The meteorological boundary conditions are provided to the model from the ECHAM5 A1B scenario simulation without nudging available from its website (Url-2). The land use and the vegetation data are used by the Global Land Cover Characterization (GLCC) data at 30 sec resolution. SST data are obtained using the NOAA Optimum Interpolation. The given set-up of RegCM4.1 is utilized for both the short-term and the long-term simulations. Only the ICBC data is different for short-term study.

### 2.1.1 Short term

Two simulations representing March 2008 are done, which includes a strong mineral dust transport event over the Mediterranean. The first simulation is performed without any aerosol, and the second simulation is performed including only mineral dust aerosol. In order to reproduce the specific meteorological conditions, which generated the selected mineral dust, episode the model is driven by NCEP/NCAR Reanalysis data available at 6-h intervals with a resolution of $2.5^o$ x $2.5^o$ in the horizontal and 18 pressure levels.

### 2.1.2 Long term

In the second phase of this thesis study, a set of decadal simulations are performed, in order to assess the impact of mineral dust on the Mediterranean region for three different periods: present climate conditions (1991-2000); near future climate conditions (2041-2050); end of 21th century (2091-2100). The reference period, 1991-2000, is selected to make a reference period for ten years periods with a same interval. The first future simulation is done for the interval of 2041-2050, which is the breaking point according to the studies of Gao (2006) and Giorgi (2006). The final simulation period shows the end of century, which used to be taken as the end period of climate simulations since the ECHAM5 data is available until 2100. Since the simulations with

dust module has high computational cost and also takes longer simulation time, ten years periods are selected for each term. In order to show the dust effect over the specified periods, all the simulations are done for both dust module activated and not activated.

## 2.2  Datasets

Along with the RegCM4.1 simulations, several different datasets are used for validation, verification as well as in depth analysis. The dust transport is very important in the Mediterranean Region, since it affects the air quality, the aerosol optical properties and the radiative forcing. Therefore, first of all, effects of dust episodes on $PM_{10}$, aerosol optical properties and radiative forcing (both in shortwave and longwave spectrum) over Eastern Mediterranean using the new version 4.1 of RegCM model (Giorgi, 2012) are investigated. In RegCM4, different soil and soil texture distribution from sub-grid emissions used according to Laurent et al. (2008). Dust emission size distributions are calculated according to Kok (2011), which has 12 more prognostic equations. Model outputs are analyzed for aerosol optical properties and radiative forcing (SW, LW). Results of this simulation are compared with AERONET sun/sky radiometer measurements and satellite data for evaluating the simulated aerosol optical properties.

### 2.2.1  Short term

Istanbul is a megacity located in the Eastern Mediterranean; it is the most populated city in Turkey with over 13 million inhabitants (18% of total Turkey population of Turkey, TUIK-Turkish Statistical Institute 2010). Istanbul is highly affected from $PM_{10}$ pollution during winter and spring months. Source of $PM_{10}$ is aerosol from local sources, such as anthropogenic sources from urban and surrounding regions, and natural sources from the forest of Istanbul. Istanbul is also exposed to long-range sources as anthropogenic sources from Europe and natural sources from Saharan Desert (Kindap, 2006). It has been found that Istanbul's background $PM_{10}$ concentration is affected by 0.5-13 %.

This section is focused on the effect of dust episodes on the aerosol optical properties and radiative forcing over Eastern Mediterranean. In this study, the contribution of mineral dust on $PM_{10}$ concentrations in Istanbul is investigated and RegCM4.1 for an

important episode, when there is an increase in $PM_{10}$ levels concentrations significantly, over the region was evaluated. Aerosol optical properties (AOD, SSA) and radiative forcing (SW, LW) over the region are analysed.

$PM_{10}$ measurements, taken from the Turkish Ministry of Environment and Urbanization (National Air Quality Observation Network) are analysed by R studio. The daily mean of $PM_{10}$ data is calculated by taking the average of hourly data of each station. Then mean of the stations were taken to have only one point. This data are evaluated for seven years (2004-2010) according to the EU Council Directive 1999/30/EC. When $PM_{10}$ concentration exceeds 50 $\mu g/m^3$, this day is checked by the DREAM Model of Barcelona Supercomputing Center to see if there is a possible dust event.

**Table 2.1 :** March 2008 Evaluation.

| | 2008 March | | | |
|---|---|---|---|---|
| | $PM_{10}$ | D | Over 50 | Wind |
| 1 | **75.18** | | 1 | SW |
| 2 | 39.02 | | 0 | |
| 3 | **93.41** | | 1 | SW |
| 4 | **72.15** | | 1 | SW |
| 5 | **52.79** | 1 | **1** | SW |
| 6 | **59.65** | 1 | **1** | N |
| 7 | 48.14 | | 0 | |
| 8 | **91.71** | 1 | **1** | SW-NW |
| 9 | **101.81** | 1 | **1** | SW |
| 10 | **68.43** | 1 | **1** | SW |
| 11 | **63.65** | 1 | **1** | S-SE |
| 12 | **97.46** | 1 | **1** | E |
| 13 | **51.99** | | 1 | SW |
| 14 | **56.23** | | 1 | NW-S |
| 15 | **55.45** | | 1 | SW-S |
| 16 | **61.37** | | 1 | SW |
| 17 | **50.62** | 1 | **1** | SW |
| 18 | 46.81 | | 0 | |
| 19 | 49.23 | | 0 | |
| 20 | 49.31 | | 0 | |
| 21 | **58.45** | 1 | **1** | NW-NE |
| 22 | **75.40** | 1 | **1** | SW-E |
| **23** | **139.30** | 1 | **1** | SW-SE |
| 24 | **120.77** | 1 | **1** | SW |
| 25 | 48.62 | | 0 | |
| 26 | 47.92 | | 0 | |
| 27 | **51.41** | | 1 | E-NE |
| 28 | 49.11 | | 0 | |
| 29 | 41.94 | | 0 | |
| 30 | 37.56 | | 0 | |
| 31 | **57.88** | 1 | **1** | N-NW |

Wind direction is also evaluated to check if there is dust transport on that day. Then the final episode is selected according to the highest number of events in months and years. Table 2.1 summarizes the evaluation of March 2008. In this table, $PM_{10}$ indicates the daily average of $PM_{10}$ concentration of Istanbul, D shows the situation of the day, which exceeds 50 $\mu g/m^3$, and wind shows the direction of the wind on the selected day.

The selected episode is simulated by RegCM4.1 with and without the dust module activated. Results of this simulation are compared with AERONET sun/sky radiometer measurements and satellite images of OMI (Ozone Monitoring Instrument) and MISR (Multi-angle imaging spectrometer) for evaluating the aerosol optical properties.

Dream (Dust REgional Atmospheric Model) is a component of the NCEP/ETA model, which predicts the atmospheric life cycle of dust. The first work is done by Nickovic and Dobricic (1996) for developing DREAM Model. Skiron forecasting system is the main atmospheric modeling system in this model. It has been developed to evaluate the dust cycle in the atmosphere. Figure 2.4 shows a dust transport episode on 23th March 2008.
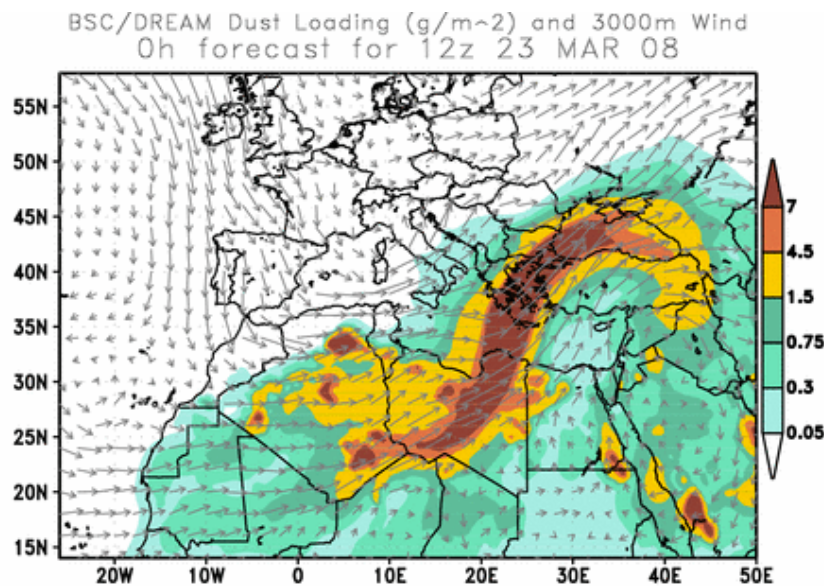


**Figure 2.4 :** Episodic event on 23 March 2008 (DREAM).

## 2.2.2 Long term

Meteorological boundary conditions are provided to the model from the ECHAM5 A1B scenario simulation without nudging available from Url-2. The ECHAM5 data are available at a 6 hours temporal resolution and at 1.875°x1.875° horizontal resolution, with 17 pressure levels. Land use and vegetation data was used by the Global Land

Cover Characterization (GLCC) data at 30 sec resolution. SST data were obtained NOAA Optimum Interpolation.

To assess the model performance of the RegCM4.1 with the dust module for the long-term simulations, the gridded datasets of CRU are used. The data, provided by University of East Anglia, UK (Mitchell and Jones 2005), is available at 0.5° grid spacing over the land areas only.

The dust budget and the radiative forcing are evaluated. Furthermore, the changes in aerosol optical depth, the surface dust emission, the dry deposition, the wet deposition, the column burden, and the short-wave and long-wave at the surface and at the top of the atmosphere are investigated in detail. Temperature and precipitation changes are also defined and discussed.

# 3. RESULTS AND DISCUSSIONS

Results and discussion are given for two different cases in this section. First, results of short-term study are shown in order to investigate the relationship between high $PM_{10}$ concentrations and dust transport using atmospheric modeling, satellite data as well as in-situ observations and determining the aerosol optical properties and direct radiative effects of aerosols for a dust transport episode on 21-24 March 2008. In a second phase, results of long-term study are shown. A comprehensive analysis of the dust budget, including surface emissions, column burden, dry deposition, wet deposition, aerosol optical depth, radiative forcing for present and future climate are presented in this case.

## 3.1 Results for the Short Term Study

Daily $PM_{10}$ concentration distribution for Turkey is shown in Figure 3.1. In 2008 $PM_{10}$ spring concentration is higher than summer and fall concentration. In order to have a detailed research on mineral dust transport episodes, Istanbul megacity is selected since there are long time period observations. A megacity has a total population over 10 million and Istanbul megacity has a 13.710.512 population according to the census of Turkish Statistical Institute (2012). Istanbul is the 23rd megacity based on the population criteria (Url-4).

$PM_{10}$ data is obtained by Turkish Ministry of Environment and Urbanization (National Air Quality Observation Network). Data is evaluated according to the EU directive 1999/30/EC. Annex 4 of this directive regulates the 24 hour limit value for $PM_{10}$ for the protection of human health, as number of days which exceeded 50 $\mu g/m^3$ cannot exceed more than 35 times per year. In this study, the effect of mineral dust on $PM_{10}$ concentration was investigated.

$PM_{10}$ data revealed that winter has the highest $PM_{10}$ concentration over the Anatolian Peninsula (110 $\mu g/m^3$ for 2008, 100 $\mu g/m^3$ for 2009 and 85 $\mu g/m^3$ for 2010). This is due to the fact that, during winter periods activity from anthropogenic emission sources such as residential heating and vehicles are highest. During this period meteorological

conditions also affect the $PM_{10}$ concentration. For example, inversion can be observed frequently. Under normal conditions fall period is expected to have the second highest $PM_{10}$ levels. However in the case of 2008, spring has higher concentration levels as compared to fall (80 μg/m$^3$ for spring and 70 μg/m$^3$ for fall).

In order to investigate this unusual behaviour of $PM_{10}$ concentration, it is hypothesized that dust outbreaks might be the main reason for this increase in $PM_{10}$ concentrations measured during spring 2008 in several stations in Turkey.
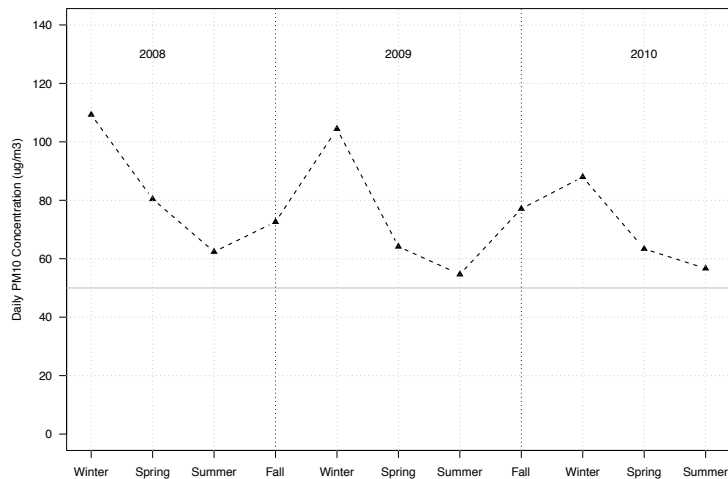


**Figure 3.1:** Seasonal $PM_{10}$ concentration for Turkey.

In order to investigate this hypothesis, $PM_{10}$ measurements are utilized which are conducted for Istanbul (which has the longest record of $PM_{10}$ data). The city has been operating $PM_{10}$ measurement network at 10 different sites since 2004. First the daily $PM_{10}$ data are compared against EU directive of 50 μg/m$^3$ and days exceeding this threshold are identified. Then in order to identify the days with Saharan influence, output of the Barcelona Supercomputing Center - Dust Regional Atmospheric Model (BSC-DREAM8b, Nickovick et al., 2001; Pérez et al., 2006; Basart et al., 2012) is used. BSC-DREAM8b is a dust model based on NCEP/ETA model, aims to predict the atmospheric life cycle of dust, and it is used in several studies to investigate Saharan Dust Transport (Jimenez-Guerrero, 2008; Papanastasiou, 2010; Nastos, 2012).

The number of $PM_{10}$ concentration exceedance days for the city of Istanbul, are provided in Table 3.1, along with information on dust days based on BSC-DREAM8b Model. On the average there are 171 (almost half of the year) days where $PM_{10}$ levels are higher than 50 μg/m$^3$. Analysis reveals that Saharan dust transport occurs on 39% of these days (i.e. 67 days). It should be noted that number of exceedance days and dust

days are different for each year between 2004 and 2010. The highest number of exceedance occurs in 2007 and 2008, where 282 and 200 days are over the limit respectively. These two years also have the highest number of dust days (113 and 77 respectively). For Istanbul, the highest number of exceedance days occurs in spring (49 days on the average), followed by winter (45), fall (41) and summer (36 days). Spring also has the highest dust days with over 58 % of the exceedance days. This number ranges between 50 and 76% for the years 2004 and 2010. These numbers reveal that spring period has the highest contribution from Saharan dust transport, and especially spring 2008 has the most significant dust outbreaks. Therefore, in this study spring 2008 is selected as the main period to be analysed.

**Table 3.1 :** Seasonally dust days and $PM_{10}$ exceedance days in Istanbul.

|  | 2004 | | 2005 | | 2006 | | 2007 | | 2008 | | 2009 | | 2010 | | Average | |
|---|---|---|---|---|---|---|---|---|---|---|---|---|---|---|---|---|
|  | PM | D % | PM | D % | PM | D % | PM | D % | PM | D % | PM | D % | PM | D % | PM | D % |
| MAM | 34 | 56 | 43 | 53 | 48 | 56 | 69 | 55 | 63 | 76 | 43 | 56 | 42 | 50 | 49 | 58 |
| JJA | 12 | 8 | 0 | 0 | 61 | 30 | 92 | 37 | 39 | 28 | 10 | 70 | 38 | 29 | 36 | 33 |
| SON | 29 | 52 | 42 | 29 | 36 | 17 | 75 | 44 | 29 | 55 | 36 | 19 | 43 | 47 | 41 | 38 |
| DJF | 35 | 26 | 45 | 22 | 43 | 19 | 46 | 17 | 69 | 3 | 49 | 47 | 29 | 52 | 45 | 24 |
| Annual | 110 | 40 | 130 | 35 | 188 | 31 | 282 | 40 | 200 | 39 | 138 | 44 | 152 | 44 | 171 | 39 |

In order to make regional analysis, $PM_{10}$ stations other than Istanbul in the Marmara Region and Aegean Region are used in this analysis. Figure 3.2 shows the air quality stations selected to be used in this study. Red circles show the selected stations in Marmara Region and blue triangles show the selected stations in Aegean Region.

High $PM_{10}$ concentrations are observed for the selected regions with values exceeding 50 µg/m$^3$ during March 2008 (shown in Figure 3.3). However the highest level occurs (as high as 180 µg/m$^3$) on the selected episode of 21-24 March 2008 as seen in the Figure 3.3. It should be noted that average $PM_{10}$ concentration for Marmara and Aegean Region behave similarly as they peak on March 24, 2008.
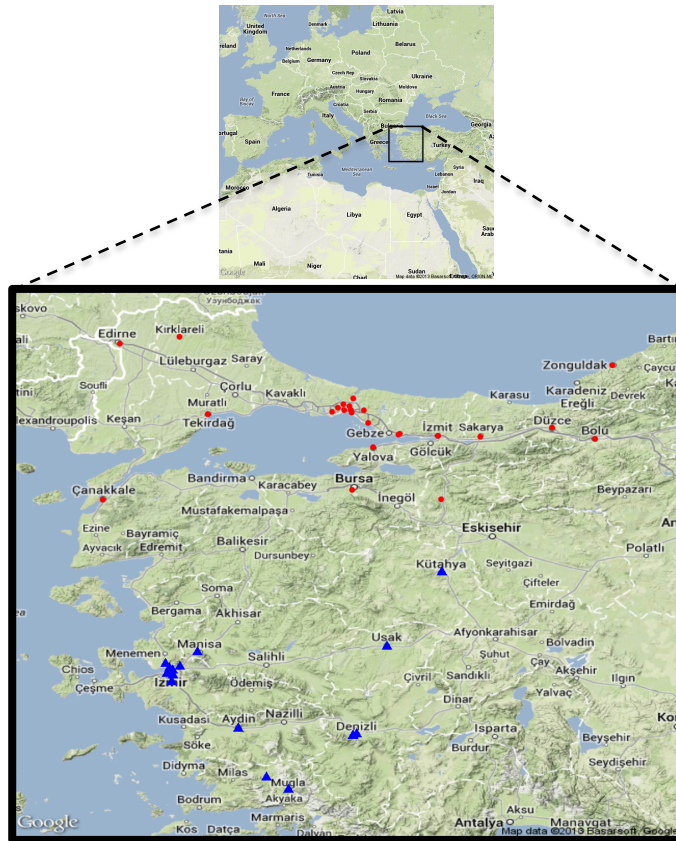
**Figure 3.2:** Stations in Marmara Region are shown by red circles and stations in Aegean Region are shown by blue triangles.
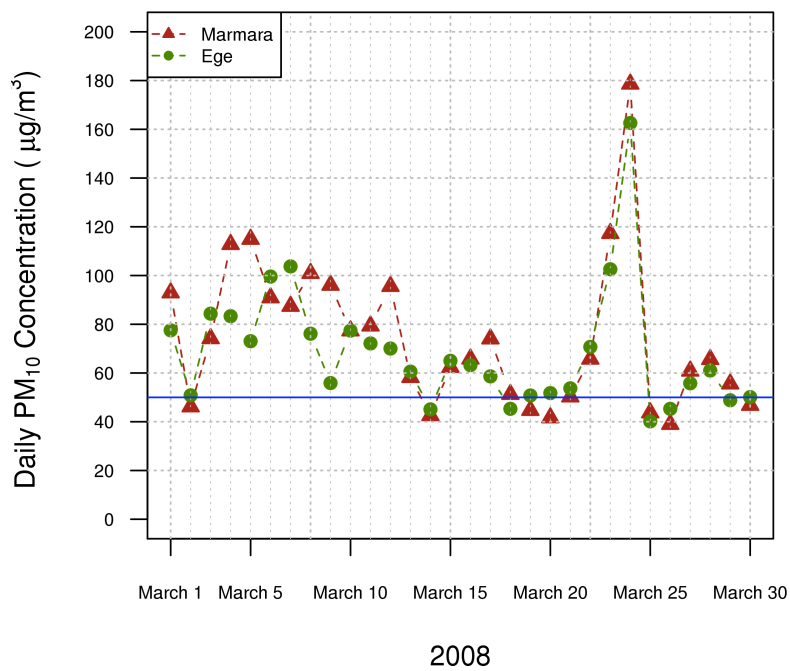


**Figure 3.3:** PM$_{10}$ levels during March 2008 episode.

In order to have an idea about the observations, satellite image was also shown to compare the results visually. Figure 3.4 shows Meteosat-9 Dust RGB Image on 23 March 2008 12:00 UTC. It is seen that dust lifted from Libya and transported by the southwesterly wind to Greece, Turkey and Eastern Bulgaria. Green plume shows the dust transport over Turkey. As it is seen from the Figure 3.4, dust emissions are mainly originated from Libya in this episode. Dust transported to Greece, Turkey and Eastern Bulgaria passing through Mediterranean Sea, Crete and Aegean Sea and reaching to Marmara Region with a mean column burden up to 2 g/m$^2$ over Marmara Region.
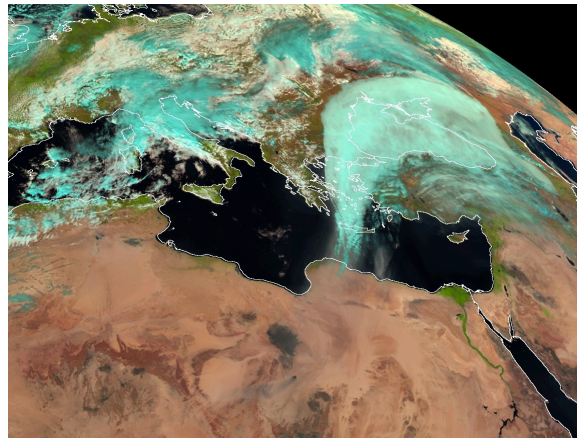


**Figure 3.4:** Saharan Dust transport to Istanbul on 23 March 2008 at 12:00 UTC Satellite Image Met-9 RGB NIR1.6, VIS0.8, VIS0.6 (Url-3).

Figure 3.5 shows the DREAM Model output for the same day, in which dust transport observed also according to the satellite image retrieved by Met-9. DREAM Model can model the dust transport similar to the satellite image. The dust pattern simulated by RegCM4.1 is similar to the satellite observations from Meteosat-9 (Figure 3.4). Column burden corresponds to the mineral dust concentration peak reaching the Eastern Mediterranean is similar to the satellite image and also DREAM output.
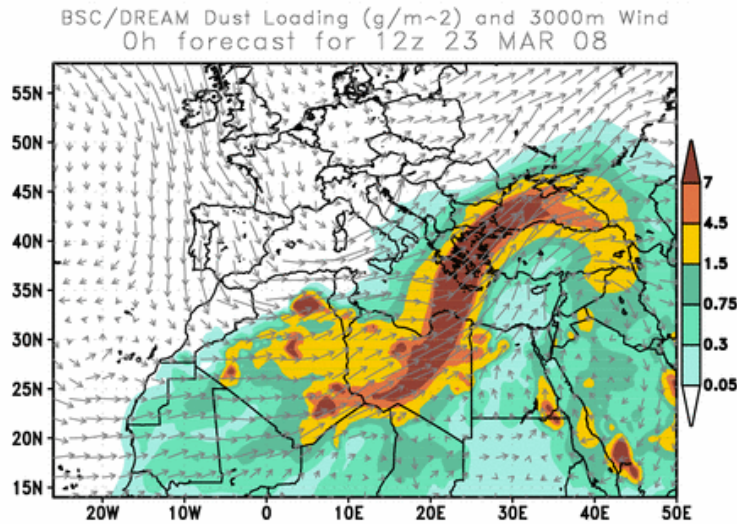
**Figure 3.5:** BSC-DREAM8b Model Output for 23 March 2008.

### 3.1.1 Meteorological situation

In order to understand the dust transport mechanism, meteorological conditions should be evaluated. There are different wind systems over Mediterranean Sea (Kubilay, 1997). Westerlies, easterlies, and the coastal land-sea breezes are common in summer and autumn. Local winds poyraz and sirocco are important in winter and spring (Özsoy, 1981). In late winter and spring southwest flow along the North African coast is most frequent and in winter and spring south and southwest flow from the north of African continent is most frequent (Dayan, 1986). It causes important dust episodes during spring affecting the Eastern Mediterranean Region.

In order to show the meteorological conditions affecting the selected time period, NCEP data are used for spring 2008. One of the important parameters, sea level pressure provides us to get information about meteorological conditions at surface. Therefore, it makes easier to interpret dust pattern behaviour. Mean sea level pressure for spring 2008 given in Figure 3.6 shows that air mass moves from high pressure to low pressure. So that higher SLP over Atlantic leads the air mass to move west. Saharan dust transports by this pressure system especially during spring months.
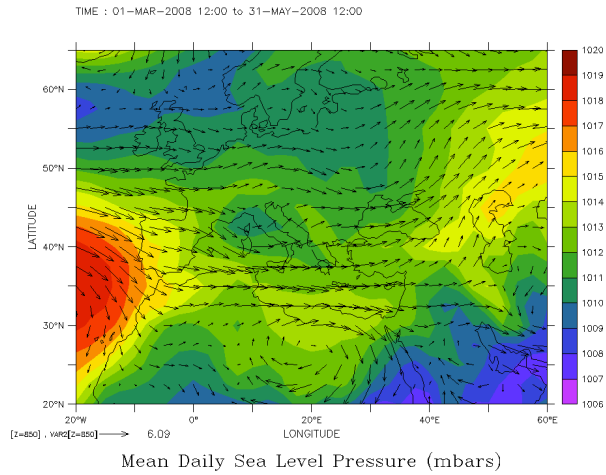
Mean Daily Sea Level Pressure (mbars)

**Figure 3.6:** Sea level pressure at spring 2008.

Figure 3.7 shows wind direction at 850 mbar on 23rd March 2008. It is seen that there is tunnel effect because of the temperature difference between southeast and southwest which leads dust to be carried to Anatolian Peninsula. Westerly winds changes to south westerly over Libya, which transports dust from Libya to Anatolian Peninsula and north of it.
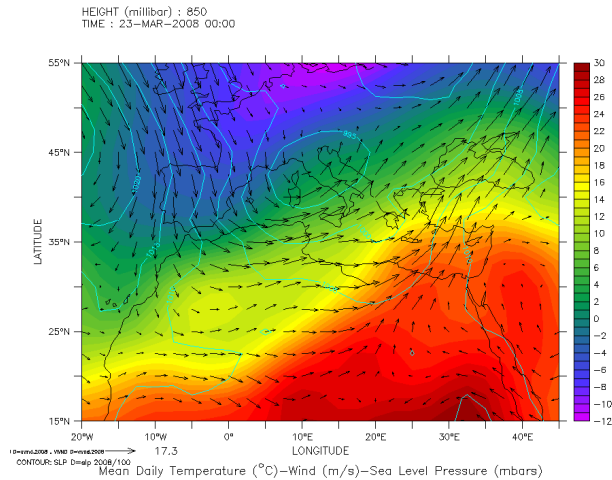


HEIGHT (millibar) : 850
TIME : 23-MAR-2008 00:00

Mean Daily Temperature (°C)-Wind (m/s)-Sea Level Pressure (mbars)

**Figure 3.7:** Wind direction and temperature at 850 mbar
at spring 23 March 2008.

Vertical condition of the atmosphere is also important that helps to explain how far dust transports vertically in the atmosphere.  Thus, the skew-T diagram is used to show the vertical structure of the atmosphere in Istanbul on 23 March 2008. The increase in the temperature with height shows that there is inversion. On this day, inversion occurs at 665 m height.
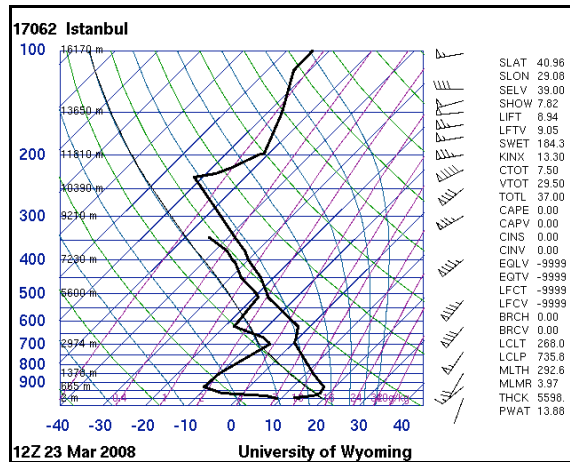
**Figure 3.8:** Vertical distribution of temperature in Istanbul on 23 March 2008, 12z by Radiosonde of University of Wyoming.

Model results obtained by RegCM4.1 were investigated and also compared with the observations. Figure 3.9a shows the daily mean temperature and wind direction at 850 mbar for 12z at 23 March 2008 as the model output. Figure 3.9b shows the daily mean temperature and wind direction at 925 mbar for the same time. It can be seen from these figures that there is a south westerly current because of the temperature difference.
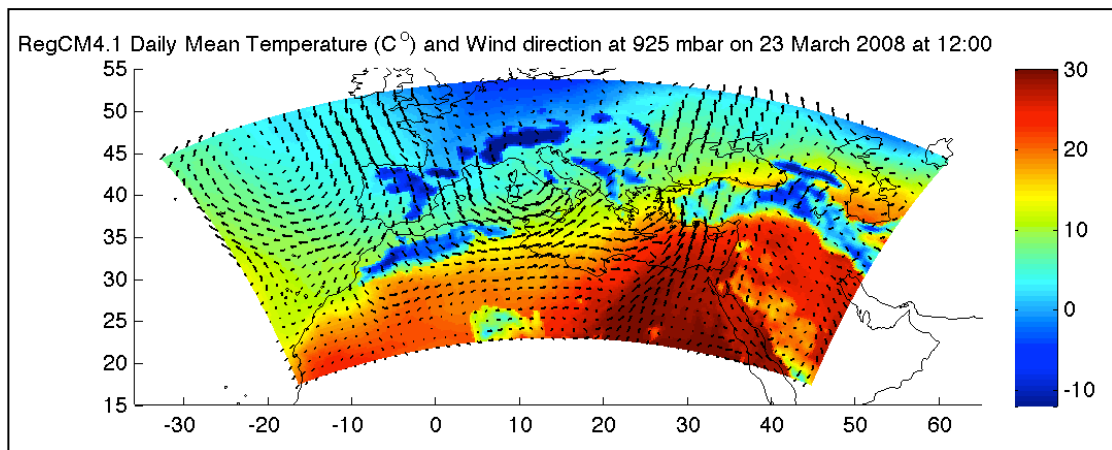
**a)**
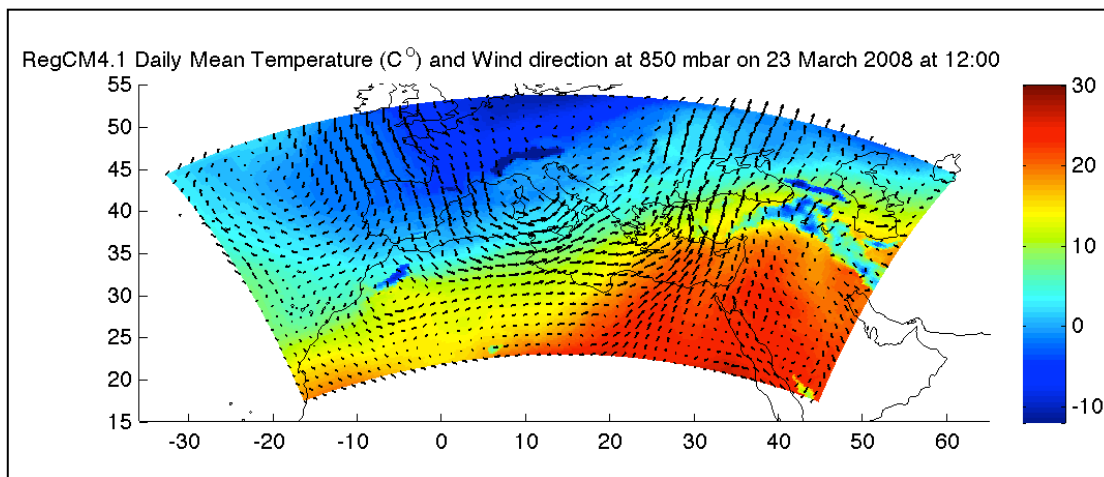
**b)**



**Figure 3.9:** Daily Mean Temperature and Wind direction at 850 and 925 mbar for 12z 23 March 2008.

### 3.1.2 Model performance

In order to have idea about the microphysical properties of dust particles, observation at different locations is necessary (Tafuro et al., 2006). Aerosol optical depth is an important parameter to investigate the effect of aerosol on radiative forcing. Instrumental design, calibration, and good identification of clear sky conditions determine the quality of the data (Dubovik et al., 2000). The Aerosol Robotic Network ground based aerosol monitoring network (AERONET, Holben et al., 1998), was developed by NASA. Automatic sun-sky scanning spectral radiometers are used by this network to provide globally distributed near-real time observations of aerosol optical depth and aerosol size distributions (Dubovik et al., 2000). AERONET has more than 300 sites all over the world (Holben et al. 1998, 2001).

In this study Level 2 Aeronet data were used (i.e., pre and post field calibrated, automatically cloud cleared and manually inspected) for Sevastopol (44.62 N°, 33.52 E°) and Eilat (29.50 N°, 34.92 E°). For Erdemli (36.56 N°, 34.25 E°) station Level 1.5 data (i.e., Real Time Cloud Screened data but may not have the final calibration applied) are used, as Level 2 data are not always available. Figure 3.10 shows the locations of the stations selected.

**Figure 3.10:** Locations of selected stations (Map provided by INEG Image NASA Terra Metrics 2014).

Figure 3.11 shows the corrected AOD values for 550 nm for the AERONET stations for the selected period and stations: a) Erdemli; b) Sevastopol; and c) Eilat along with RegCM outputs. It should be pointed out that AERONET doesn't provide AOD measurements at 550 nm, the Angstrom wavelength exponent $\alpha_{440-870}$ has been used as a conversion factor to calculate the AOD at 550 nm. AOD at 440 nm and $\alpha_{440-870}$ are provided by the AERONET measurements, then AOD at 550 nm is calculated by the following formula: $AOD_{550} = AOD_{440}\, e^{\,-\alpha_{440-870}\,\ln(550/440)}$

Figure 3.11 shows the observed and simulated AOD time series for Erdemli station, which is located in South Turkey and among the selected AERONET station it is the closest to the pathways of Saharan dust transport episodes. Between March 1st and 20th, there is high correlation between model and observations as RegCM values follow the observations, even capturing the small peak around March 8th. Then largest peak occurs between March 20th and 25th both for the observations and RegCM outputs, which corresponds to a main dust transport episode hitting the Anatolian peninsula, simulated also by the BSC-DREAM8b model and with high $PM_{10}$ concentrations measured in the Marmara and Aegean regions (Figure 3.3). For this period, RegCM overestimates AOD by 18% on the average (ranging between 9 percent to almost 40 percent). Overall, the

correlation between the model and the observations were significant as the correlation coefficient was estimated to be 0.6.

Figure 3.11b present the results for Sevastopol, which is located in Ukraine on the northern coasts of Black Sea. The model results seem to have similar pattern as compared to the observations. As two peaks where AOD values are the highest were also captured by the model (March 7-11 and March 24-25). It should be noted that Sevastopol station has 14 out of 30 days measurements during March 2008 and this significantly reduces model performance analysis for this site.

Eilat station (Figure 3.11c) is located in Israel and thus East of the considered dust transport pathways and with possible influences from dust emissions from the Arabian Peninsula. The model captures more than 60 percent variability in the data (correlation coefficient between model and observations are estimated to be 0.63). It should also be pointed out that, both for the model and observations, the largest peak at Eilat occurs at March 17-18, which is not the same dust episode originated from North Africa that resulted in high $PM_{10}$ concentrations in Marmara and Aegean regions, but very probably originated from the Arabian peninsula (BSC-DREAM8b, Figure 3.6).

Analysis of these results suggests that RegCM captures the temporal variation in the observation and hence can be used to understand dust transport towards the Eastern Mediterranean. On the other hand we generally observed an AOD overestimation of the model during the main dust episodes. Aerosol Optical Depth (AOD) results obtained by the RegCM model for the selected episode, are discussed in the following section.
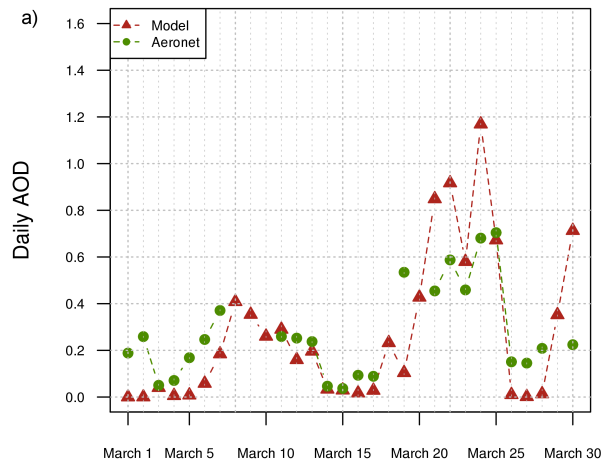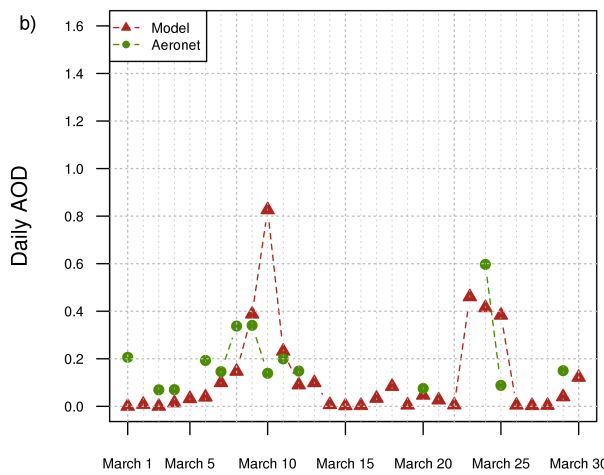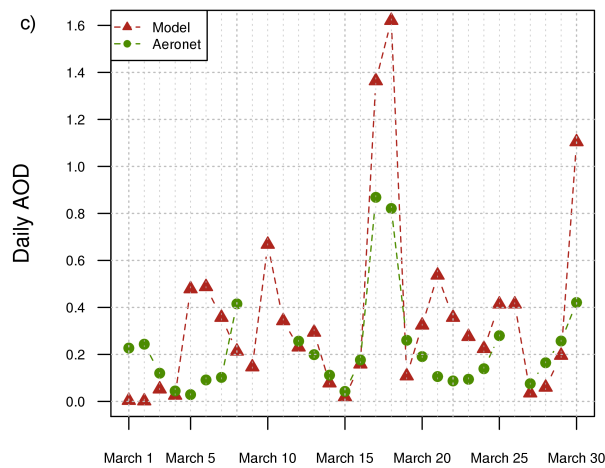
**Figure 3.11:** Corrected AOD values for 550 nm for different Aeronet stations
(a) Erdemli (b) Sevastopol  (c) Eilat.

### 3.1.3 Episode analysis

An important problem for understanding the contribution of aerosols to radiative processes occurs due to the lack of information on macrophysical and microphysical properties of aerosols. Aerosols macrophysical properties such as sources, sinks, and loading and microphysical properties such as composition, size distribution, chemical interaction, lifetime, and diurnal variation gives significant information to determine the effects of aerosols (Dubovik et al., 2000).

Figure 3.12 shows the AOD distribution over the Mediterranean as simulated by RegCM for the main dust transport episode (21-24 March 2008) to the Anatolian peninsula. On March 21$^{st}$, AOD values over central Algeria (Northwest of Hoggart Massif in southeast Algeria) were highest reaching values over 2.0 (Figure 3.12a). This region is one of the main dust sources in Sahara. It should also be pointed that AOD values over 1 are observed over the Eastern Mediterranean, reaching as far as Crete and Southwest Anatolia. In clear-sky conditions the AOD is generally less than 0.1, while AOD values larger than 1 corresponds to hazy conditions due to high aerosol concentrations. Therefore, the model suggests there is an ongoing significant transport of dust on the first day. On the second day (March 22$^{nd}$, Figure 3.12b), the peak AOD values seem to disperse over Algeria and there is a transport of dust towards East. The dust intrusion over Anatolia still continues on the second day reaching values as high as 1. On the third day (Figure 3.12c), the model suggests that the peak values of AOD are over Libya and the values over the Aegean Sea and western Anatolia are highest. On the last day (Figure 3.12d), the dust intrusion seems to disperse and AOD values are less than 1.0 over most of the region.

At it can be seen in Figure 3.5, Meteosat-9 Dust RGB Image was given for 23 March 2008 12:00 UTC. It shows that dust is lifted from Libya and transported by the south westerly wind to Greece, Turkey and Eastern Bulgaria. Green plume shows the dust transport over Turkey. This figure supports model's findings the dust transports towards western Anatolia.
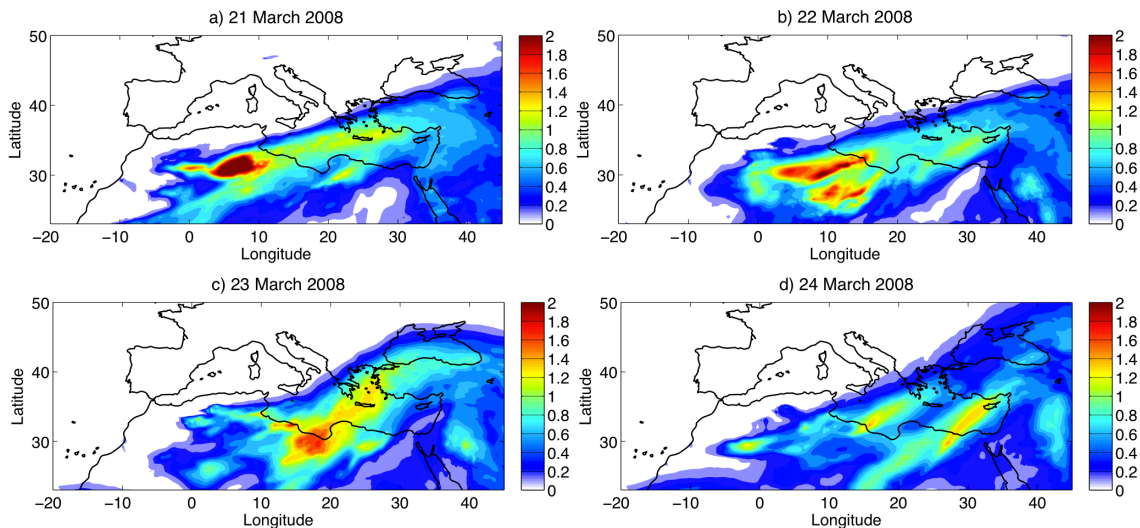
**Figure 3.12:** Daily mean aerosol optical depth during the episode.

Ozone Monitoring Instrument (OMI) is an instrument from Netherlands's Agency for Aerospace Programs (NIVR) with the Finnish Meteorological Institute (FMI) to the Aura Mission, which classifies aerosol types, and can measure cloud pressure and coverage. It is possible to have tropospheric ozone from this data. Total ozone and other parameters concerning ozone chemistry and climate, recorded by TOMS, and are recorded by OMI. Instruments on the Aura platform interact with OMI measurements. Solar backscatter radiation in the visible and ultraviolet wavelength is observed by OMI's hyperspectral imaging (Url-3). OMI follows NASA's TOMS and ESA's GOMES, which measure more parameters than TOMS with a better resolution. OMI has an important role on monitoring of ozone layer. The total column amount of atmospheric ozone $NO_2$, atmospheric dust, smoke and other aerosols are measured by OMI (Url-3).

OMAERUVd, provides information on aerosols, has a resolution of 1.00 x 1.00 degree grid has been used for this study. Aerosol Extinction Optical Depth at 500 nm and aerosol single scattering albedo at 500 nm were plotted for the comparison. Figure 3.13 shows the mean daily aerosol optical depth from the model and OMI output. Model shows the source region in Sahara similarly to the satellite image. Also, aerosol optical depth is over 1 in the model and satellite image. However, model does not capture the source region in the southeast, and dust transport is not observed in the OMI output because of the possible cloud cover.
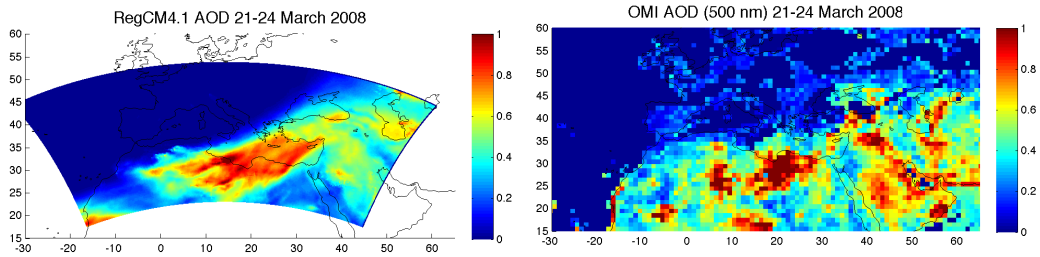
**Figure 3.13:** Daily mean aerosol optical depth during the episode.

In order to understand the interaction of aerosol and processes, global satellite data is an important tool, but not enough (Tanre et al, 1997). Following the improvements on aerosol optical depth, uncertainties in aerosol transport is reduced by MISR and MODIS instruments (Kahn, 2010) which lead to reduce the uncertainty of aerosol effects on climate (IPCC, 2007). Aerosol Optical Depth (AOD) at 550 nm by MODIS (Figure 3.15) shows the dust transport from Libya to Anatolian Peninsula. AOD has a value up to 0.9. There is no image over Turkey because of the cloud formation over the region.
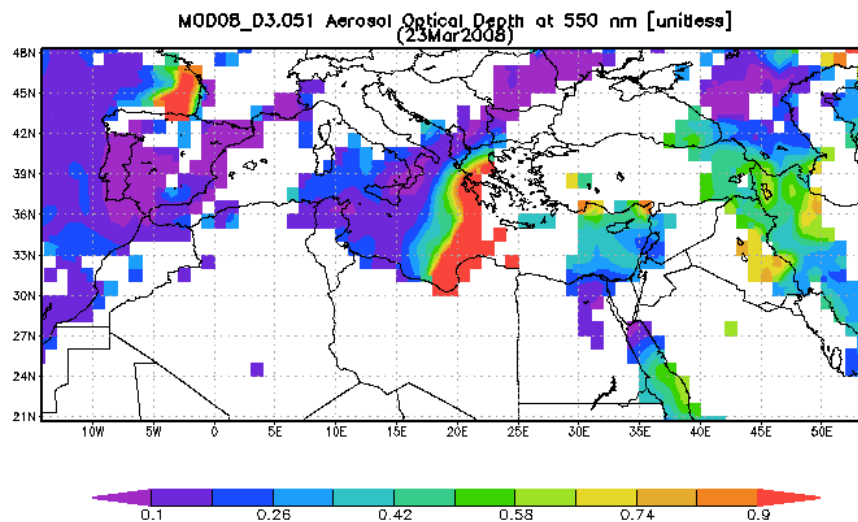


**Figure 3.14:** Modis Satellite Image on 23rd March 2008.

According to the regression analysis between daily AOD and $PM_{10}$ levels for March 2008 over three regions, $R^2$ resulted over 0.4 for March. Figure 3.15 shows the time series for $PM_{10}$ concentrations versus AOD values for the three different regions over Turkey. It can be seen that there is high variability in AOD during the month. There is a high correlation between $PM_{10}$ and AOD during the episode in the three regions.
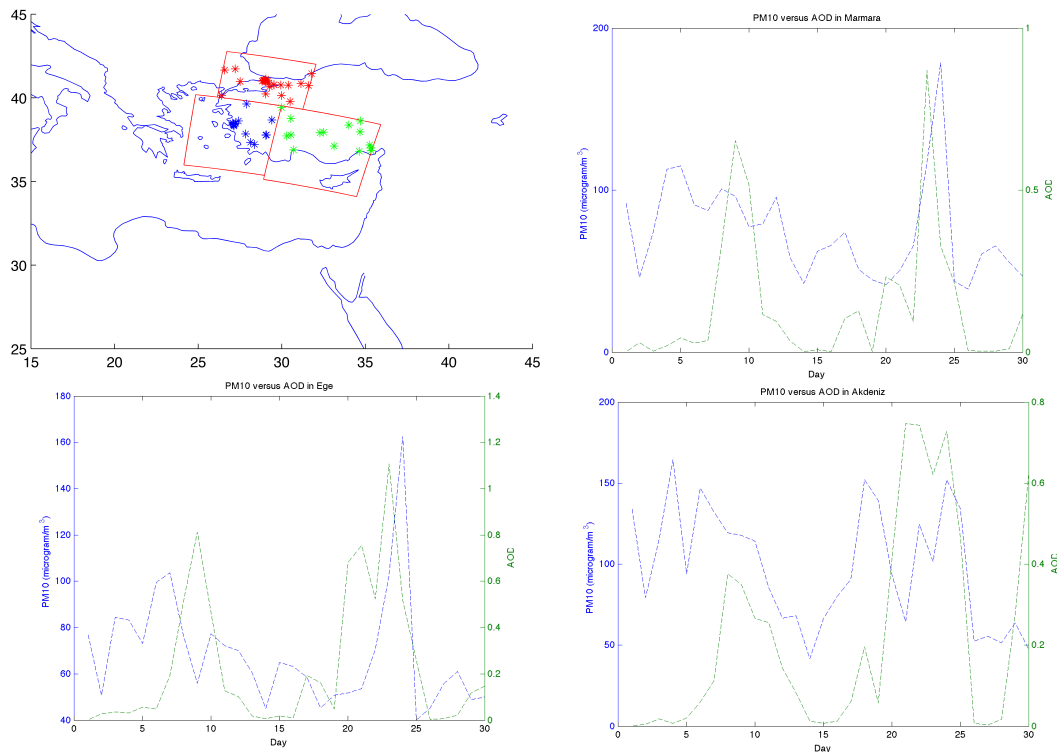
**Figure 3.15:** PM$_{10}$ versus AOD for three regions.

Simulations, conducted by RegCM4.1 provide AOD (350-640 nm model band) values ranging between 0.09 and 0.87 in Marmara, 0.52-1.11 in Ege, 0.62-0.75 in Akdeniz during the episode. Dust transport on 21$^{st}$ and 22$^{nd}$ March 2008 affects the Central Anatolia with 0.9 daily mean AOD value. On 23th March 2008, the dust plume reaches the Marmara Sea and AOD increases up to 1 over the region according to RegCM4.1 model outputs. AOD is generally less than 0.1 under the clear-sky conditions while it is larger than 1 corresponds to hazy conditions due to high aerosol concentrations. Although AOD is high over the regions during 7-8-9 March, PM$_{10}$ levels are not as high as the second episode in the month (Figure 3.15).

The single scattering albedo (ω) is the fraction of light extinction that is scattered by a particle, is ranging from 0 (absorbing particle) to 1 (scattering particle) where the asymmetry parameter (g) is the average direction (angle) of the scattering. Single scattering albedo is 0.93 and asymmetry parameter is 0.62 on average during the episode, which means Saharan dust is highly scattering and leads forward scattering.

Figure 3.16 shows the corrected SSA (single scattering albedo) for Barcelona (41.39 N°, 2.12 E°). Parameter for the 550 nm wavelength has been calculated using linear interpolation between 440 nm and 675 nm values. Single scattering albedo for Barcelona station is in the confidence range. On the other hand, this station was not

affected by the dust episode. But it was used to check the clear sky conditions. So that this station was taken as a validation point. Red line shows the model output and blue points show the observations.
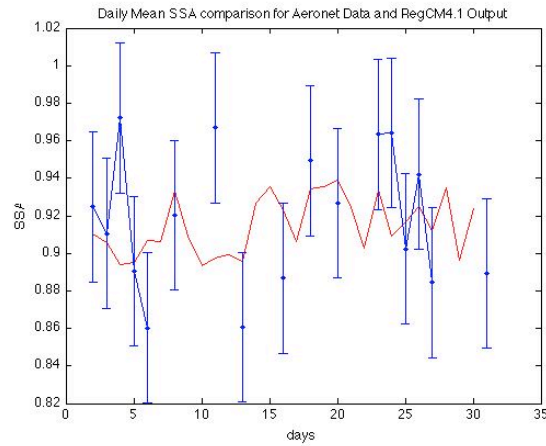


**Figure 3.16:** Corrected SSA values for 550 nm for Barcelona for Level 1.5.

The time series of simulated column burden as mg/m$^2$ averaged over the selected regions (i.e., Marmara and Aegean) are given in Figure 3.17. During most of the month March column burden values are less than 100 mg/m$^2$ for both Marmara and Aegean (Marmara has a median value of 23 and Aegean has a median value of 60 mg/m$^2$). However, in the second week (between March 8$^{th}$ and 10$^{th}$) both Aegean and Marmara regions have column burden values over 200 mg/m$^2$.
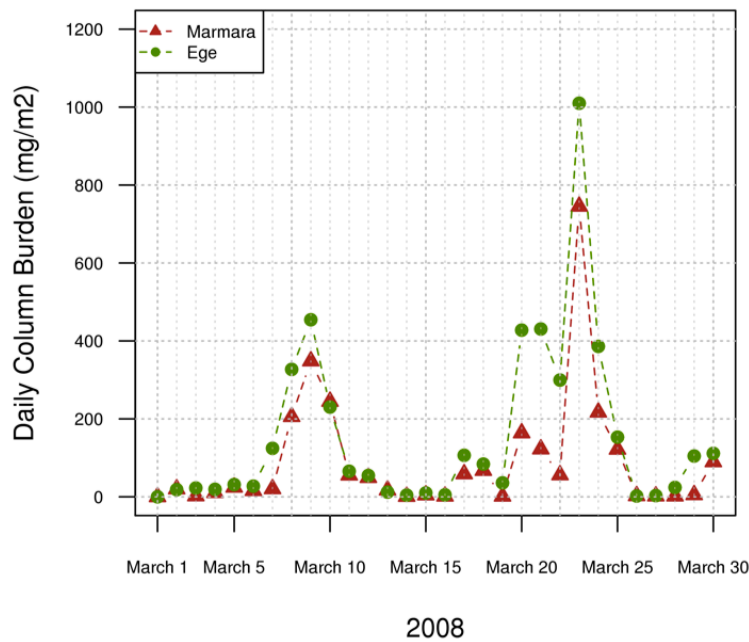


**Figure 3.17:** Daily and Regional Mean Column burden at March 2008.

The peak occurs on March 23rd for both regions with a column burden value over 600 (1009 mg/m$^2$ for Aegean and 745 mg/m$^2$ for Marmara).

According to the simulated daily dust burden averaged over the different regions, the mean burden on 23 March is larger than 1 g/m$^2$ in the outflow of Libya, 0.6 g/m$^2$ over Greece and 0.7 g/m$^2$ over Marmara, 1 g/m$^2$ over Ege, and 0.4 g/m$^2$ over Akdeniz. Total column burden is 152 g/m$^2$ in Marmara, 309 g/m$^2$ in Ege, 160 g/m$^2$ in Akdeniz, 675 g/m$^2$ in south and 165 g/m$^2$ over Greece on 23th March 2008. On the same day Marmara has 0.09 g/m$^2$, Ege has 0.20 g/m$^2$, Akdeniz has 0.13 g/m$^2$ dry deposition on 23th March 2008.
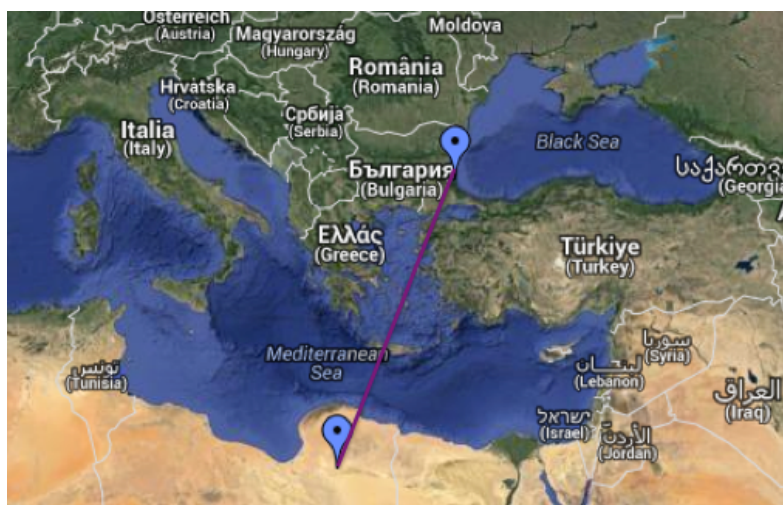


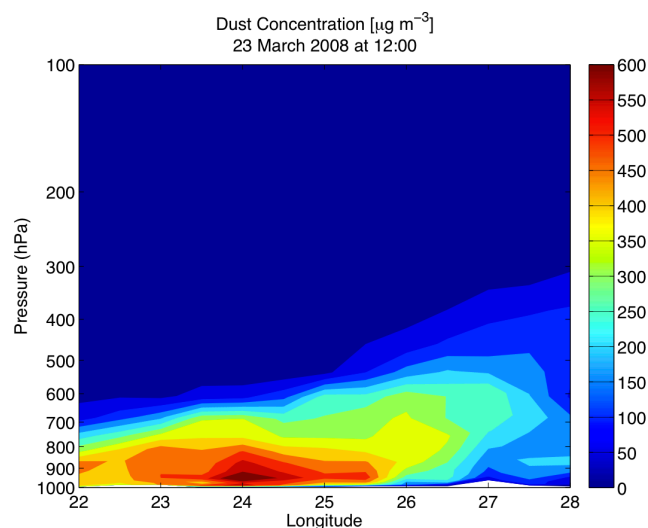**Figure 3.18:** Cross section from Libya to Istanbul.



**Figure 3.19:** Vertical cross section from Libya to Istanbul on 23$^{rd}$ March 2008 at 12:00.

Figure 3.18 shows the selected coordinates Libya [22 N, 30 E] to Istanbul [28 N, 42 E] to give the dust concentration in vertical cross section. Figure 3.19 shows the vertical cross section of dust concentrations along this line on 23rd March 2008.

As it is seen from the figure, dust concentrations are higher near the surface at the source region and lifting up by the south westerly wind and transports to the Marmara Region on 23rd March. Dust concentration is around 500 µg/m$^3$ from Libya to Crete near the surface, below the 850 hPa. Then the dust plume is lifted up to 500 hPa with 200 µg/m$^3$ and surface concentrations reaching Istanbul were below 100 µg/m$^3$.

### 3.1.4    Mineral dust direct radiative forcing

Aerosol direct radiative forcing (RF, e.g. IPCC 2001; Forster et al. 2007) is a measure of radiative impact caused by an external perturbation introduced into the system, due to changes in aerosol concentrations. In this section we analyse the effect of a mineral dust outbreak from Saharan desert into the Mediterranean. Figure 3.20 shows the shortwave direct radiative forcing at surface and at TOA due to the dust transport peaking on the 23$^{rd}$ March 2008.
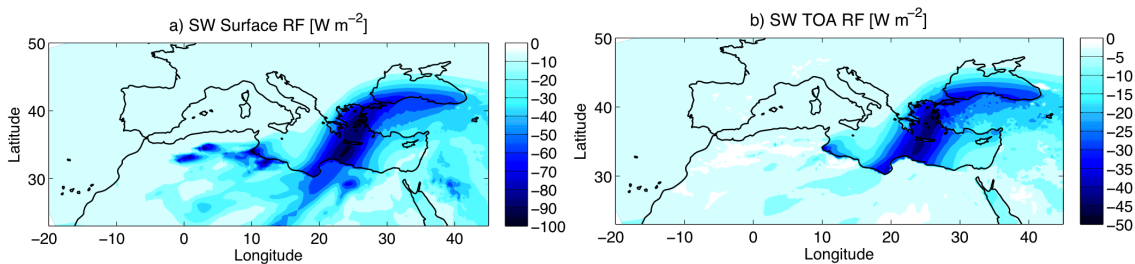


**Figure 3.20: a)**Daily mean SW forcing at surface    **b)** at ToA.

At surface the peak in mineral dust concentrations (Figure 3.12) over the Eastern Mediterranean produces a cooling with a daily mean SW radiative forcing up to -90 W/m$^2$ at surface and -40 W/m$^2$ at TOA. The evolution of the episode in terms of surface concentration, burden, and aerosol optical depth averaged over two regions of the Anatolian peninsula is summarized in Table 3.2, the SW and LW radiative forcings are listed in Table 3.3. In the Marmara region aerosol radiative forcing reaches -62 W/m$^2$ at surface and -29 W/m$^2$ at TOA on 23 March 2008, when AOD is 0.87 and dust burden more than 700 mg/m$^2$. The effect of dust in the Aegean region is larger, the average AOD in the region is 1.11 on March 23$^{rd}$, and the dust burden is over 1000 mg/m$^2$. In this region the SW radiative forcing reaches -71 W/m$^2$ and -33 W/m$^2$ at surface and TOA, respectively. The forcing efficiency at surface is calculated as the ratio between

surface radiative forcing and aerosol optical depth. Forcing efficiency is between -39.7 W/m$^2$ and -71.1 W/m$^2$ in Marmara region during the dust episode. These values are in the range of what found by Santese et al. (2010), where two different dust outbreaks in the Mediterranean were analysed. Santese et al. (2010) estimated a daily-mean SW surface forcing efficiency of -76 W/m$^2$ and -80 W/m$^2$ for two episodes, corresponding to direct radiative forcings at surface of -24 W/m$^2$ and -25 W/m$^2$ and the AOD of 0.52 and 0.54. The forcing efficiency at TOA is ranging between -23.9 W/m$^2$ and -33.2 W/m$^2$ in the Marmara region and between -14.9 and -33 in the Aegean region. Santese et al. (2010) shows smaller daily-mean SW direct radiative forcing, -3.4 W/m$^2$, and forcing efficiency, -6.5 W/m$^2$. The radiative forcing of mineral dust at the TOA is more sensitive to surface albedo, with opposite signs over bright surfaces like a desert and dark surfaces like ocean and deciduous forests. Averaging over a large domain, all Mediterranean basin, like in Santese et al. (2010), compared to an average over a small region mainly only over land, may produce the differences in SW radiative forcing and forcing efficiency at TOA between these two studies.

Table 3.2 : Atmospheric properties during the episode.

| Ege | PM µg/m$^3$ | AOD | Std | Mean Dry Deposition mg/m$^2$ | Std | Mean Column Burden mg/m$^2$ | Std |
|---|---|---|---|---|---|---|---|
| 21-Mar | 53.7 | 0.75 | 0.07 | 50.41 | 14.07 | 430.6 | 31.25 |
| 22-Mar | 70.71 | 0.52 | 0.17 | 42.28 | 30.15 | 299.67 | 92.84 |
| 23-Mar | 102.56 | 1.11 | 0.33 | 201.13 | 193.74 | 1009.9 | 337.39 |
| 24-Mar | 162.57 | 0.52 | 0.26 | 188.99 | 128.12 | 386.06 | 223.62 |
| Marmara | | | | | | | |
| 21-Mar | 50.24 | 0.21 | 0.04 | 37.21 | 14.88 | 122.52 | 24.37 |
| 22-Mar | 65.75 | 0.09 | 0.05 | 10.69 | 4.92 | 56.12 | 31.22 |
| 23-Mar | 117.31 | 0.87 | 0.38 | 96.67 | 104.6 | 745.37 | 386.94 |
| 24-Mar | 178.61 | 0.33 | 0.18 | 138.41 | 110.1 | 217.08 | 116.27 |

The coarse fraction of mineral dust particles has absorbing properties in the infrared wavelengths, thus impacting the long-wave radiation budget (Figure 3.21). In our simulation the LW aerosol radiative forcing at surface was quantified around 6.9 W/m$^2$ and 10.7 W/m$^2$ over Marmara and Aegean regions, when averaged at dust peak day, and ranging between 0.5 W/m$^2$ and 4.1 W/m$^2$ during the entire episode, which is in the range of the values estimated by Santese et al. (2010). The corresponding LW forcing efficiency, which is the radiative forcing divided by AOD, at surface ranges between

5.5 W/m$^2$ and 10 W/m$^2$ over the Marmara and Aegean regions. A good agreement between our study and Santese et al. (2010) is also found for LW radiative forcing at TOA, which is ranging between 0.5 W/m$^2$ and 4.4 W/m$^2$ during peak dust concentrations, with LW forcing efficiency at TOA of 1.5 – 4.6 W/m$^2$.
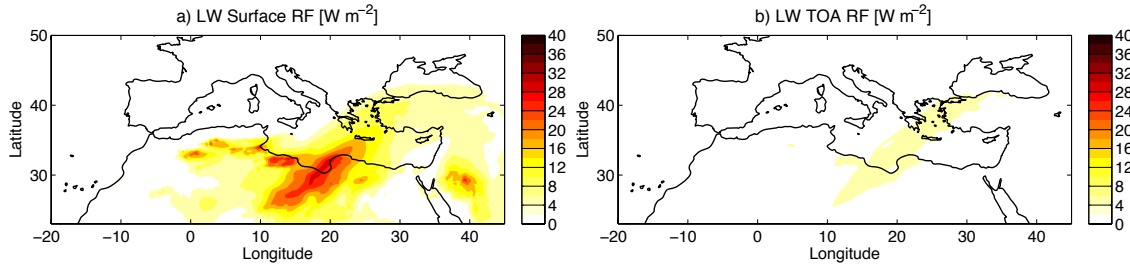


**Figure 3.21:** a) Daily mean LW forcing at surface    b) at ToA.

**Table 3.3 :** Radiative properties during the episode.

| Ege | SRF LW W/m$^2$ | FE | TOA LW W/m$^2$ | FE | SRF SW W/m$^2$ | FE | TOA SW W/m$^2$ | FE |
|---|---|---|---|---|---|---|---|---|
| **21-Mar** | 4.12 | 5.49 | 2.16 | 2.88 | -41.99 | -55.99 | -23.48 | -31.31 |
| **22-Mar** | 3.2 | 6.15 | 1.17 | 2.25 | -25.65 | -49.33 | -14.92 | -28.69 |
| **23-Mar** | 10.68 | 9.62 | 4.39 | 3.95 | -71.4 | -64.32 | -33.01 | -29.74 |
| **24-Mar** | 5.19 | 9.98 | 0.75 | 1.44 | -32.92 | -63.31 | -17.74 | -34.12 |
| **Marmara** | | | | | | | | |
| **21-Mar** | 1.26 | 6 | 0.64 | 3.05 | -11.95 | -56.9 | -6.97 | -33.19 |
| **22-Mar** | 0.51 | 5.67 | 0.19 | 2.11 | -3.57 | -39.67 | -2.15 | -23.89 |
| **23-Mar** | 6.89 | 7.92 | 3.99 | 4.59 | -61.86 | -71.1 | -28.83 | -33.14 |
| **24-Mar** | 3.11 | 9.42 | 0.5 | 1.52 | -15.55 | -47.12 | -8.92 | -27.03 |

In order to understand the dust effect over the region, RegCM was also performed without dust module. Daily average temperature in Figure 3.22 indicates that because of the high concentration decrease in dust source is higher than the other regions. Dust causes around 1.5 C° degrees decrease over the source region. Moreover, the region influenced by the dust source for example, west of Turkey, gets cooler during the dust episode. Daily average temperature in Istanbul decreases around 1 C°. Therefore, mineral dust causes temperature decrease since it has scattering feature. Mainly, dust load causes temperature decrease, over the source regions.
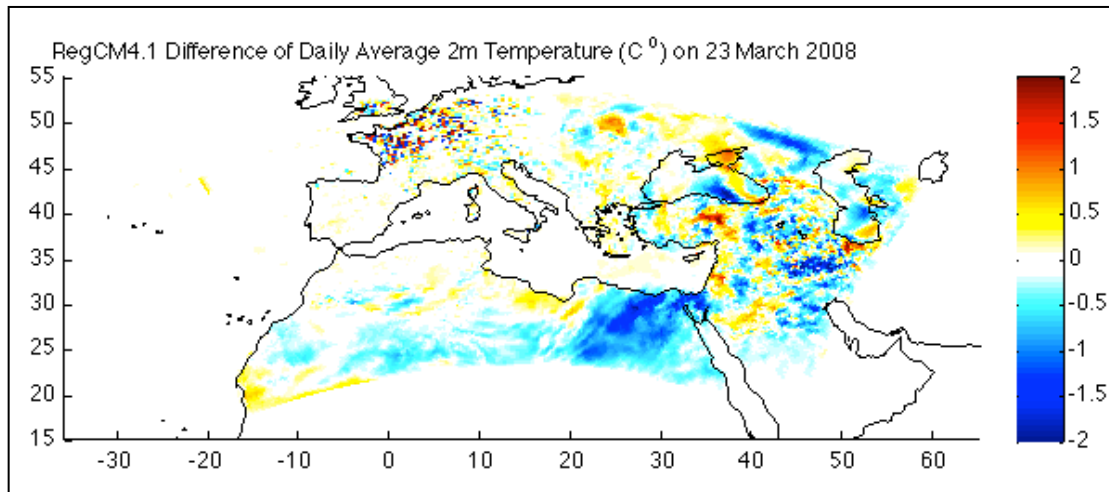
**Figure 3.22:** Daily Temperature Difference for two simulation (Dust − Nodust).

Figure 3.23 summarizes the short-term case study visually. First PM$_{10}$ concentrations were prepared and evaluated according to the EU legislation, and then it is also investigated according to the DREAM Model. The model was run and two different simulations were completed. Satellite images were compared to the model outputs, and also AERONET observations were compared to the model outputs. All analyses were conducted by using R and Matlab programs.
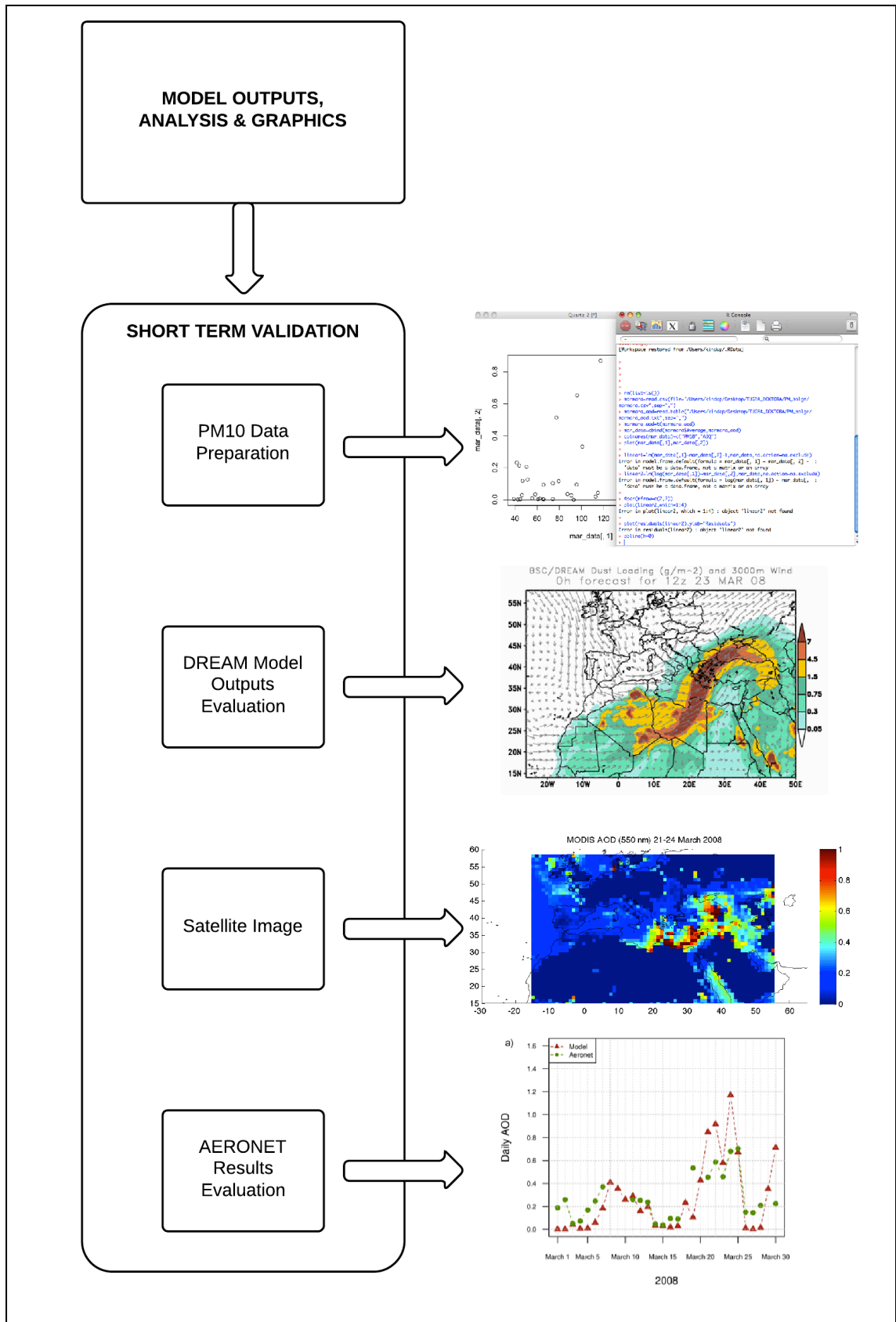
**Figure 3.23:** Summary of the short term case study.

## 3.2 Results for the Long Term Study

The emissions and transport of dust from Sahara to Europe depend on meteorological conditions, therefore climate change can affect the sources of mineral dust and its transport pathways. On the other hand dust has also an effect on climate by modifying the radiative budget in the atmosphere. In this section, results for present and future climate dust budget and climate are given.

The objective of this study is to identify the effect of mineral dust on the climate of Mediterranean. In order to quantify this effect, three 10-years time periods (1991-2000, 2041-2050, and 2091-2100) were simulated with the regional climate model RegCM-4.1.1. ECHAM5 A1B scenario (the rapid economic growth, and balanced energy sources) was used to provide boundary and initial conditions to RegCM-4.1.1. In order to show the effect of dust on climate, the RegCM-4.1.1 model was performed with and without dust module for each 10-year period.

**Table 3.4 :** Name of the simulations

| Period | With dust simulation | Without dust simulation |
|---|---|---|
| 1991-2000 | PRDU | PRnoDU |
| 2041-2050 | NFDU | NFnoDU |
| 2091-2100 | 21DU | 21noDU |

### 3.2.1   Downscaling of ECHAM5

ECHAM5, data are prepared by MPI at Hamburg (for IPCC AR4): available from 1941 to 2100, T63 (1.875°x1.875°, 17 pressure levels, in compressed binary format. In order to evaluate the model for long-term study, RegCM-4.1.1 uses ECHAM5 data as initial-boundary conditions. Resolution of ECHAM5 is around 200 km, which is not good enough to capture the surface features for the study domain.  In this step data were prepared to the model run by running the ICBC as explained in Section 2 (Figure 2.2).

Figure 3.24 shows the difference in temperature between ECHAM5 (input) after processed by ICBC and RegCM4.1 (output) for January and July no dust conditions. In this figure, it can be seen that high altitudes and coastlines have less temperature during January according to the model output. Raw data gives 2°C higher temperature over Turkey in January. The entire coastline has higher temperature according to the raw data. Model outputs give higher temperature over the Saharan Desert around 1°C. Temperature is lower along the coastline during July according to the model outputs that improved land-sea mask by the model might be the reason. Raw data gives around

1 °C less temperature over Turkey in July. Coastlines have lower temperature and Saharan Desert is also 1 °C colder according to the model outputs.
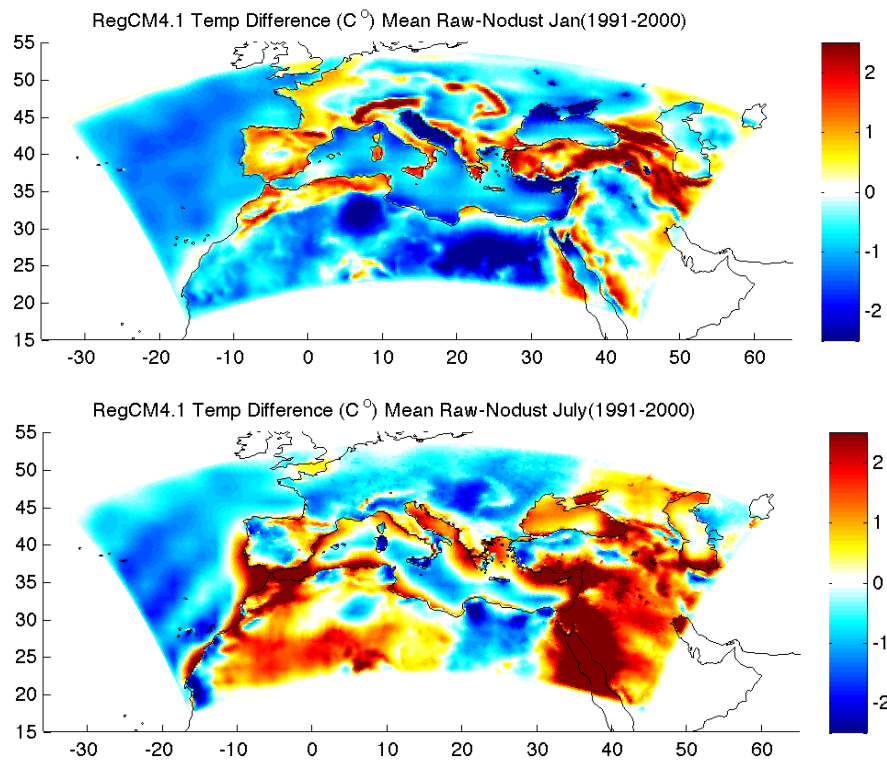


**Figure 3.24:** Mean temperature difference between ECHAM5-RegCM4.1.1 for 1991-2000.

### 3.2.2 Model performance

In order to assess the model performance, 10-year average monthly precipitation and temperature data were analyzed on both seasonal and annual time averages. Taylor diagrams (Taylor 2001) summarize the overall model performance that computes the root mean square difference (RMSD), variability and pattern correlation between the model outputs and observation. The gridded datasets of Climate Research Unit (CRU) of the University of East Anglia, UK (Mitchell and Jones 2005) were used as observation. The CRU data are available at $0.5^o$ grid spacing over the land areas. Therefore, model simulation outputs were interpolated to the CRU grids, and the grid points over the seas are masked accordingly. Since the model domain is quite large, we particularly focus on eastern Mediterranean and Sahara regions.

Figure 3.25 shows the Taylor diagram for temperature and precipitation over the Eastern Mediterranean (blue dots) and Saharan (red dots) regions on seasonal and annual time averages. Radial and angular coordinates correspond to the magnitude of

standard deviation and correlation against the observation, respectively. Distance from reference point indicates RMSD between model and data.

Model simulations indicate a decent agreement with the observation as they are close to the reference point (Figure 3.25a). Pattern correlations are ranged between 0.95 and 0.99 for the both two sub-domains. RMSD indicates quite small values for both sub-domains, however, Eastern Mediterranean region has relatively smaller RMSD.

In contrast to temperature, the Taylor diagram for precipitation identifies that model simulations have highly distributed structure (Figure 3.25b). The pattern correlations for the sub-domains lie in the range between 0.6 and 0.9. However, the variability in the Eastern Mediterranean region is higher than those in Sahara region. Moreover, RMSD in the Eastern Mediterranean is large compared to the Sahara region. These findings are related with the remarkable contrasting features in topography, land-sea boundary and landscape in the eastern Mediterranean region, in which local climate features are predominantly controlled by these features.

In Figure 3.25, the radial distance from the origin gives the standard deviation, the distance from reference point gives the RMSD, and the angular coordinate gives the correlation. RMSD is normalized by the standard deviation of the observation. The numbers represent the seasonal (1-4) and annual (5) means for the eastern Mediterranean (blue dots) and Sahara (red dots).
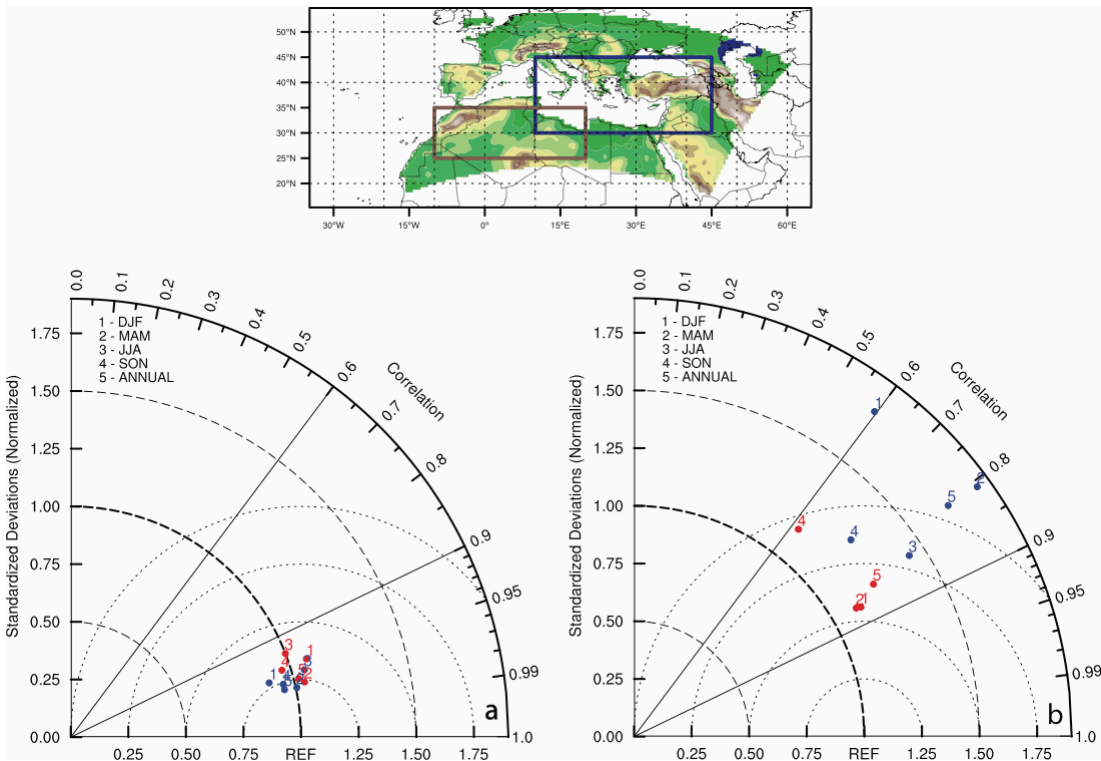
**Figure 3.25:** Taylor diagrams of 10-year averaged temperature (a) and precipitation (b) for the model simulations**.**

### 3.2.3   Average Sea Level Pressure

Figure 3.26a shows the mean sea level pressure (SLP) and wind directions in the 1991-2000 according to the ECHAM5 A1B scenario. Figure 3.26b shows the difference of SLP and wind speed between 2041-2050 and 1991-2000. Figure 3.26c shows the SLP and wind speed differences between 2091-2100 and 1991-2000.

It can be seen that Azores High causes a westerly wind in 1991-2000 period, which transport dust to the east. In the second period, dust transports back to the west and goes to Atlantic Ocean that causes a decrease in dust over Turkey. Since the Azores High strengthens in the future period, dust transports to south and because of the low-pressure system on Africa, dust transports to west. This meteorological situation explains all the dust processes, which will be given in the following section.
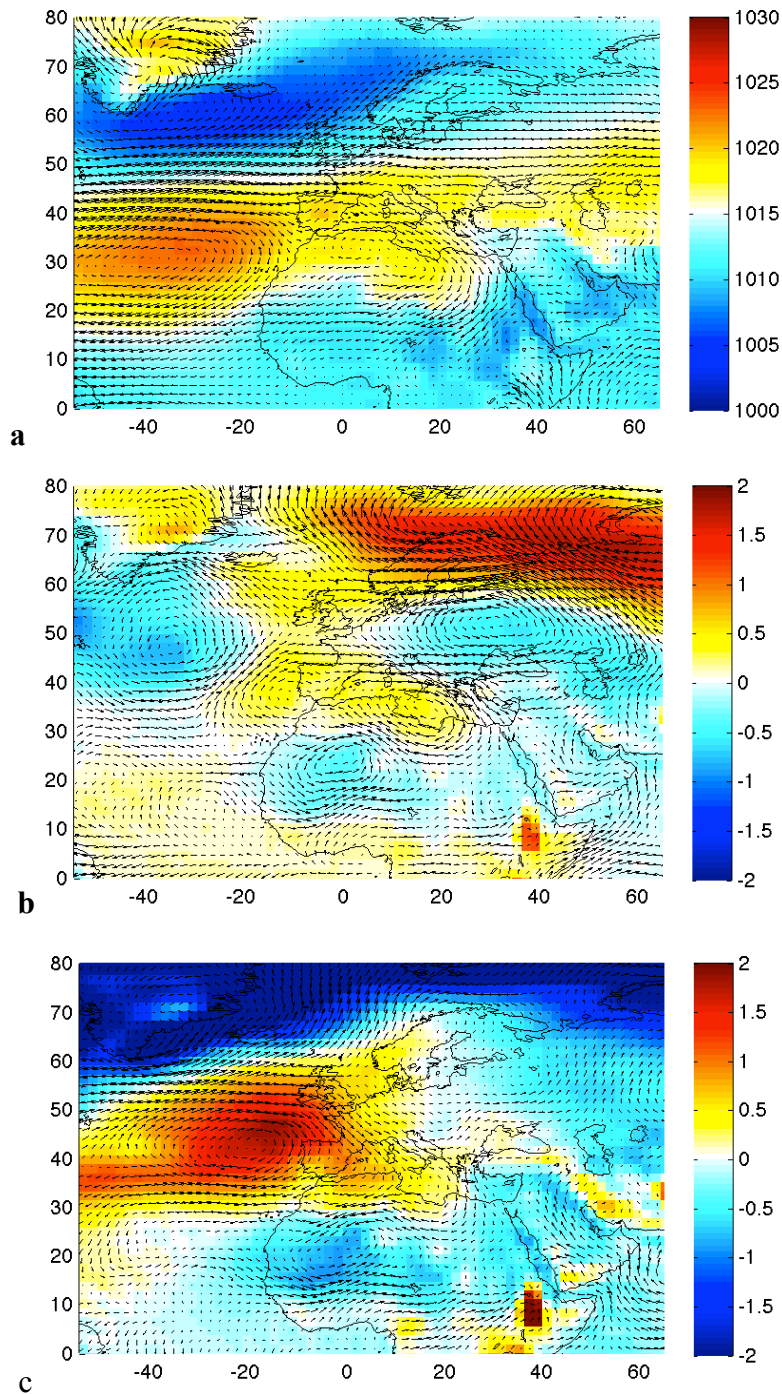
**Figure 3.26:** Mean sea level pressure (hPa) according to ECHAM5.

### 3.2.4 Dust budget

Amount of dust transport may change according to the change in the climate (e.g. precipitation, wind stress, humidity, and changes in the dust sources). Dust source is important which may change by change in land cover because of anthropogenic changes and climate change (Harrison, 2001). Anthropogenic way is the change by human; for example the land use changes modifiy the surface and change climate, which alters the

dust emissions. Besides size bin is also important for emissions (Seinfeld, 2006). In this section, the dust budget (Surface emissions, dry deposition, wet deposition and column burden) for the present, near future and future period are presented for all of dust bins.

Figure 3.27 shows mean surface emission for 1991-2000 calculated by averaged 6 hourly values for each month and then all these monthly values are averaged. According to the PRDU simulation, surface emissions are more than 2000 mg/m$^2$-day dust on the north of Saharan desert. South of the Saharan desert has a surface emission in the range between 500-1500 mg/m$^2$-day. Syrian Desert has a surface emission around 700 mg/m$^2$-day and Nefud Desert has a range between 1800-2000 mg/m$^2$-day surface emission.
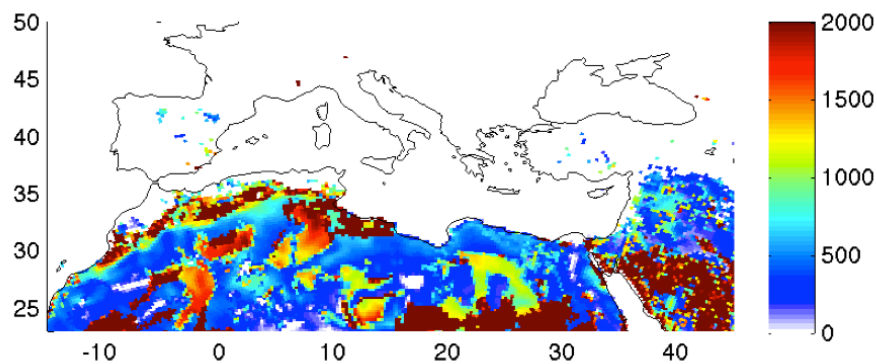


**Figure 3.27:** Mean surface emission for 1991-2000.

Figure 3.28 shows the differences between near future and future conditions between present conditions for the mean surface emission. According to the differences of NFDU and PRDU simulations, there is a slight decrease on the north part of the African continent and also an increase on the south of the continent around 10%. Surface emission decreases up to 10% on the east of Turkey.

Surface emission decreases on the northern part of African Continent and increases on the southern part of Saharan Desert from PRDU to 21DU. In 21DU simulation, surface emission decreases up to 10% on the north of Africa and increases up to 10% in the Saharan Desert. This shift can be explained by the intense Azores High that transports the dust to the south.
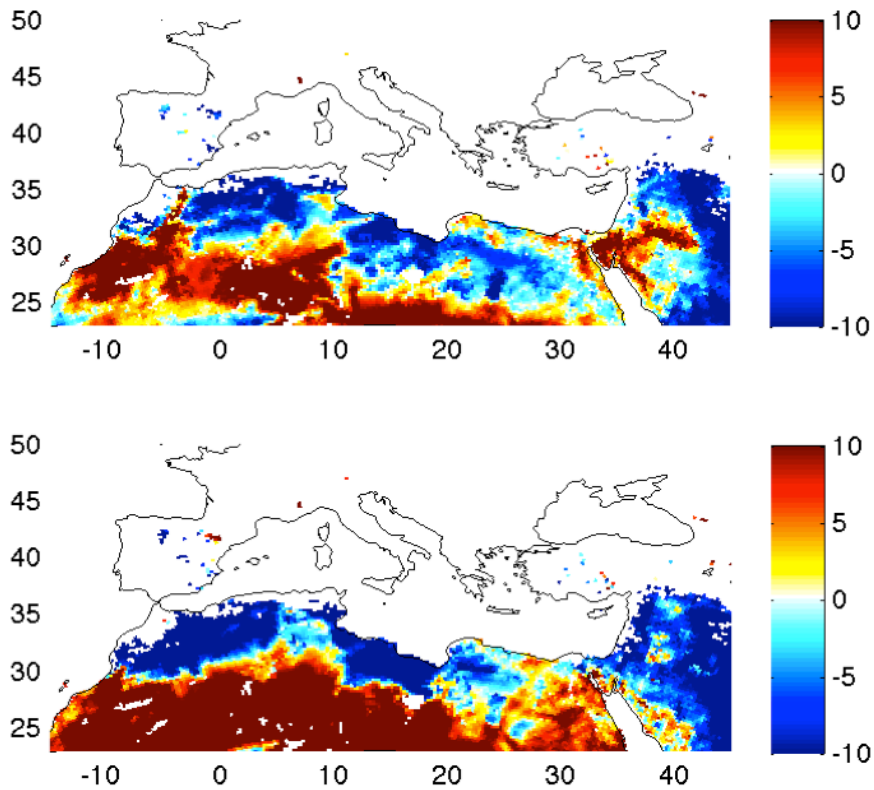
**Figure 3.28:** Change in mean surface emission (%)
a) 2041-2050-1991-2000  b) 2091-2100-1991-2000.

Figure 3.29 shows the time series of surface emissions with upper and lower limits. Values are calculated by taking the sum of each month, and then monthly surface emissions expressed in Tg. Average of each month of 10 years were taken. PRDU shows a surface emission around 700 Tg during the spring seasons and 350 Tg surface emission during autumn seasons.

All the other simulations show a similar pattern to PRDU with slight differences. It can be seen by the figure that surface emission in 21DU is higher than PRDU period in spring season. Domain was divided into two regions from the 20 East and values are shown below.
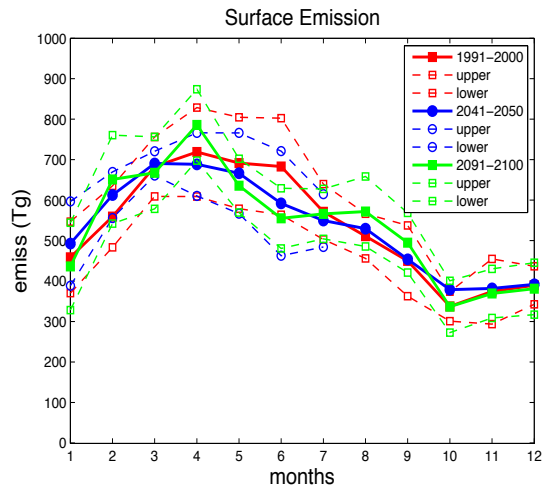
**Figure 3.29:** Seasonal cycle of mean surface emission.

Figure 3.30 shows that emissions of eastern part increases in the summer season and emissions of western part increases in the spring period.
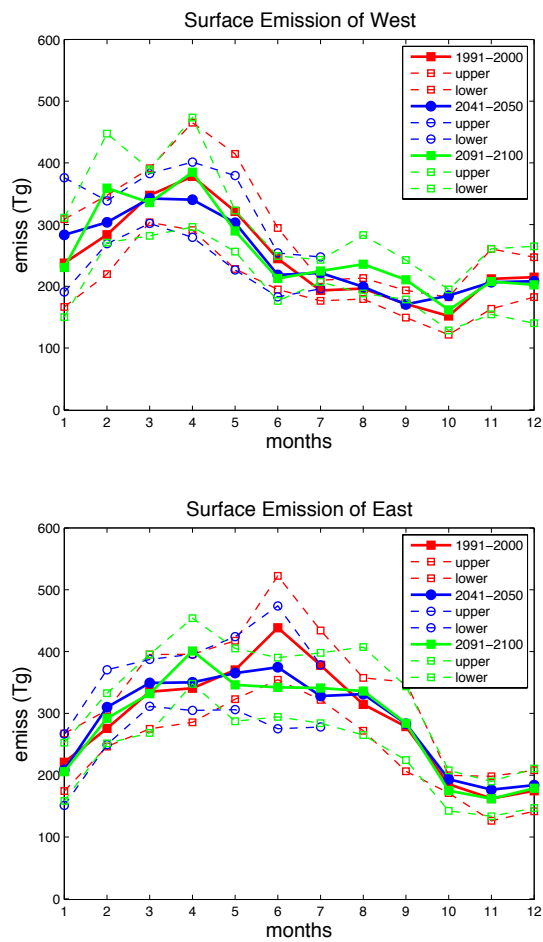




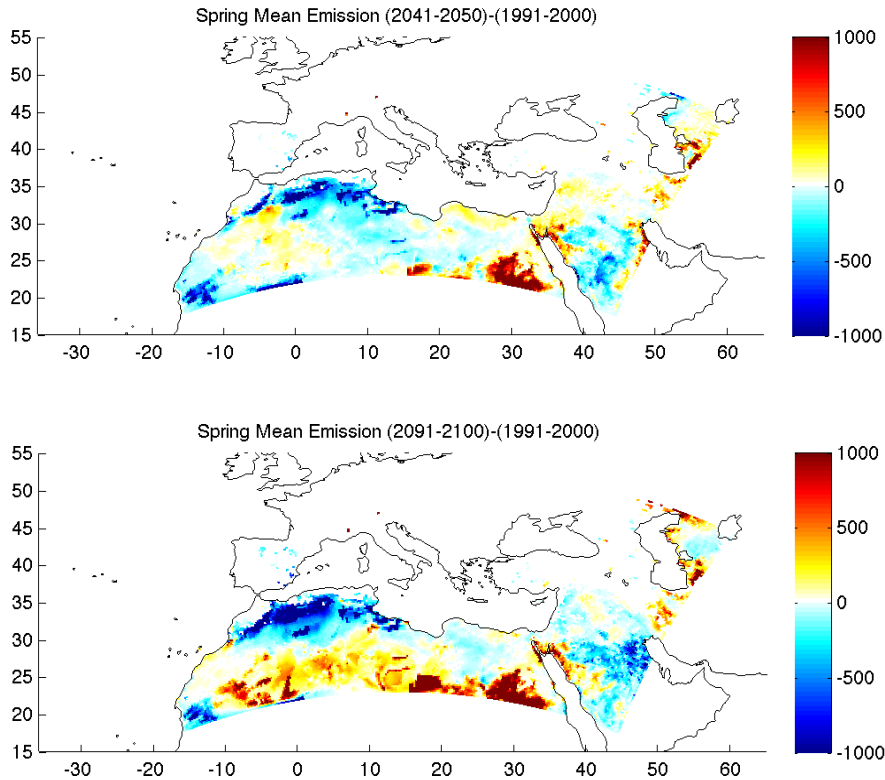**Figure 3.30:** Time series of surface emission at the west and east.

**Figure 3.31:** Change in spring mean surface emission (mg/m$^2$-day)
a) 2041-2050-1991-2000  b) 2091-2100-1991-2000.

It is necessary to show the domain on map in order to see the change in different regions in spring session. Figure 3.31 shows the change in spring mean surface emission. According to the spring mean surface emissions, there is a decrease in the dust emission in North Africa in 2041-2050. There is a higher decrease as seen in 2091-2100 period. There is an increase in the southern part of Africa in 2091-2100.

Figure 3.32 shows the mean dry deposition at 1991-2000. Present dry deposition is calculated by averaging the monthly values averaged by 6 hourly values and then the average of ten years is calculated. Dry deposition at PRDU goes up to 2000 mg/m$^2$-day at the north of the African Continent. It is in between the ranges from 1000 to 1500 mg/m$^2$-day at Nefud Desert. Dry deposition increases from PRDU to NFDU and 21DU in the south part of Saharan desert, since the surface emission increases in the same region. Also, decrease in dry deposition is similar to the decrease in surface emission, which may lead by the northerly wind carrying the dust from north to the south of continent.
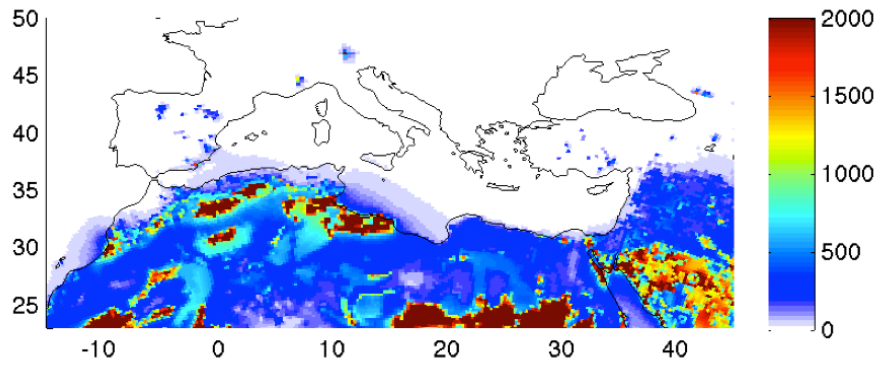
**Figure 3.32:** Mean dry deposition 1991-2000.

Dust is transported to the northwest of the domain for the 2041-2050 period due to the wind system shown in Figure 3.26a. For the 2091-2100 period dust is transported to the Atlantic due to the wind and pressure systems also shown in Figure 3.26b.
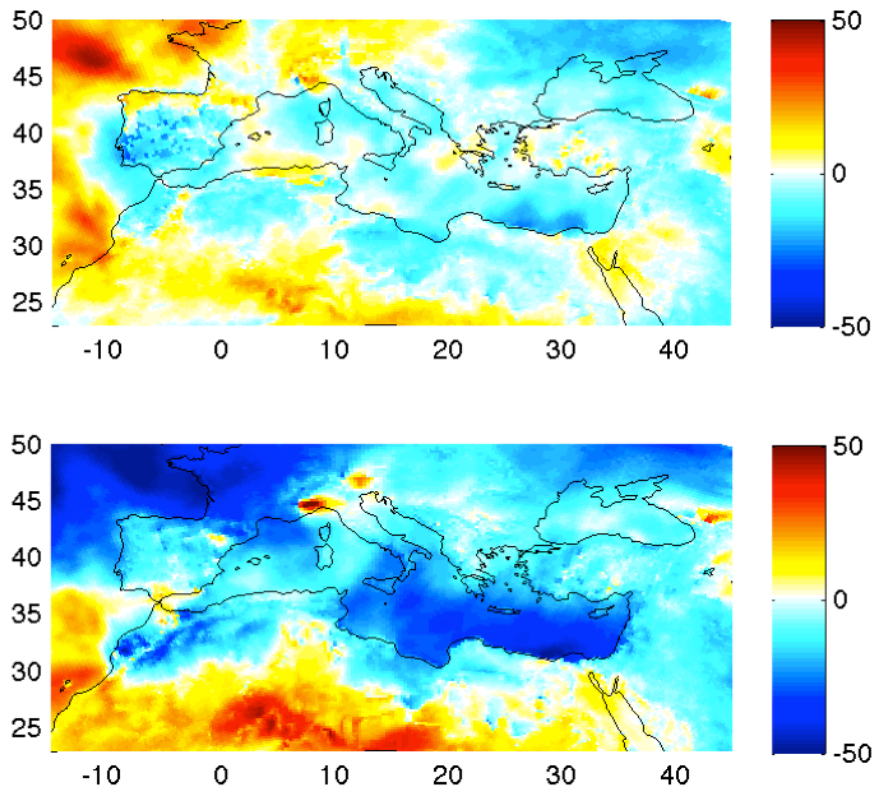


**Figure 3.33:** Change in mean dry deposition (mg/m$^2$-day)
a) 2041-2050-1991-2000   b) 2091-2100-1991-2000.

Figure 3.34 shows the time series of surface dry deposition with the upper and lower limits. Values are obtained by sum of each month and all the months are averaged for ten years periods. This figure has similar pattern with surface emission. PRDU simulation has a dry deposition around 350 Tg during the spring season. As the surface

emission increases from PRDU to 21DU, surface dry deposition also increases in the same period. The highest deposition occurs in spring also shown in the short-term case.
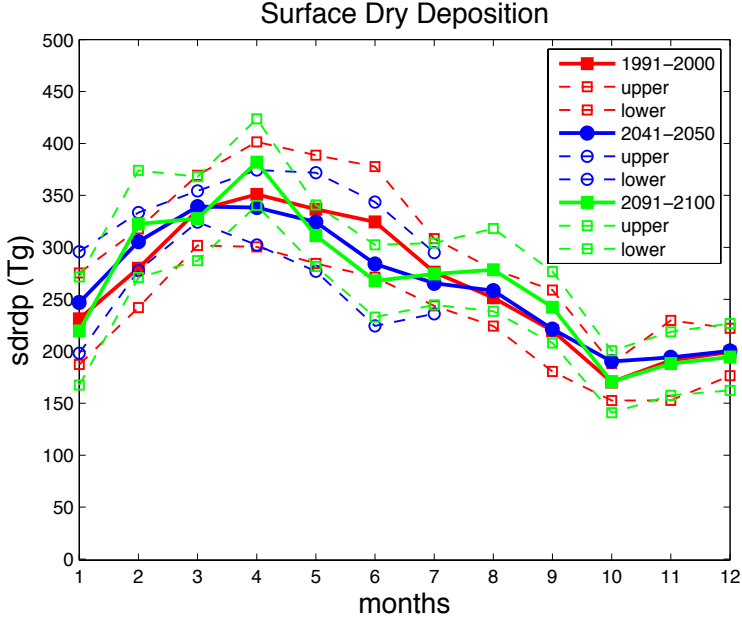


**Figure 3.34:** Seasonal cycle of surface dry deposition for three different periods.
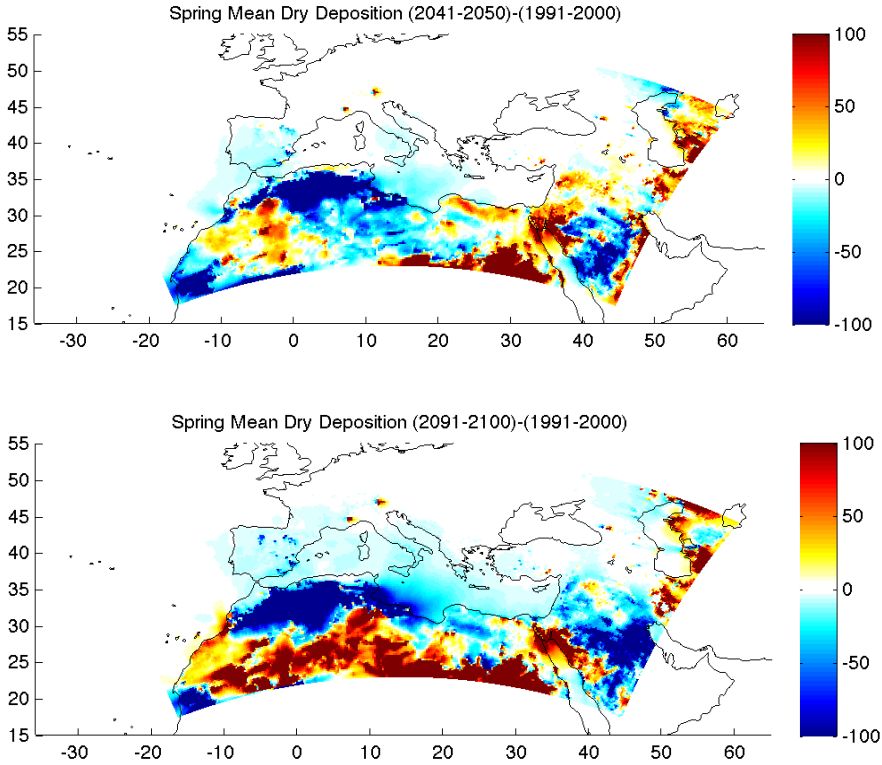


**Figure 3.35:** Difference in Spring Mean Dry Deposition (mg/m$^2$-day)
a) 2041-2050-1991-2000   b) 2091-2100-1991-2000.

Figure 3.35 shows the difference in spring mean dry deposition session. Dry deposition decreases in the North Africa and increases in the west of Africa in the two future periods. There is an increase in 2091-2100 in the south of Africa.
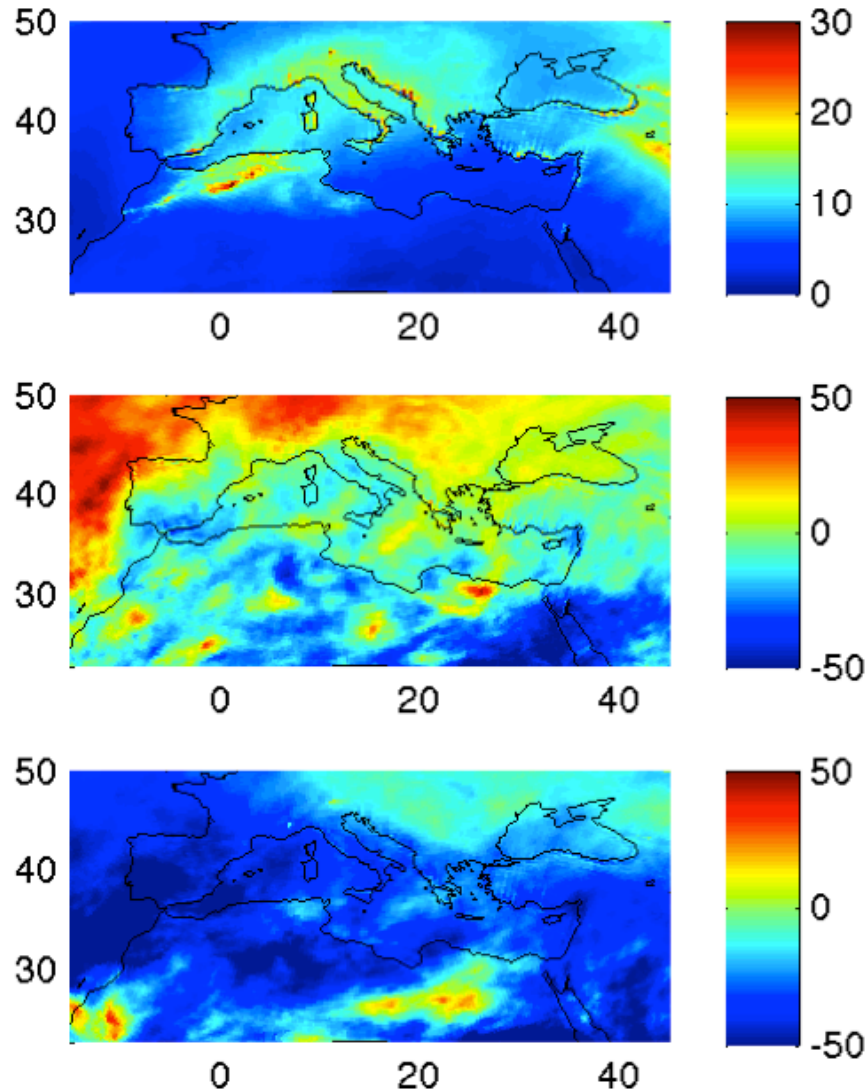


**Figure 3.36:** Daily Mean Wet Deposition mg/m$^2$-day and
Change in  % (2041-2050-1991-2000) – (2091-2100-1991-2000).

Daily mean wet deposition for three periods is given in Figure 3.36. At PRDU, wet deposition is high near the coast of Mediterranean since there is high precipitation. It is seen that wet deposition range from 10 to 20 mg/m$^2$-day at PRDU. Also, there is wet deposition around 18 mg/m$^2$-day in North Africa since there is high surface emission and more precipitation at the coast.

There is an increase at the northern Europe increasing by the latitude and there is a decrease increasing at the southern part of the domain at NFDU. There is a decrease up

to 50% all over the domain at 21DU, related to the precipitation decrease all over the domain.

Figure 3.37 shows the time series of wet deposition. Values are the total of each month and all the months are averaged for ten years periods. PRDU has a total of 9 Tg wet deposition during March and April. It is obvious that, there is high wet deposition during spring for the three different periods. Wet deposition during summer is around 2 Tg during the summer.
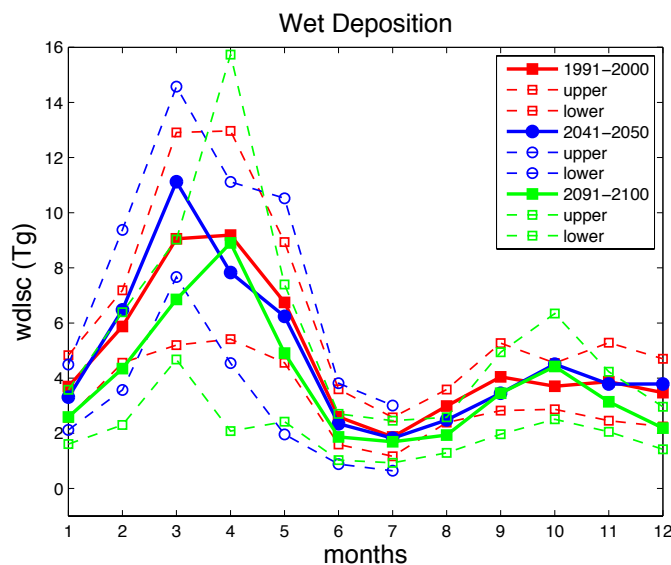


**Figure 3.37:** Seasonal cycle of wet deposition
for three different periods.

Figure 3.38 shows the daily mean column burden at PRDU, and Figure 3.39 shows the difference between NFDU and PRDU and 21DU and PRDU. Values represent the daily averages. Column burden is shown very high in the source regions in comparison with the north of the domain at PRDU.

When the difference between PRDU and NFDU is compared, there is an increase at the west of the domain within a range between 10-40% can be seen. There is an increase around 20% at the south part of Saharan Desert, which is related to the surface emission increase at the 21DU.
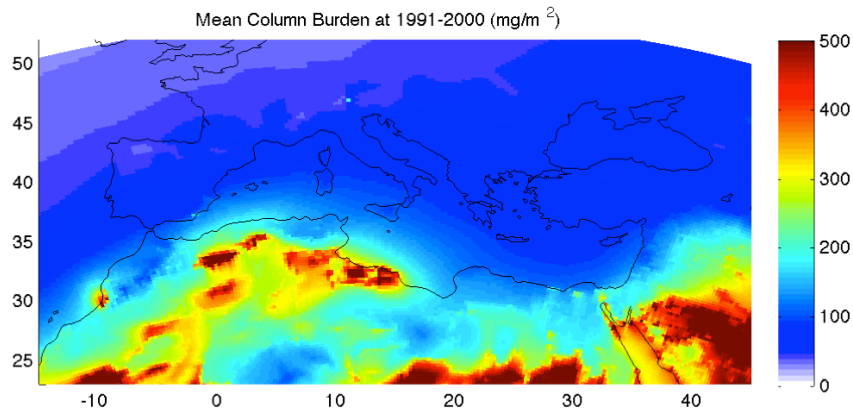
**Figure 3.38:** Mean Column Burden at 1991-2000 (mg/m$^2$-day).
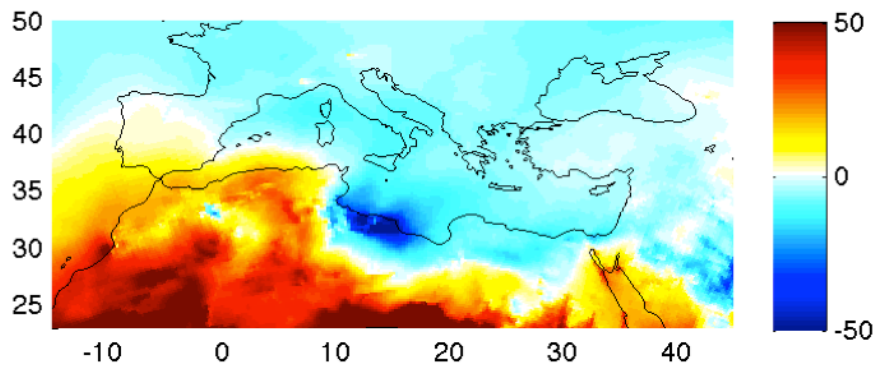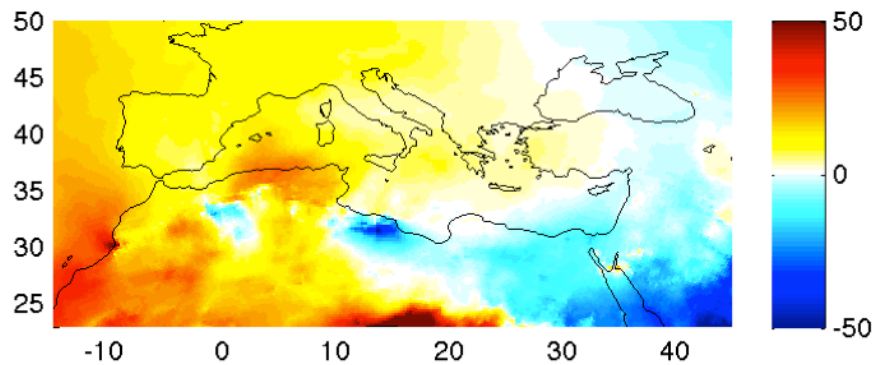


**Figure 3.39:** Difference of column burden (%)
a) 2041-2050-1991-2000   b) 2091-2100-1991-2000.

Figure 3.40 shows the total column burden as the time series of column burden data. It indicates that total column burden is higher during the spring, which is similar to the surface emission pattern. PRDU gives 170 Tg total column burden during May, which is the highest column burden on average. Actually surface emission was highest on April for the same period. On the other hand, April has higher dry and wet deposition than May. It is expected to have higher column burden during May as it can be seen by Figure 3.40.
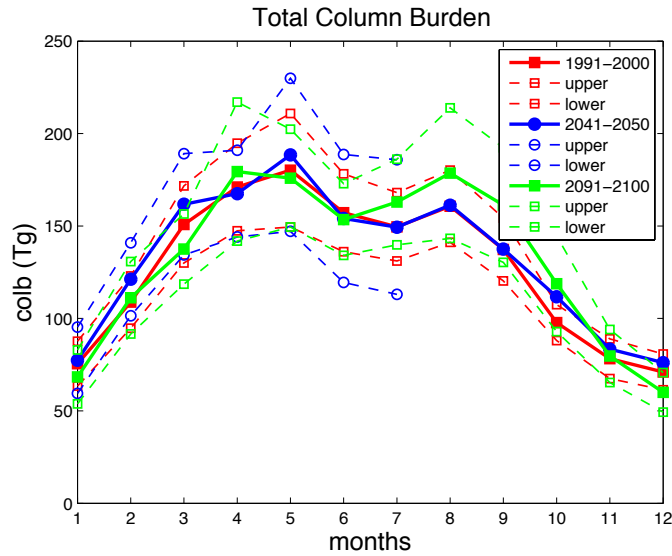
**Figure 3.40:** Total column burden (Tg) for three different periods.

### 3.2.5 Aerosol optical depth

According to the Figure 3.41, AOD is between 0.3 and 0.5 at the source region at PRDU. It is even higher at Nefud, which is around 0.6. AOD has similar pattern with column burden. In Figure 3.42, AOD increases at the west of the domain at NFDU period since emissions increase and also wind direction is southerly in the NFDU period which carries the dust to the north of the domain. Also, there is a decrease at the west of the domain around 10%.
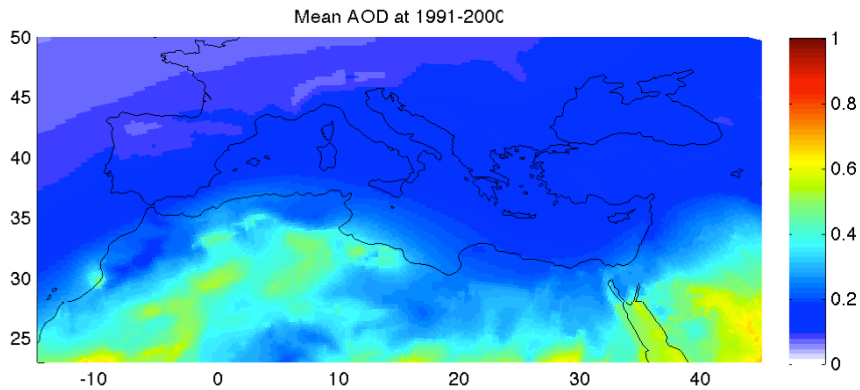


**Figure 3.41:** Mean AOD at 1991-2000.
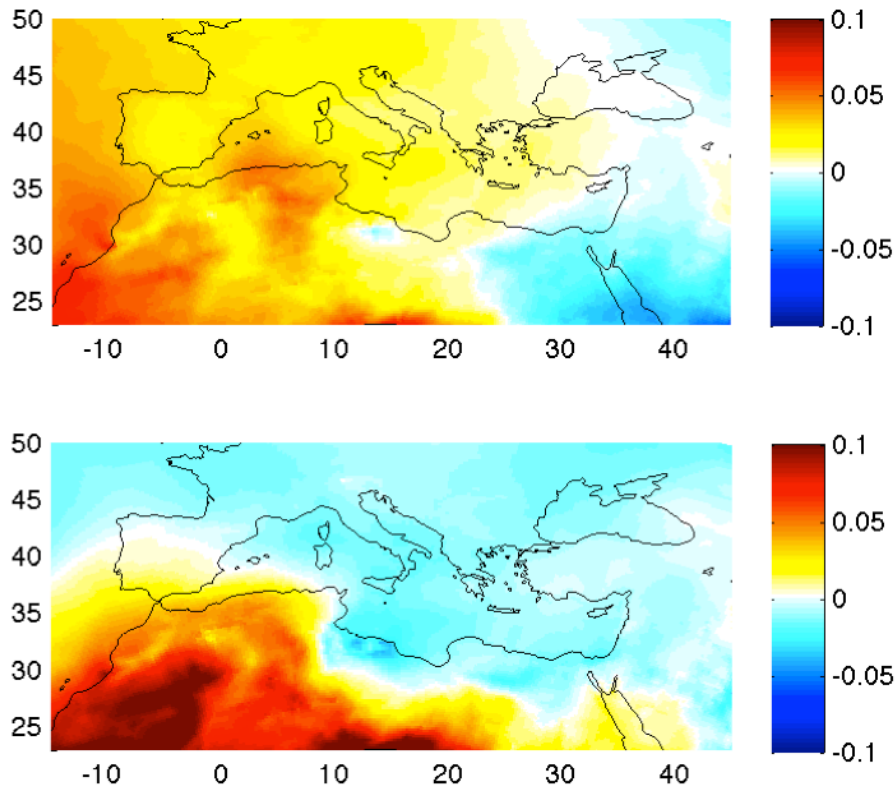
**Figure 3.42:** Change in AOD at
a) 2041-2050-1991-2000   b) 2091-2100-1991-2000.

When the time series are plotted, it is seen that west of the domain has one peak during spring. But the east of the domain has two peaks in the spring and autumn. This is caused by the other dust sources in the eastern region, Nefud and Syrian Deserts. Also, this might be explained by the increase in episodic events in Sahara during the spring months.
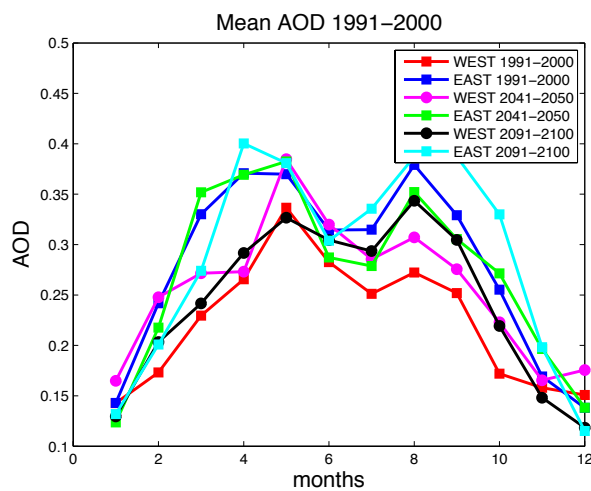


**Figure 3.43:** Seasonal Cycle of AOD.
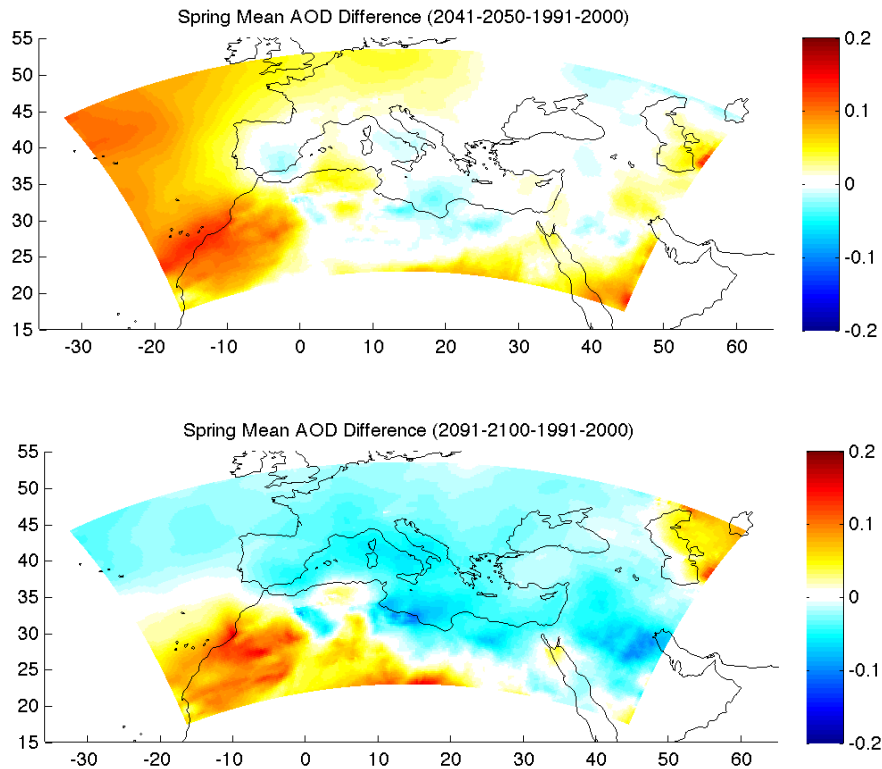
**Figure 3.44:** Difference in Spring Mean AOD
a) 2041-2050-1991-2000   b) 2091-2100-1991-2000.

Figure 3.44 shows the difference in spring mean AOD. AOD increases in 2041-2050 in the west of Africa. There seems to be no change on Turkey in the same period. There is similar increase in 2091-2100 in the west of Africa where, there is a slight decrease over Eastern Mediterranean.

### 3.2.6   Present and future dust optical properties and radiative forcing

According to the studies, mineral dust leads, decrease in SW radiation. A study done by Mallet (2009) shows that, dust aerosol decreased the SW radiation by up to -137 W/m$^2$ (regional mean) in North Africa, resulting in a significant decrease in surface temperature and sensible heat. Another study conducted by Takemura (2003) shows, dust caused a monthly mean SW surface forcing of -2.0 W/m$^2$ over East Asia. According to Huang (2009), dust aerosol caused a daily-mean surface SW forcing of up to -41.9 W/m$^2$ over the Taklamakan desert (Huang, 2009).

Mineral dust also leads increase in long wave radiation. There are many studies showing the effect of mineral dust on long wave radiation. Vogelmann (2003) found that Asian dust contributed to a surface LW forcing of up to 10 W/m$^2$. Another study shows that the LW forcing compensated about 20% of the SW cooling (Markowicz,

2003). According to Huang (2009), one-third of the SW surface cooling is because of the Asian dust is compensated by its LW warming effect (Huang, 2009).

Figure 3.45 shows the longwave at the surface and the top of the atmosphere for the three time periods and Figure 3.46 shows the short wave at surface and top of the atmosphere. Longwave at surface increases around 5 $W/m^2$ over the source regions and 1 $W/m^2$ over the north of the source regions. Longwave at the top of the atmosphere also increases around 1 $W/m^2$ over the source regions. Short wave at the surface decreases up to 20 $W/m^2$ over the source regions and 5 $W/m^2$ over the north of the domain. Short wave at the top of the atmosphere decreases 3 $W/m^2$ over the source region. The surface radiative forcing is reduced by dust around 1-2 $W/m^2$ (Tegen et al., 1996, Woodward et al., 2001) where top of the atmosphere forcing tend to be less (Zhang, 2009). The study of Zhang (2009) shows that short wave forcing is negative both at the surface and top of the atmosphere with values around -25 $W/m^2$ and -7.5 $W/m^2$ over the source regions.
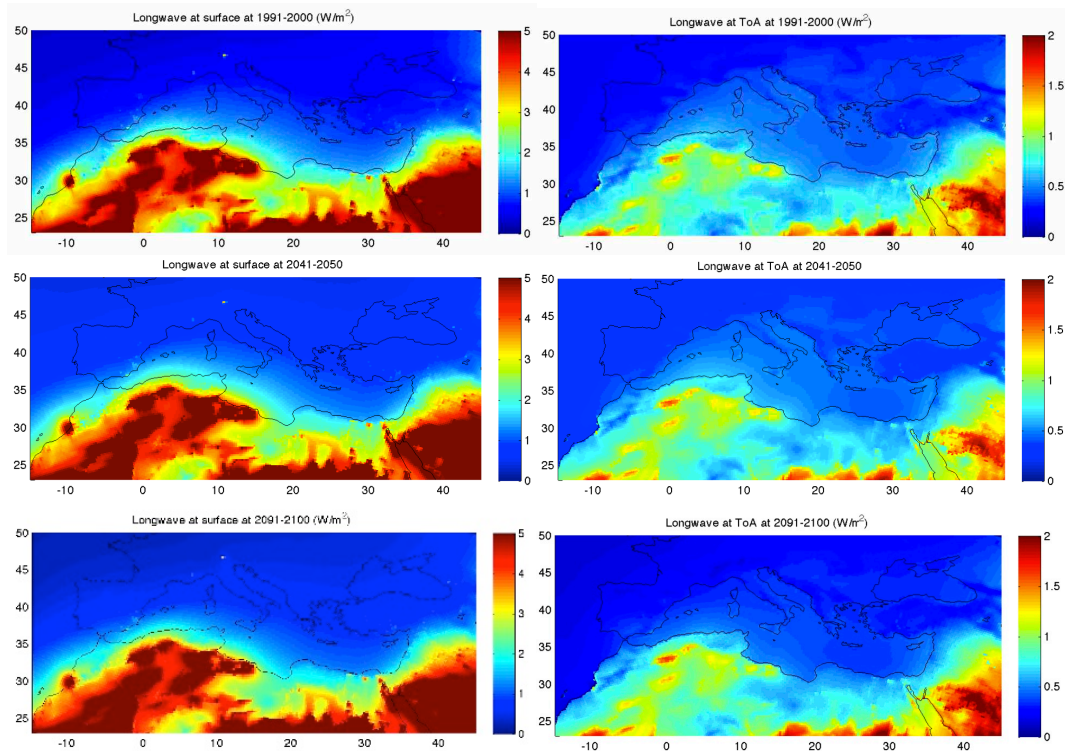


**Figure 3.45:** Longwave at surface and ToA (W/m$^2$).

Long wave effect of dust at the surface is 10 $W/m^2$ and 2.5 $W/m^2$ according to the same study. According to the study of Solmon (2006), dust loads and high temperatures in the Saharan desert causes a long wave absorbtion and positive radiative forcing at ToA

(Top of atmosphere). It is found that radiative forcing at the surface is negative and causes cooling. Values increase when the AOD increases (Solmon, 2008).
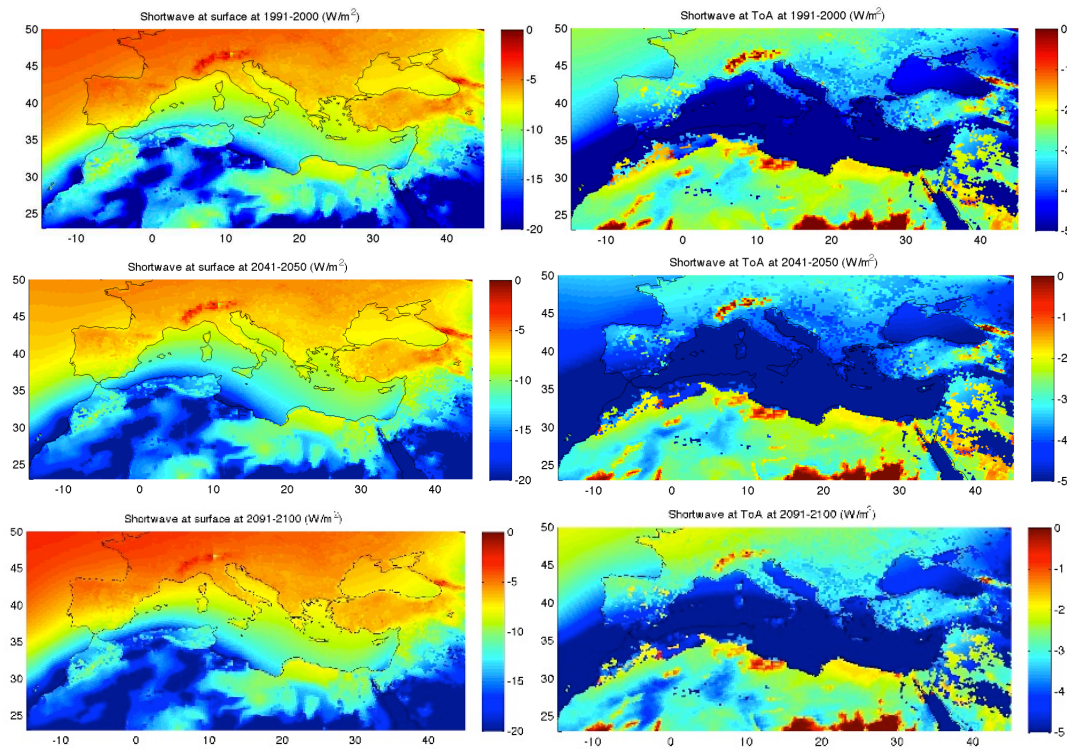


**Figure 3.46:** Shortwave at surface and ToA (W/m$^2$).

## 3.3. Effect of Dust on Temperature and Precipitation

Climatic effects of dust are given in this section. Figure 3.47 shows effect of mineral dust on temperature. Figure shows the difference of average temperature of the 10 years simulations performed both with dust and without dust. Dust causes a decrease around 0.2 C° over Turkey and Europe and a decrease around 0.5 C° over the African continent for the mean of 1991-2000. This result is valid also for the 2041-2050. Dust effect decreases at 2091-2100 period since the column burden decreases over Turkey in the future. According to IPCC (2007), aerosols lead 0.5 W/m$^2$ decrease in radiative forcing directly and 0.7 W/m$^2$ decrease by cloud albedo effect. Zhang et al. (2009) found 1 C° decrease over the source region.

Figure 3.48 shows the difference between dust and no-dust simulation for temperature of four different region in the domain. Dust leads temperature decrease in the spring season in 1991-2000. There is a smooth decrease in 2041-2050 period and it decreases in autumn in the four regions in 2091-2100. When the average of all year is taken there is a decrease in total temperature in case of dust is included in the simulation.
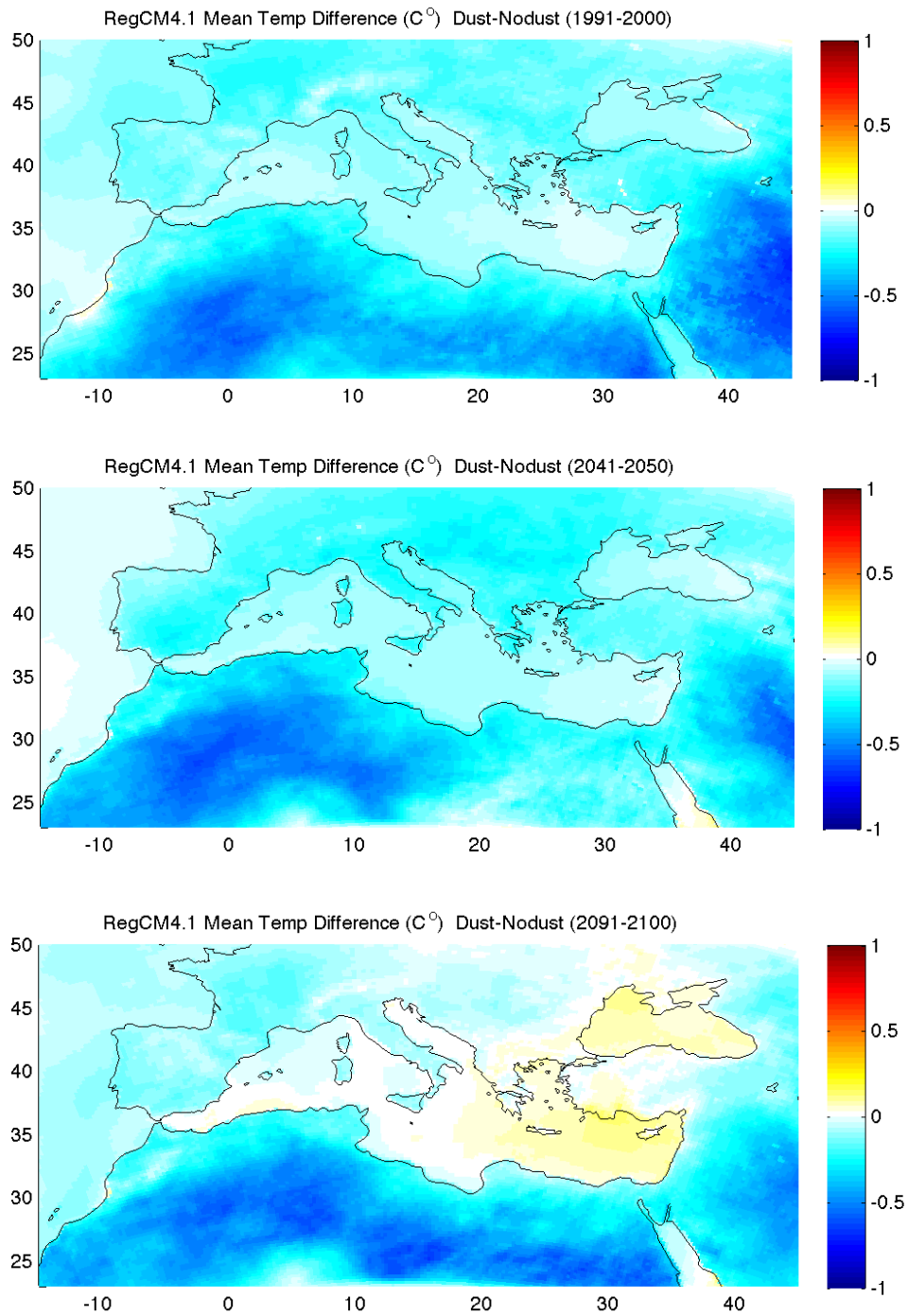
**Figure 3.47:** Temperature differences for each period with dust and without dust.
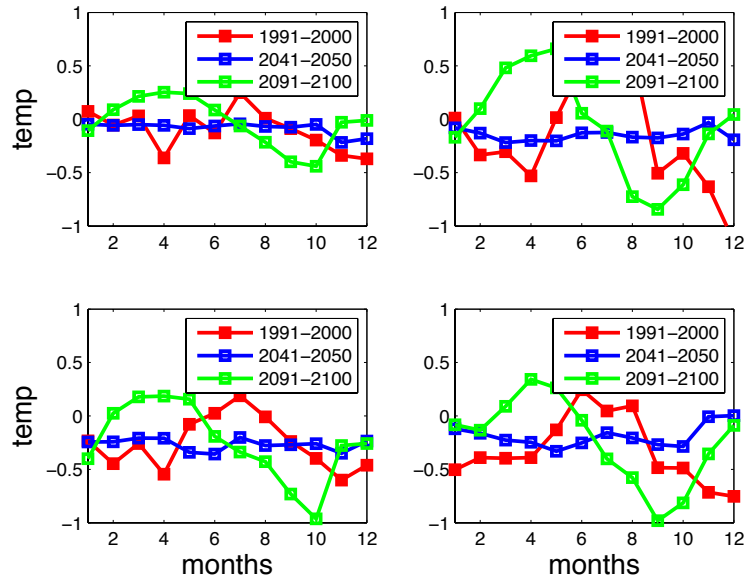
**Figure 3.48:** Difference of dust-nodust simulations
for temperature difference of ten year means.
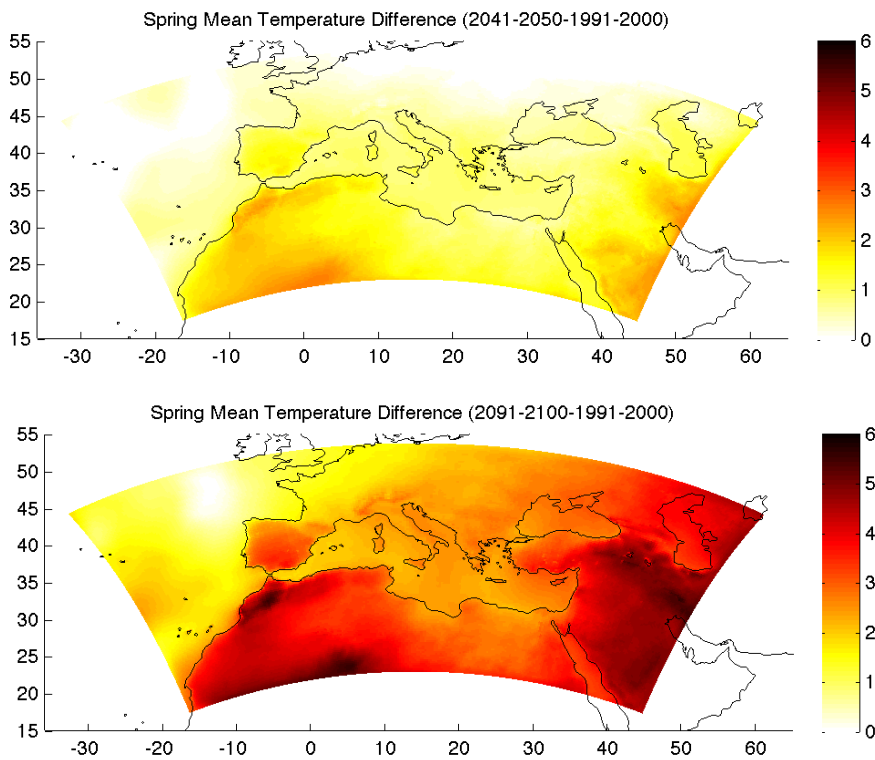


**Figure 3.49:** Difference in Spring Mean Temperature
a) 2041-2050-1991-2000   b) 2091-2100-1991-2000.

Figure 3.49 shows the difference in spring mean temperature with dust between the periods. There is an increase over all domains in the both periods in temperature. The increase is higher in the 2091-2100 period. These figures are showing both greenhouse

effect (A1B scenario from ECHAM5 output) and dust effect so that temperature increase is around 4 C over Africa in 100 year difference. These results are similar in IPCC 4th Assessment Report (2007) A1B scenario.
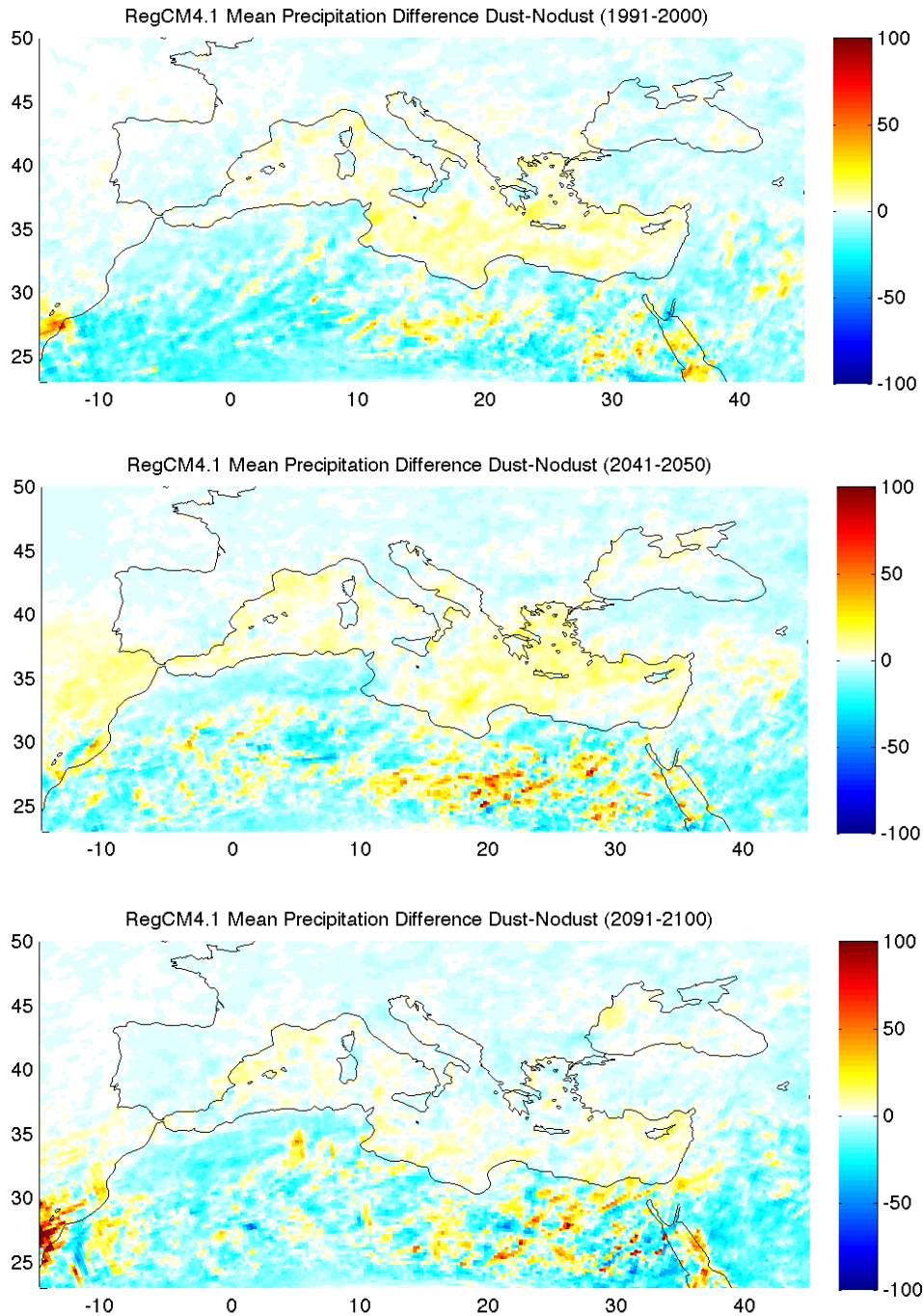


**Figure 3.50:** Precipitation differences for each periods with dust and without dust.

Precipitation change caused by dust is given in Figure 3.50. It shows the difference of average of the 10 years simulations with dust and without dust for three time periods. It is seen that precipitation decreases over the domain around 0.2 kg/m$^2$-day. According to

Solmon et al. (2008), dust causes a decrease of precipitation over Sahel region. In our study, it is seen that precipitation decreases over the all lands and increase over the sea.

Figure 3.51 shows the difference between dust and no-dust simulation for precipitation of four different regions for three different time periods. The difference of the dust and no-dust simulation averaged over all months of each term and each region. Dust leads a decrease over all domain and all regions. There is an increase in the spring period in the northwest of domain in 1991-2000 period.
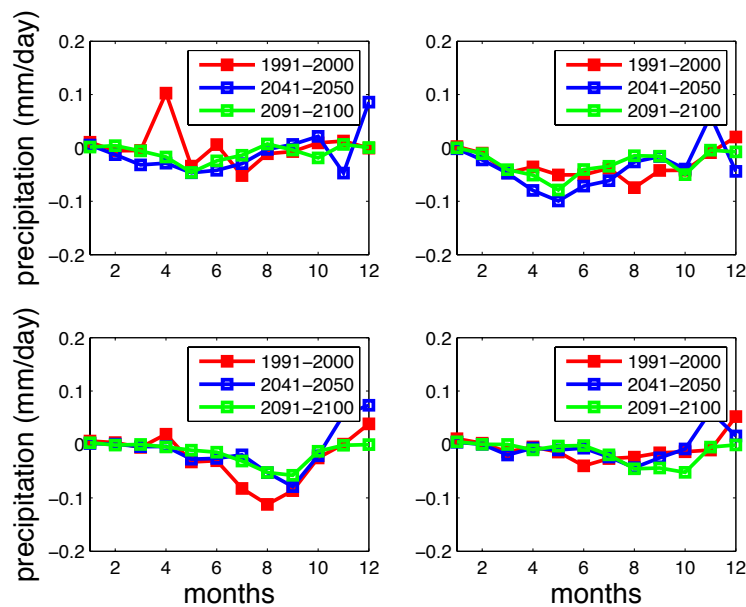


**Figure 3.51:** Difference of dust-nodust simulations
for precipitation difference of ten year means.

Figure 3.52 shows the difference between periods in total precipitation in spring. There is a decrease over Northern Europe and increase over Russia in the first time period in total precipitation. There is an increase in Northern Europe and decrease in the Southern Europe in 2091-2100 average period.

Figure 3.53 shows the summary of the long term study. As it is explained in this section model set up was done, ECHAM5 data were downloaded and prepared to the simulation. After simulations were completed model outputs were post-processed and analysis and visualization were done by Matlab. Afterwards model inputs processed by ICBC and then outputs of the model were compared. Also Taylor diagrams were made for model validation.
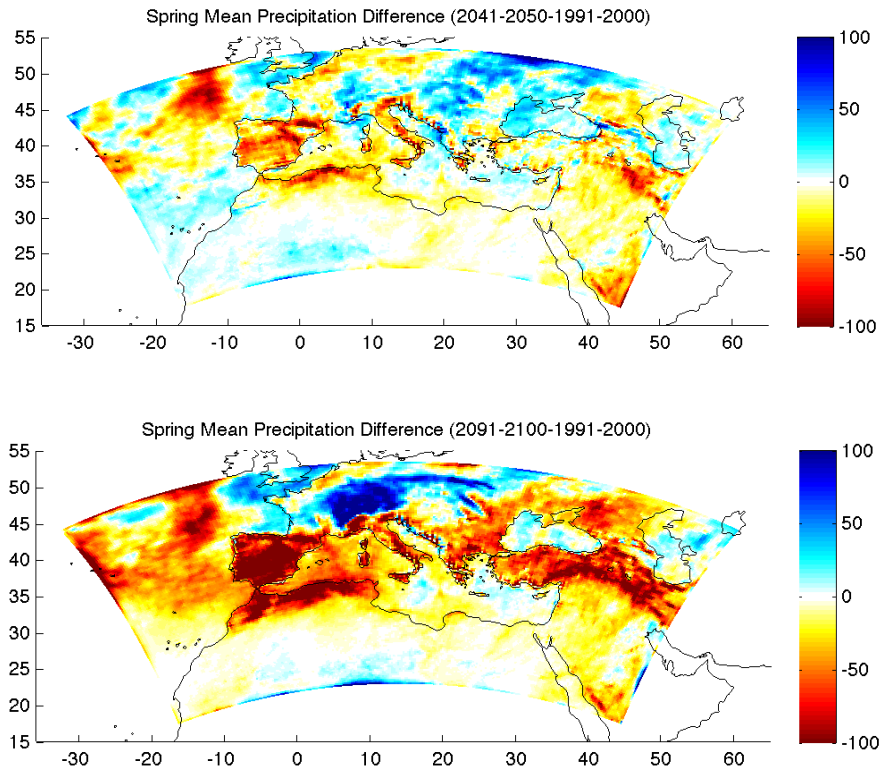
**Figure 3.52:** Difference in Spring Total Precipitation (kg/m$^2$)
a) 2041-2050-1991-2000   b) 2091-2100-1991-2000.
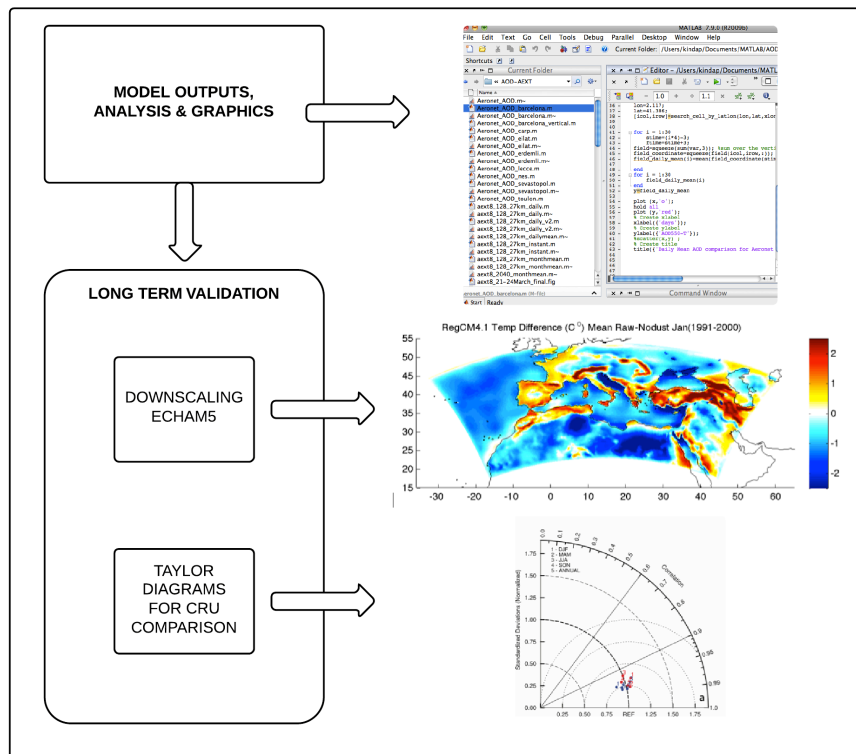


**Figure 3.53:** Summary of Long Term Study.

# 4. CONCLUSIONS AND FUTURE WORK

This section gives the conclusion of the study and future work planned following to this study. Saharan desert is an important component of the Mediterranean climate system. Meteorological conditions are the driving factors of the emissions and transport of dust from Sahara, so that climate change can affect the mineral dust sources and its transport pathways. Dust also affects the Mediterranean climate by modifying its radiative budget at regional scale.

This thesis showed the impact of dust transport on air quality and climate by two cases (short-term and long-term). The purpose of the short-term case is to investigate the relationship between high $PM_{10}$ concentrations and dust transport using atmospheric modelling, satellite data as well as in-situ observations and determining the aerosol optical properties and direct radiative effects of aerosols for a dust transport episode during March 2008. $PM_{10}$ values for the three selected regions and, for the episode in Turkey and at 10 different stations in Istanbul for the period 2004-2010 were provided by the Turkish Ministry of Environment. After determining the most affected season, which is spring, $PM_{10}$ concentrations for this season were evaluated and then an important episode during March 2008 was selected.

In this study, RegCM4.1 was used to model to further investigate the Saharan dust transport in the selected episode. During the period between March 21st and 24th, 2008, observed daily mean of $PM_{10}$ concentrations reached up to 180 μg/m$^3$ in Marmara region and 160 μg/m$^3$ in Aegean region. According to the RegCM4.1 model outputs, station Erdemli had highest AOD on 23$^{rd}$ March 2008, around 1.2, where it was 0.7 according to the AERONET observations. Daily average AOD in Marmara Region was found to be around 1.0 on the same day. Daily average column burden was 1000 mg/m$^2$ in Marmara Region and 750 mg/m$^2$ in Aegean Region. Daily mean short wave (all sky) radiative effect at surface and ToA was -62 W/m$^2$ and -29 W/m$^2$ in Marmara and -71 W/m$^2$ and -33 W/m$^2$ in Aegean Region respectively. In parallel, long wave forcing at

surface and ToA is 7 W/m$^2$ and 4 W/m$^2$ in Marmara and 11 W/m$^2$ and 4 W/m$^2$ in Aegean Region.

The second case is the long-term study, which was aimed to investigate the effect of mineral dust on climate. Three 10-year time periods (1991-2000, 2041-2050, and 2091-2100) were simulated with the regional climate model RegCM-4.1.1 in order to quantify the changes in dust distribution, optical properties, direct radiative forcing and its impacts on temperature and precipitation. The dust budget components (surface emissions, dry deposition, wet deposition and column burden) are simulated for the present, near future and end of century in order to compare them in present climate and future climate projections.

The model domain covers the entire Mediterranean Basin. The horizontal resolution is 27x27 km$^2$ and grid number is 128x256 with 18 vertical layers from surface to 50 hPa. Initial and boundary conditions were obtained from ECHAM5 simulations of the A1B scenario. Two sets of simulations were performed, with and without mineral dust. Monthly average precipitation and temperature data over 10 years are analyzed on both seasonal and annual time averages. Taylor diagrams (Taylor 2001) that compute the root mean square difference (RMSD), variability and pattern correlation between the model outputs of no-dust simulations and gridded datasets of Climate Research Unit (CRU) observations, allow us to assess the overall model performance.

Mineral dust emissions are expected to shift towards southern latitudes of Saharan Desert in the future compared to present climate. Dust emissions are increasing by 15% and 20% in 2040s and 2090s in the southern part of the domain. This occurs because of the general pattern of surface winds, which are strengthening at lower latitudes, associated to a strengthening and relocation of the Azores anticyclone towards north in future climate conditions. This leads to an increase (8%) in dust burden in the west of the domain and a decrease (10%) in the east of the domain. Aerosol optical depth also changes similarly to the dust burden. In the 2040s, AOD is increasing by 15% in the Western Mediterranean and decreasing by up to 10% in the Eastern Mediterranean. Similar changes are also simulated for the end of the 21st century.

Short wave net radiation at surface is decreasing up to 20 W/m$^2$ over the source regions and 8 W/m$^2$ over Mediterranean Sea and South Europe and 3 W/m$^2$ over the source region at the top of atmosphere since mineral dust has scattering feature. Also dust

caused a decrease in mean temperature around 0.2 Cº over Europe and 0.5 Cº over the African continent for the period 1991-2000. A similar impact is found also for the 2041-2050. Smaller temperature changes are simulated for the end of the 21st century.

## 4.1 Conclusions for the episodic study

Model results highly correlated with $PM_{10}$ concentrations and satellite image. It is found that RegCM4.1 is able to model March 2008 episode and it can capture the dust pattern correctly in comparison with the satellite image.

1) On March 23th 2008, when the dust episode affecting Aegean and Marmara Regions intensively, daily mean $PM_{10}$ level was 102.6 $\mu g/m^3$ in Aegean Region and 117.3 $\mu g/m^3$ in Marmara Region according to the data provided by Turkish Ministry of Environment and Urbanization.

2) Model performance was evaluated through the AOD model outputs and AERONET observations. Three stations were selected which are affected stations such as Erdemli and Sevastopol and control station Eilat. Correlation coefficient was calculated around 0.6.

3) On the same day, AOD was 1.11 in Aegean Region and 0.87 in Marmara Region according to the RegCM4.1 model results. Mean dry deposition is 201.13 $mg/m^2$ and 96.67 $mg/m^2$ and column burden was 1009.9 $mg/m^2$ and 745.37 $mg/m^2$, respectively.

4) Dust transport causes change in radiative forcing because of the highly scattering feature of mineral dust. Short wave at surface and at ToA decreases around 71.4 $W/m^2$ and 33 $W/m^2$ in Aegean Region and 61.9 $W/m^2$ and 28.8 $W/m^2$ in Marmara Region, respectively. Long wave at surface and ToA increases around 10.7 $W/m^2$ and 4.4 $W/m^2$ in Aegean Region and 6.9 $W/m^2$ and 4 $W/m^2$ in Marmara Region, respectively.

This study shows the atmospheric properties and radiative forcing during an important dust episode affecting west of Turkey.

**4.2 Conclusions for the Long Term**

A comprehensive analysis of the dust budget, including surface emissions, burden, deposition and effect of dust on radiation, temperature and precipitation for present and future climate were investigated in this section.

1) Compared to present climate, a shift of mineral dust emissions towards southern latitudes of Saharan Desert was observed in the future. It was found that Saharan dust episodes occur more in spring season. Surface emissions shifted to south in near future and future periods. Emissions increased around 10 mg/m$^2$-day (2%). In the southern part of the domain dust emissions were increasing by 15% and 20% in 2040s and 2090s, respectively. This is due to a change in the general pattern of surface winds, which are strengthening at lower latitudes, probably due to a strengthening and relocation of the Azores anticyclone towards north in future climate conditions.

2) This generated a change in dust burden over the Mediterranean with decreases particularly in the Eastern Mediterranean (10%) and increases in the West Mediterranean (8%). Column burden and AOD is related to dust emissions and changes in wind pattern. The changes in burden of dust determine also a change in the distribution of the aerosol optical depth (AOD) and the dust radiative forcing. In the 2040s AOD is increasing by 15% in the Western Mediterranean and decreasing by 10% in the Eastern Mediterranean. Similar changes were also simulated for the end of the 21$^{st}$ century.

3) Dry deposition is related to dust emissions and wet deposition is related to dust emissions and the precipitation. Dry deposition increases around 10 mg/m$^2$-day (10%) in 2041-2050 by shifting to south. It decreases around 7-8 mg/m$^2$-day in the east.

4) The impact of dust on the net radiative budget was quantified for the single 10-years periods by comparing the simulations with dust and without dust. Shortwave net radiation at surface is decreasing up to 20 W/m$^2$ over the source regions and 8 W/m$^2$ over Mediterranean Sea and South Europe. Shortwave net radiation at the top of atmosphere is decreasing 3 W/m$^2$ over

the source region.

5) Dust causes an average decrease of 0.2 C° over Europe and 0.5 C° over the African continent for the period 1991-2000. A similar impact was found also for the 2041-2050. Smaller temperature changes simulated for the end of the 21$^{st}$ century. No significant changes were observed in precipitations for the 3 periods.

6) In this study we have seen that lack of land use change, which is a very important issue to be solved in RegCM-4 model. As a result of climate change, it is expected to have more dust sources in the future than reference period. Because of warmer temperatures, dust sources and dust storms may increase. So that land use change will be important in evaluating the effect of dust on climate.

## 4.3 Future Work

Since Saharan desert is an important component of the Mediterranean climate system, it should be noted that dust storms should be more investigated in terms of frequencies. As a further work, intense dust events over the Mediterranean Region for the three time periods should be counted and frequency should be calculated. In order to do this, it is necessary to count events over a given threshold for AOD or daily total deposition by taking daily average of all days for ten years.

This study showed that dust has significant impact on air quality, especially on $PM_{10}$. There should be studies that can set different limits to dust transport episodes according to the EU Council Directive 1999/30/EC. $PM_{10}$ concentration exceeds 50 $\mu g/m^3$ even if there is no residential heating, so that this issue can be solved in order to prevent unfair applications. Experimental studies also can be done to calculate the ratio of mineral dust in particulate matter in order to support this idea.

In this study ECHAM5 A1B scenario data according to the IPCC 4$^{th}$ Assessment Report were used. New data are available at the IPCC 5$^{th}$ Assessment Report Group. New simulations can be performed according to the new emission scenarios.

Land surface model of RegCM4.1 is BATS. Although it is a good option, it is known that land use will change as a result of climate change. In this study this change becomes very important since the effects are calculated according to the dust transport.

A module which also provides land use change in the future periods can be adapted to the climate models.

# REFERENCES

**Alfaro, S. C., and Gomes, L.** (2001). Modeling mineral aerosol production by wind erosion : Emission intensities and aerosol size distribution in source areas, *J. Geophys. Res.*, 106, 18,075–18,084.

**Andreae, T. W., M. O. Andreae, C. Ichoku, W. Maenhaut, J. Cafmeyer, A. Karnieli, and L. Orlovsky.** (2002). Light scattering by dust and anthropogenic aerosol at a remote site in the Negev desert, Israel, *J. Geophys. Res.* ,107 (D2), doi:10.1029/2001JD900252.

**Balkanski, Y., Schulz, M., Claquin, T., and Guibert, S.** (2007). Reevaluation of Mineral aerosol radiative forcings suggests a better agreement with satellite and AERONET data, *Atmos. Chem. Phys.*, 7, 81–95, doi:10.5194/acp-7-81-2007.

**Basart, S., Pérez, C., Nickovic, S., Cuevas, E., Baldasano J. M.** 2012. Development and evaluation of the BSC-DREAM8b dust regional model over Northern Africa, the Mediterranean and the Middle East, Tellus B, 64, 18539.

**Brusseurs, G.P.** (2003). *Atmospheric Chemistry in a Changing World*. Springer.

**Dayan, U.** (1986). Climatology of back trajectories from Israel based on synoptic Analysis, *J. Climate Application Meteorology*, 25(5): 591-595.

**DREAM Model** < (http://www.bsc.es/projects/earthscience/BSC-DREAM/)>

**Dickinson, R. E., Errico, R. M., Giorgi, F., and Bates, G. T.** (1989). A regional climate model for the western United States, *Climatic Change*, 15, 383–422.

**Dickinson, R. E., Henderson-Sellers, A., and Kennedy, P. J.** (1993). Biosphere-atmosphere transfer scheme (bats) version 1e as coupled to the ncar community climate model, Tech. rep., National Center for Atmospheric Research.

**Dubovik, O., and M. D. King.** (2000). A flexible inversion algorithm for retrieval of aerosol optical properties from sun and sky radiance measurements. *J. Geophys. Res.*, 105, 20 673–20 696.

**Elguindi, N., Bi, X., Giorgi, F., Nagarajan, B., Pal, J., Solmon, F., Rauscher, S., Zakey, A.** (2007). RegCM Version 3.1 User's Guide, Trieste, Italy.

Elguindi, N., Bi, X., Giorgi, F., Nagarajan, B., Pal, J., Solmon, F., Rauscher, S., Zakey, A. (2010). RegCM Version 4.0 User's Guide, Trieste, Italy.

Escudero, M., Stein, A.F., Draxler, R.R., Querol, X., Alastuey, A., Castillo, S., Avila, A. (2011). Source apportionment for African dust outbreaks over the Western Mediterranean using the HYSPLIT model, Atmospheric Research, 99, 518–527.

Formenti, P., et al. (2001). Aerosol optical properties and large-scale transport of air masses: Observations at a coastal and a semiarid site in the eastern Mediterranean during summer 1998, *J. Geophys. Res.*, 106 , 9807–9826.

Forster, P; Ramaswamy, V; Artaxo, P; Berntsen, T; Betts, R; Fahey, DW; Haywood, J; Lean, J; Lowe, DC; Myhre, G; Nganga, J; Prinn, R; Raga, G; Schultz, M; Van Dorland, R. (2007). Climate change 2007: The physical science basis. Contribution of Working Group I to the Fourth Assessment Report of the Intergovernmental Panel on Climate Change, Cambridge University Press.

Ginoux, P., Chin, M., Tegen, I., Prospero, J. M., Holben, B., Dubovik, O., and Lin, S.J. (2001). Sources and distributions of dust aerosols simulated with the GOCART model, Geophys.Res.106, 20255-20274 10.1029/2000JD000053.

Ginoux, P., J. M. Prospero, T. E. Gill, N. C. Hsu, and M. Zhao (2012). Global-scale attribution of anthropogenic and natural dust sources and their emission rates based on MODIS Deep Blue aerosol products, Rev. Geophys., 50, RG3005, doi:10.1029/2012RG000388.

Giorgi, F., Coppola, E., Solmon, F., Mariotti, L., Sylla, M. B., Bi, X., Elguindi, N., Diro, G. T., Nair, V., Giuliani, G., Cozzini, S., Guettler, I., O'Brien, T. A., Tawfik, A. B., Shalaby, A., Zakey, A. S., Steiner, A. L., Stordal, F., Sloan, L. C., and Brankovic, C. (2012). RegCM4: model description and preliminary tests over multiple CORDEX domains, *Clim. Res.*, 52, 7–29, doi:10.3354/ cr01018.

Giorgi, F., M. R. Marinucci, and G. T. Bates, (1993). Development of a second generation regional climate model (regcm2): Boundary layer and radiative transfer processes, *Mon. Wea. Rev.*, 121, 2794–2813, 1993b.

Giorgi, F., Marinucci, M. R., Bates, G. T., and DeCanio, G. (1993). Development of a second generation regional climate model (regcm2) ii: Convective processes and assimilation of lateral boundary conditions, *Mon. Wea. Rev.*, 121, 2814–2832.

Giorgi, F., and Mearns, L. O. (1999). Introduction to special section: Regional climate modeling revisited, *J. Geophys. Res.*, 104, 6335–6352.

**Grell, G.** (1993). Prognostic evaluation of assumptions used by cumulus parameterizations, *Mon. Wea. Rev.,* 121 , 764–787.

**Hansen, J., M. Sato, and R. Ruedy,** (1997). Radiative forcing and climate response. *J. Geophys. Res.,* 102, 6831-6864, doi:10.1029/96JD03436.

**Haywood, J. and O. Boucher** (2000). A comparison of the climate impacts of tropospheric aerosols: A *review,* Reviews of *Geophysics, 38, 513*-543.

**Holtslag, A. A. M., E. I. F. de Bruijn, and H.-L. Pan.** (1990). A high resolution air mass transformation model for shortrange weather forecasting, *Mon. Wea. Rev.,* 118, 1561–1575.

**Huneeus, N., M. Schulz, Y. Balkanski, J. Griesfeller, S. Kinne, J. Prospero, S. Bauer, O. Boucher, M. Chin, F. Dentener, T. Diehl, R. Easter, D. Fillmore, S. Ghan, P. Ginoux, A. Grini, L. Horowitz, D. Koch, M.C. Krol, W. Landing, X. Liu, N. Mahowald, R.L. Miller, J.-J. Morcrette, G. Myhre, J.E. Penner, J.P. Perlwitz, P. Stier, T. Takemura, and C. Zender.** (2011). Global dust model intercomparison in AeroCom phase I. *Atmos. Chem. Phys.,* **11**, 7781-7816, doi:10.5194/acp-11-7781-2011.

***Intergovernmental Panel on Climate Change (IPCC), Climate Change*** (2007). The Physical Science Basis, in: Contribution of WGI to the IPCC AR4, edited by: Solomon, S., Qin, D., Manning, M., Chen, Z., Marquis, M., Averyt, K. B., Tignor, M., and Miller, H. L., Cambridge University Press, Cambridge, UK and New York, NY, USA.

**Jaenicke, R.** (1993). Tropospheric Aerosols. *International Geophysics,* Volume 54, Pages 1-31.

**Jacobson, M.** (2005). *Fundamentals of Atmospheric Modeling,* Cambridge.

**J. Haywood and O. Boucher.** (2000). A comparison of the climate impacts of tropospheric aerosols: A review, *Reviews of Geophysics,* 38, 513-543.

**Jimenez-Guerrero, P., Perez, C., Jorba, O., Baldasano, J.M.** (2008). Contribution of Saharan dust in an integrated air quality system and its on-line assessment, Geophysical Research Letter, VOL. 35, L03814, doi:10.1029/2007GL031580.

**Kocak, M., Kubilay, N., Mihalopoulos, N.** (2004). Ionic composition of lower tropospheric aerosols at a Northeastern Mediterranean site: Implications regarding sources and long- range transport, *Atmospheric Environment,* 38, 2067-2077.

**Kocak M, Mihalopoulos N, Kubilay N.** (2007). Chemical composition of the fine and coarse fraction of aerosols in the northeastern Mediterranean. Atmospheric Environment; 41: 7351–68.

**Kocak M, Mihalopoulos N, Kubilay N.** (2009). Origin and source regions of PM10 in the Eastern Mediterranean atmosphere. Atmospheric Research, Volume 92, Issue 4, June 2009, Pages 464–474.

**Kiehl, J. T., Hack, J. J., Bonan, G. B., Boville, B. A., Breigleb, B. P., Williamson, D. and Rasch, P.** (1996). Description of the Ncar community climate model (ccm3), Tech. Rep. NCAR/TN-420+STR, National Center for Atmospheric Research.

**Kubilay, N., Saydam, C., Yemenicioğlu, S., Kelling, G., Kapur, S., Karaman, C., Akça, E.** (1997). Seasonal chemical and mineralogical variability of atmospheric particles in the coastal region of the Northeast Mediterranean. Catena 28 : 313-328.

**Kubilay, N., Nickovic, S., Moulin, C., Dulac, F.** 2000. An illustration of the transport and deposition of mineral dust onto the eastern Mediterranean. Atmospheric Environment, 1293-1303.

**Kubilay, N., Oguz, T., Koηak, M., Torres, O.** 2005. Ground-based assessment of Total Ozone Mapping Spectrometer (TOMS) data for dust transport over the northeastern Mediterranean. *Global Biogeochemical Cycles* 19, GB1022, doi:10.1029/2004GB002370.

**Laurent, B., Marticorena, B., Bergametti, G., Leon, J.F., Mahovald, N.M.** 2008. Modeling mineral dust emissions from the Sahara desert using new surface properties and soil database. Journal of Geophysical Research, DOI: 10.1029/2007JD009484

**Lelieveld, J., Berresheim, H., Borrmann, S., Crutzen, P. J., Dentener, F. J., Fischer, H., Feichter, J., Flatau, P. J., Heland, J., Holzinger, R., Korrmann, R., Lawrence, M. G., Levin, Z.,Markowicz, K. M., Mihalopoulos, N., Minikin, A., Ramanathan,V., de Reus, M., Roelofs, G. J., Scheeren, H. A., Sciare, J., Schlager, H., Schultz, M., Siegmund, P., Steil, B., Stephanou, E. G., Stier, P., Traub, M.,Warneke, C.,Williams, J., and Ziereis, H.** 2002. Global Air Pollution Crossroads over the Mediterranean, Science, 298, 794–799, doi:10.1126/science.1075457.

**Lohmann, U., Feichter, J.** (2001). Can the direct and semi-direct aerosol effect compete with the indirect effect on a global scale?, *Geophys. Res. Lett.*, 28, 159–161.

**Longueville, F., Hountondji, Y-C., Henry, S., Ozer, P.** (2010). What do we know about effects of desert dust on air quality and human health in West Africa compared to other regions? Science of the Total Environment 409, 1–8.

**Malavelle, F., Mallet, M., Pont, V., Liousse, C., and Solmon, F.** 2011. Long-term simulations (2001–2006) of biomass burning and mineral dust optical properties over West Africa: comparisons with new satellite retrievals,

Atmos. Chem. Phys. Discuss., 11, 28587–28626, doi:10.5194/acpd-11-28587-2011.

**Marticorena, B., and G. Bergametti.** (1995). Modeling the atmospheric dust cycle : 1-design of a soil derived dust production scheme, *J. Geophys. Res.*, 100, 16, 415–16, 430.

**Meloni, D., Sarra, A., Monteleone, F., Pace, G., Piacentino, S., Sferlazzo, D.M.** 2008. Seasonal transport patterns of intense Saharan dust events at the Mediterranean island of Lampedusa, Atmospheric Research, 88, 134–148.

**Mitchell TD, Jones PD.** (2005). An improved method of constructing a database of monthly climate observations and associated high- resolution grids. *Int. J. Climat.* 25:693–712.

**Nabat, P., Solmon, F., Mallet, M., Kok, J.F.,Somot, S.** (2012). Dust emission size distribution impact on aerosol budget and radiative forcing over the Mediterranean region: a regional climate model approach, *Atmos. Chem. Phys.*, 12, 10545–10567, 2012, doi:10.5194/acp-12-10545-2012

**National Air Quality Obser. Net.** <http://www.havaizleme.gov.tr/Default.ltr.aspx>

**Nastos, P. T.** 2012. Meteorological Patterns Associated with Intense Saharan Dust Outbreaks over Greece in Winter. Advances in Meteorology Volume, Article ID 828301.

**Nickovic, S., A. Papadopoulos, O. Kakaliagou, and Kallos, G.** 2001. Model for prediciton of desert dust cycle in the atmosphere, J. Geophys. Res., 106, 18,113–18,129.

**Özsoy, E.** (1981). On the atmospheric factors affecting the Levantine Sea. European Center for Medium Range Weather Forecasts (ECMWF) Technical Report 25, 29 pp.

**Pal, J. S., Small, E. E. and Eltahir, E. A. B.** (2000). Simulation of regional-scale water and energy budgets: Representation of subgrid cloud and precipitation processes within RegCM, *J. Geophys. Res.-Atmospheres*, 105 (D24), 29, 579–29, 594.

**Pal, J. S., Giorgi, F., Bi, X. et al.** (2007). The ICTP RegCM3 and RegCNET: Regional climate modeling for the developing world, Bull. Amer. Meteor. Soc., 88 , 1395–1409.

**Papanastasiou, D.K., Poupkou, A., Katragkou, E., Amiridis,V., Melas, D., Mihalopoulos, N., Basar, S., P´erez, C., and Baldasano, J.M.** An Assessment of the Efficiency of Dust Regional Modelling to Predict Saharan Dust Transport Episodes Advances in Meteorology, Volume 2010, Article ID 154368, doi:10.1155/2010/154368

**Penner, J. E., Andreae, M., Annegarn, H., Barrie, L., Feichter, J., Hegg, D., Jayaraman, A., Leaitch, R., Murphy, D., Nganga, J., and Pitari, G.** (2001). Aerosols, their Direct and Indirect Effects. In Climate Change 2001: The Scientific Basis, Cambridge University Press, Cambridge, UK.

**Pérez, C., Nickovic, S., Pejanovic, G., Baldasano, J. M., and Ozsoy, E.:** Interactive dust radiation modeling: A step to improve weather forecasts, 2006. J. Geophys. Res., 11, D16206, doi:10.1029/2005JD006717, 2006b.

**Pey J., X. Querol, A. Alastuey, F. Forastiere, and M. Stafoggia,** 2013. African dust
outbreaks over the Mediterranean Basin during 2001-2011: $PM_{10}$ concentrations, phenomenology and trends, and its relation with synoptic and mesoscale meteorology. Atmos. Chem. Phys., 13, 1395-1410.

**Prospero, J., P. Ginoux, O. Torres, and S. E. Nicholson.** (2002), Environmental Characterization of Global sources of atmospheric soil dust derived from the NIMBUS-7 TOMS absorbing aerosol product, Rev. Geophys., 40 (1), 1002, doi:10.1029/20000GR000095.

**Raes, F., Dingenen, R. V., Vignati, E., Wilson, J., Putaud, J.P., Seinfeld, J., Adams, P.** (2000). Formation and cycling of aerosols in the global troposphere. *Atmospheric Environment*, Volume 34, Issue 25, 26 July, Pages 4215-4240.

**Ramanathan, V., Crutzen, P. J., Kiehl, J. T., Rosenfeld, D.** (2001). *Science 294*, 2119.

**Reddy, M. S., Boucher, O., Balkanski, Y., Schulz, M.** 2005. Aerosol optical depths and direct radiative perturbations by species and source type. Geophysical Research Letters, VOL. 32, L12803, doi:10.1029/2004GL021743.

**Salvador, P., Artíñano, B., Molero, F., Viana, M., Pey, J., Alastuey, A., Querol, X.** (2013). African dust contribution to ambient aerosol levels across central Spain: Characterization of long-range transport episodes of desert dust. Atmospheric Research, 127, 117–129.

**Santese, M., Perrone, M.R., Zakey, A.S., Tomasi, F.D., Giorgi, F.** (2010). Modeling of Saharan dust outbreaks over the Mediterranean by RegCM3: case studies, *Atmos. Chem. Phys.*, 10, 133–156.

**Sathees, S.K., Moorthy, K.K.,** (2005). Radiative effects of natural aerosols : A review, *Atmospheric Environment*, 39, 2089-2110.

**Seinfeld, J.H., Pandis, S.N.** (2006). *Atmospheric Chemistry and Physics: From Air Pollution to Climate Change*, 2nd Edition.

**Sokolik, I. N., D. M. Winker, G. Bergametti, D. A. Gillette, G. Carmichael, Y. J. Kaufman, L. Gomes, L. Schuetz, and J. E. Penner.** (2001). Introduction to special section: Outstanding problems in quantifying the radiative impacts of mineral dust, *J. Geophys. Res.*,106 (D16), 18,015–18,027, doi:10.1029/2000JD900498.

**Solmon, F., Giorgi, F., Liousse, C.** (2006). Aerosol modeling for regional climate studies: application to anthropogenic particles and evaluation over a European/African domain, *Tellus*, 58B, 51-72.

**Solmon, F., Mallet, M., Elguindi, N., Giorgi, F., Zakey, A., Konare, A.** (2008). Dust aerosol impact on regional precipitation over western Africa, mechanisms and sensitivity to absorption properties, *Geophys. Res. Lett.*, 35, L24705, doi:10.1029/2008GL035900.

**Solomon, S., D. Qin, M. Manning, Z. Chen, M. Marquis, K.B. Averyt, M. Tignor and H.L. Miller.** 2007. Contribution of Working Group I to the Fourth Assessment Report of the Intergovernmental Panel on Climate Change. Cambridge University Press, Cambridge, United Kingdom and New York, NY, USA.

**Sportisse, B.** (2008). *Fundamentals in Air Pollution: From Processes to Modelling*, Springer.

**Tanaka, T.Y., Chiba, M. (2006).** A numerical study of the contributions of dust source regions to the global dust budget Global and Planetary Change 52, 88–104.

**Taylor, K.E.** (2001). Summarizing multiple aspects of model performance in a single diagram. *J.Geophysics Research.*

**Tegen, I.** (2003). Modeling soil dust aerosol in the climate system: An overview. Quarternary Science Reviews , 22, 1821 - 1834.

**Url-1** <http://regclim.coas.oregonstate.edu/dynamical-downscaling/model-description/index.html >. Retrieved January 19, 2014.

**Url-2** <http://users.ictp.it/~pubregcm/RegCM4/globedat.htm#part4>. Retrieved May 19, 2013.

**Url-3** <http://earthobservatory.nasa.gov/GlobalMaps/ >, Retrieved December 5, 2013.

**Url-4** < http://www.citypopulation.de/world/Agglomerations.html>. Retrieved December 5, 2013.

**Warneck, P.** (1988). Chemistry of the natural atmosphere, Academic Press.

**Woodage, M. J., A. Slingo, S. Woodward, R. E. Comer,** 2010. U.K. HiGEM: Simulations of Desert Dust and Biomass Burning Aerosols with a High-Resolution Atmospheric GCM. *J. Climate*, 23, 1636–1659.

**Zakey, A.S., Solmon, F., Giorgi, F.** (2006). Implementation and testing of a desert dust module in a regional climate model, *Atmospheric Chemistry and Physics*, 6, 4687-4704.

**Zender, C. S., Bian, H., and Newman, D.** (2003). Mineral Dust Entrainment and Deposition (DEAD) model: Description and 1990s dust climatology, *J. Geophys. Res.*, 108, 4416, doi:10.1029/2002JD002775.

**Zhang, D.F., Zakey, A.S., Gao, X.J., Giorgi, F., Solmon, F.** (2009). Simulation of dust aerosol and its regional feedbacks over East Asia using a regional climate model, *Atmos. Chem. Phys.*, 9, 1095–1110.

**CURRICULUM VITAE**

**Name Surname:** Tuğba AĞAÇAYAK

**Place and Date of Birth:** İstanbul, 30.09.1982

**Address:** Istanbul Technical University, Eurasia Institute of Earth Sciences

**E-Mail:** agacayak@itu.edu.tr

**B.Sc.:** ITU, Environmental Engineering (2000-2004)

**M.Sc.:** ITU, Environmental Sciences and Engineering & ITU, Management Sciences (2004-2007)

**PhD :** ITU, Eurasia Institute of earth Sciences, Earth System Science (2007-2014)

**Professional Experience and Rewards:** Research Assistant (2009-2013)

**List of Publications and Patents:**

**PUBLICATIONS/PRESENTATIONS ON THE THESIS**

1. **Agacayak, T.**, Kindap, T., Unal, A., Pozzoli, L., Mallet, M., Solmon, F. 2014. A case study for Saharan dust transport over Turkey via RegCM4.1 Model Atmospheric Research, DOI: 10.1016/j.atmosres.2014.09.012

2. **Agacayak, T.**, Kindap, T., Unal, A., Pozzoli, L., Mallet, M., Gokturk, O.M., Bozkurt, D., Solmon, F., Dulac, F. and Karaca, M. Change in the Mineral Dust Budget of the Mediterranean Region with a Future Climate, *European Geosciences Union General Assembly 2014, Vienna, Austria.* Vol. 16, EGU2014-11657, 2014.

3. **Agacayak, T.**, Kindap, T., Unal, A., Pozzoli, L., Mallet, M., Bozkurt, D., Solmon, F., Dulac, F. and Karaca, M. Impact of Mineral Dust Direct Radiative Effect on Mediterranean Climate, *European Geosciences Union General Assembly 2014, Vienna, Austria.* Vol. 16, EGU2014-11974, 2014.

4. **Agacayak, T.,** Kindap, T., Unal, A., Pozzoli, L., Mallet, M., Gokturk, O.M. (2013, October). Impact of Mineral Dust on Mediterranean Climate. *Mesaep, 17th International Symposium on Environmental Pollution and its Impact on Life in the Mediterranean Region*, Istanbul, Turkey

5. **Agacayak T.,** Kindap T., Unal A., Pozzoli L., Göktürk, O.M., Mallet M., 2013: Impacts of Aerosols on Eastern Mediterranean Region Climate. *Tikdek 2013*, June 3-5, 2013, Istanbul, Turkey.

6. **Agacayak, T**., Kindap, T., Unal, A., Pozzoli, L., Mallet, M., Dulac, F. 2012 : Investigation of Mineral Dust Impacts on the Climate of the Eastern Mediterranean Region. *Charmex 3$^{rd}$ Workshop,* Corsica, France, 5-9 November 2012.

7. **Agacayak, T.,** Kindap, T., Unal, A., Mallet, M., Pozzoli, L., Karaca, M., Solmon, F., 2012. Impact of Dust on Air Quality and Radiative Forcing : An Episodic Study for the Megacity Istanbul Using RegCM-4.1, *European Geosciences Union General Assembly 2012,* Vienna, Austria, 22-27 April 2012.

8. **Agacayak, T.,** Kindap, T., Unal, A., Mallet, M., Pozzoli, L., Karaca, M., 2011. Effect of Meteorological Conditions on PM$_{10}$ in Istanbul, *MedCLIVAR Final Conference,* Lecce, 6-9 June 2011.